ELECTROMAGNETIC RADIATION PROPERTIES OF CEMENTLESS ALKALI ACTIVATED MATERIALS REINFORCED WITH POLYPROPYLENE AND STEEL FIBERS

Iyad AHMED

2021
MASTER THESIS
CIVIL ENGINEERING

Thesis Advisor
Assoc. Prof. Dr. İlker TEKİN

ELECTROMAGNETIC RADIATION PROPERTIES OF CEMENTLESS ALKALI ACTIVATED MATERIALS REINFORCED WITH POLYPROPYLENE AND STEEL FIBERS

Iyad AHMED

T.C.
Karabuk University
Institute of Graduate Programs
Department of Civil Engineering
Prepared as
Master Thesis

Thesis Advisor
Assoc. Prof. Dr. İlker TEKİN

KARABUK
June 2021

I certify that in my opinion the thesis submitted by Iyad AHMED titled "ELECTROMAGNETIC RADIATION PROPERTIES OF CEMENTLESS ALKALI ACTIVATED MATERIALS REINFORCED WITH POLYPROPYLENE AND STEEL FIBERS" is fully adequate in scope and in quality as a thesis for the degree of Master of Science.

Assoc. Prof. Dr. İlker TEKİN .....
Thesis Advisor, Department of Civil Engineering

This thesis is accepted by the examining committee with a unanimous vote in the Department of Civil Engineering as a Master of Science thesis. June 24, 2021

Examining Committee Members (Institutions)	Signature
Chairman : Prof. Dr. Metin İPEK (SUBU)	ONLINE
Member : Assoc. Dr. Ahmet BEYCİOĞLU (ATU)	ONLINE
Member : Assoc. Dr. İlker TEKİN (KBU)	.....

The degree of Master of Science by the thesis submitted is approved by the Administrative Board of the Institute of Graduate Programs, Karabuk University.

Prof. Dr. Hasan SOLMAZ .....
Director of the Institute of Graduate Programs

"I declare that all the information within this thesis has been gathered and presented in accordance with academic regulations and ethical principles and I have according to the requirements of these regulations and principles cited all those which do not originate in this work as well."

Iyad AHMED

ABSTRACT

M. Sc. Thesis

ELECTROMAGNETIC RADIATION PROPERTIES OF CEMENTLESS ALKALI ACTIVATED MATERIALS REINFORCED WITH POLYPROPYLENE AND STEEL FIBERS

Iyad Ahmed

Karabuk University
Institute of Graduate Programs
Department of Civil Engineering

Thesis Advisor:
Assoc. Prof. Dr. İlker TEKİN
June 2021, 139 pages

Concrete production can increase carbon dioxide emission into the atmosphere remarkably. This emission is caused mainly by Portland cement production, which is one of the main concrete components. Increasing the carbon dioxide emissions in the atmosphere is related directly to global warming and could accelerate it. Thus, researchers have been trying to develop new environmental-friendly binding materials have a similar mechanical and physical properties to Portland cement, and alkali activated material is one of the promising materials.

Currently, pollution caused by Electromagnetic Fields (EMFs) is increasing day after day. Bluetooth devices, mobile phones, microwave devices, and other wave generators widespread increases this pollution. This pollution can affect the health of humankind as well as other creatures. Thus, researchers nowadays tried to reduce this risk by

attenuating the waves using construction materials. And alkali-activated materials could be one of these effective construction materials for this process.

In this study, white and green volcanic tuffs collected from the Bayburt region in Turkey were used as silica and alumina sources to produce an Alkali Activated Pastes (AAPs). Calcite was used as calcium sources. And as alkali activators, Sodium Hydroxide (NaOH) and Sodium Silicate (Na_2SiO_3) in combination were used. Besides, two types of fibers are used in this study (polypropylene and steel fibers) with different percentages of friction of volume to enhance the AAPs' electromagnet, mechanical, and physical properties that will be produced. The new composite materials' electromagnet absorption and reflection features are determined in the range of 100 MHz - 6000 MHz between the 28^{th} and 56^{th} days of production. In addition, the mechanical and physical properties of the pastes were examined at 2, 28, and 90 days of production. The results of this study showed that the maximum 90 days flexural and compressive strengths were 11.70 MPa and 30.72 MPa, respectively. And the maximum electromagnetic wave's absorption and reflection peaks for the AAP batches from the frequencies of 900 MHz, 1800 MHz, 2400 MHz, and 5000 MHz were -35.45 dB (at 5000 MHz) and -12.15 dB (at 5000 MHz), respectively.

Key Words : Alkali-Activated Materials, Zeolitic Tuff, Calcite, Polypropylene Fiber, Steel Fiber, Mechanical Properties, Physical Properties, Electromagnetic Properties, Wave Absorption, Wave Reflection.

Science Code : 91127

ÖZET

Yüksek Lisans Tezi

POLİPROPİLEN VE ÇELİK ELYAF TAKVİYELİ ÇİMENTOSIZ ALKALİ AKTİF MALZEMELERİN ELEKTROMANYETİK RADYASYON ÖZELLİKLERİ

Iyad AHMED

Karabük Üniversitesi
Lisansüstü Eğitim Enstitüsü
İnşaat Mühendisliği Anabilim Dalı

Tez Danışmanı:
Doç. Dr. İlker TEKİN
Haziran 2021, 139 sayfa

Beton üretimi, atmosferde karbondioksit emisyonlarını önemli ölçüde artırabilir. Bu emisyon, ana beton bileşenlerinden biri olan Portland çimentosunun üretiminden kaynaklanmaktadır. Atmosferdeki karbondioksit salınımının artması küresel ısınma ile doğrudan ilişkilidir ve onu hızlandırabilir. Bu nedenle araştırmacılar, Portland çimentosuna benzer mekanik ve fiziksel özelliklere sahip çevre dostu yeni bağlayıcı malzemeler geliştirmeye çalışmaktadırlar. Alkali ile aktifleştirilmiş malzeme de gelecek vaat eden malzemelerden birisi olarak kabul görmektedir.

Şu anda Elektromanyetik Alanların (EMF'ler) neden olduğu kirlilik her geçen gün artmaktadır. Bluetooth cihazlarının, cep telefonlarının, mikrodalga cihazlarının ve diğer dalga jeneratörlerinin yaygınlığı bu kirliliği artırmaktadır. Bu kirlilik insan sağlığını etkilediği gibi diğer canlıları da etkileyebilir. Böylece günümüzde

araştırmacılar, inşaat malzemeleri kullanıp dalgaları sönümleyerek bu riski azaltmaya çalışmışlardır. Alkali ile aktive olan malzemeler, bu süreç için etkili yapı malzemelerinden biri olabilir.

Bu çalışmada, Türkiye'nin Bayburt bölgesinden toplanan beyaz ve yeşil volkanik tüfler, Alkali Aktifleştirilmiş Pastalar (AAP'ler) üretmek için silika ve alümina kaynağı olarak kullanılmıştır. Kalsiyum kaynağı olarak da kalsit kullanılmıştır. Alkali aktivatör olarak Sodyum Hidroksit (NaOH) ile birlikte Sodyum Silikat (Na2SiO3) kullanılmıştır. Ayrıca bu çalışmada üretilecek AAP'lerin elektromıknatıs, mekanik ve fiziksel özelliklerini iyileştirmek için farklı hacim sürtünme yüzdelerine sahip iki tip fiber (polipropilen ve çelik fiber) kullanılmıştır. Yeni kompozit malzemelerin elektromıknatıs soğurma ve yansıtma özellikleri, üretimin 28. ve 56. günleri arasında 100 MHz - 6000 MHz aralığında belirlenir. Ayrıca hamurların mekanik ve fiziksel özellikleri, üretimin 2, 28 ve 90. günlerinde incelenmiştir. Bu çalışmanın sonuçları, maksimum 90 günlük eğilme ve basınç dayanımlarının sırasıyla 11.70 MPa ve 30.72 MPa olduğunu göstermiştir. Ve 900 MHz, 1800 MHz, 2400 MHz ve 5000 MHz frekanslarından AAP grupları için maksimum elektromanyetik dalga absorpsiyon ve yansıma zirveleri sırasıyla -35.45 dB (5000 MHz'de) ve -12.15 dB (5000 MHz'de) idi.

Anahtar Kelimeler : Alkali Aktif Malzemeler, Zeolitik Tüf, Kalsit, Polipropilen Elyaf, Çelik Elyaf, Mekanik Özellikler, Fiziksel Özellikler, Elektromanyetik Özellikler, Dalga Soğurma, Dalga Yansıması.

Bilim Kodu **:** 91127

ACKNOWLEDGMENT

Who does not thank people does not thank God, thus, I will try my best to thank the people who helped me during my master's degree; still, what is in the heart cannot be described well!

I am deeply thankful to my family for their great support and influence on me that helped me to succeed.

And I am grateful to my advisor, Assoc. Prof. Ilker Tekin, for his great and well supervision of this thesis. As well as I am thankful for his assistant Res.Asst. Mahfuz Pekgöz who helped me in multiple ways. And many thanks to my labmate Şeyda Hacıhasanoğlu.

At the end, I would like to thank the Scientific and Technological Research Council of Turkey (TÜBİTAK) for supporting this thesis by funding it as a part of the TUBİTAK #217M431 project "***Determination Of Electromagnetic Properties Of Geopolymers Covering And Wall Materials Powdered By Fiber Produced With Bayburt Syone And Development Of New Covering Materials Absorping-Reflecting Or Conducting Electromagnetic Wave*** (***Bayburt Taşı İle Üretilen Lifle Güçlendirilmiş Geopolimer Kaplama Ve Duvar Malzemelerinin Elektromanyetik Özelliklerinin Belirlenmesi Ve Elektromanyetik Dalga Emen-Yansıtan Veya İleten Yeni Kaplama Malzemesinin Geliştirilmesi***)".

CONTENTS

Page

Page

Page

LIST OF FIGURES

Page

Page

Page

LIST OF TABLES

Page

SYMBOLS AND ABBREVITIONS INDEX

SYMBOLS

%	: Percent Sign
m	: Meter
cm	: Centimeter
mm	: Millimeter
μm	: Micrometer
S/P	: Solution to Powder Ratio
min	: Minute
s	: Seconds
Kg	: Kilogram
M	: Molar
^{o}C	: Degrees Celsius
Hz	: Hertz
MHz	: Megahertz
THz	: Terahertz
dB	: Decibels
Na_2CO_3	: Sodium Carbonate
Na2SO4	: Sodium Sulfate
NaOH	: Sodium Hydroxide
KOH	: Potassium Hydroxide
Na_2SiO_3	: Sodium Silicate
$Ca(OH)_2$	: Calcium Hydroxide
CaO	: Calcium Oxide
CO_2	: Carbon Dioxide

ABBREVITIONS

AAM	: Alkali Activated Material
AAFA	: Alkali-Activated Fly Ash
AAS	: Alkali Activated Slag
AAC	: Alkali-Activated Concrete
AAR	: Alkali-Activated Reaction
OPC	: Ordinary Portland Cement
FA	: Fly Ash
GGBS	: Ground Granulated Blast-Furnace Slag
RHA	: Rice Husk Ash
C-S-H	: Calcium Silicate Hydrate
C-A-S-H	: Calcium aluminate silicate hydrate
N-A-S-H	: Sodium-Aluminosilicate-Hydrate
ASTM	: American Society for Testing and Material
XRD	: X-ray diffractometers
SEM	: Scanning electron microscope
GT	: Green Tuff
WT	: White Tuff
PP	: Polypropylene
EMR	: Electromagnetic Radiation
EMW	: Electromagnetic Wave
EMF	: Electromagnetic Field
EMS	: Electromagnetic Spectrum
SE	: Shielding effectiveness

PART 1

INTRODUCTION

1.1. GENERAL

Concrete is one of the most widely used materials globally for a long time because of its remarkable mechanical and physical properties and low costs. One of the main materials to produce a concrete mixture is Portland cement. However, Portland cement production is harmful to the environment because it increases Carbon Dioxide (CO_2) emissions. Approximately 5–7% of the world's total CO_2 emissions are generated by cement [1,2]. And the increase in the CO_2 amount in the atmosphere can cause climate change, which is one of the most critical environmental problems facing the world and lead to global warming [3]. Thus, global warming may cause a rise in the sea level caused by the water's thermal expansion. If the sea level rises above 0.40 meters, it will sink 11% of the area in Bangladesh, and as a result, 10 million people will be homeless [3]. Besides, cement production requires a collection of limestone hills intensively as it happens throughout the world nowadays, leading to ecological imbalance [4]. As a result of increasing awareness about the harmful effects of CO_2 emissions and it is subsequent, some researchers have been trying to find eco-friendly alternative substituting the Ordinary Portland Cement (OPC) binders partially or totally with satisfying mechanical and physical properties such as OPC, and one of the promising alternative binders that exhibits environmental performance over OPCs and gives satisfying mechanical and physical properties is alkali-activated materials (AAMs) [5–9].

AAMs are a globally growing technology that was first produced on a significant scale in the 1940s by Purdon [10]. But the global awareness of AAMs started to develop with the work generated by Glukhovsky in the the1950s in Eastern Europe [11]. AAMs are described as the geo-polymerization reaction between various sources of solid

aluminosilicate (precursors) and alkaline solution that activates these precursors to produce materials that harden over time. Many common sources of solid aluminosilicate could be used to produce the AAMs, such as Granulated Blast Furnace Slag (GGBS) [12], Metakaolin (MK) [13], Fly Ash (FA) [14], and Zeolitic tuff [15,16]. While as alkaline activators, the most common activators used individually or in combination are sodium carbonate (Na_2CO_3), sodium sulfate (Na_2SO_4), sodium hydroxide (NaOH), potassium hydroxide (KOH), sodium silicate (Na_2SiO_3), and calcium hydroxide ($Ca(OH)_2$) [17,18]. The main hydration products in OPC systems and AAMs are different than each other. Calcium-silicate-hydrate (C–S–H) is the main hydration product in OPC systems. While in AAMs, the main reaction products from the reaction are sodium-aluminosilicate-hydrate (N-A-S-H) and calcium-aluminosilicate-hydrates (C-A-S-H). Moreover, hydrotalcite and other crystalline phases also coincide in AAMs [19–21].

As AAMs technology grows day by day and gives a promising performance, many studies have started to compare concrete made with AAMs, which is called alkali-activated concrete (AAC) and OPC concrete. The results showed that AAC has exhibit more advantages over OPC concrete, such as early high strength and good growth over the long-term, high resistance to chemical attacks and freeze-thaw cycles, and lower carbonation rates [22,23]. However, previous investigations reported that AAMs show brittle behavior and are susceptible to cracking like OPC mortar or concrete under tension [24,25]. Cracking is a huge problem for concrete because it increases permeability. That would allow water, air, and aggressive chemical agents such as chloride to reach steel reinforcing under the concrete cover, leading to lower durability for the structural members. One of the techniques to solve these problems is incorporating fibers with the mixtures. Using fibers with AAM mixtures can positively affect this material's properties, such as strength, ductility, and durability. Using fibers incorporating with the mixtures can limit the cracks' width, besides inhibiting the brittle behavior with increasing the ductility. For example, Puertas et al. [26] investigated drying shrinkage and the mechanical behavior of Alkali Activated Slag (AAS) mortars reinforced with alkali-resistant glass fiber. The results showed that drying shrinkage is decreased over 20% in case of adding alkali-resistant glass fiber to the AAS mortars mix. Vilaplana et al. [27] made an investigation on the mechanical

properties of AAS pastes reinforced with carbon fibers. They concluded that the addition of carbon fibers could be suitable to control the drying shrinkage.

Currently, pollution caused by Electromagnetic Fields (EMFs) is increasing gradually. People are more constantly wondering about the possible hazardous effects of natural and human-made electromagnetic radiations that may lead to deteriorating the electromagnetic environment. The widespread use of electronic devices such as mobile phones, personal computers, video game consoles, digital audio players devices, and devices that enable technologies such as Bluetooth and Wi-Fi could increase this pollution. Although researchers have not come up with a final proof yet, these EMFs are possibly harmful to human beings. However, some studies reported a few effects regarding the EMFs, such as the possible interference with the brain's normal functioning [28], changes in glucose metabolism in the brain [29], effects on ecosystems and biosystems [30], and adverse effect on the rats' memory [31]. Therefore, these EMFs can increase the risk to the environment and human health.

However, Existing building materials could be one of the methods of controlling the risk of EMFs [32,33]. The structure and composition of construction materials reduce EMF's effect on the existing building materials due to its absorption properties of these waves. The most commonly used electromagnetic absorbers in construction materials are metal fiber [34], ferrites [35], graphite [36], graphene oxide [37], carbon nanotubes [38,39], carbon filament [40], and carbon fiber [41]. Most of these absorbers are compatible with cement, although they are expensive. Some researchers start to pay attention to developing new economic absorbers for the electromagnetic wave absorbing cement types [42,43]. For instance, Huang et al. [44] made a study on the wave absorbing properties of cement materials mixed with high-iron fly ash. They obtained a minimum reflectivity of these materials with −11 dB in the range of 9.5–18 GHz. Wen and Chung [34] studied the electromagnetic shielding effect of cement pastes and mortars reinforced with stainless steel fiber. The fiber diameter was 8 μm with 6 mm length. They obtained a shielding effectiveness of 70 dB at 1.5 GHz in cement paste that contains 0.72 vol.% stainless steel fiber. Kaushal and Singh [45] studied the effect of filler loading on the shielding of electromagnetic interference of reduced graphene oxide reinforced polypropylene (PP). PP with different percentages

(0.5, 1, 3, and 5wt%) of reduced graphene oxide were prepared to design a nanocomposite to shield the electromagnetic waves. The results showed that adding these composites are able to block up to 90% of the wave. And this composite could be a potential candidate for another kind of microwave absorbing material.

As a result of an extensive literature survey on the AAMs' properties, it was observed that the electromagnetic properties of the AAMs had not been studied widely yet. Previous investigations mainly focused on the mechanical, physical, chemical, and thermal properties of this material. However, the aim for this study is to produce Alkali Activated Pastes (AAPs) reinforced with polyproline and steel fibers with a different percent of friction of volume and determine the electromagnetic properties of these coating materials between the 28^{th} and 56^{th} days of production in the range of 100 MHz - 6000 MHz. Additionally, the mechanical and physical properties such as flexural strength, compressive strength, water absorption, and shrinkage of the AAPs will be provided after 2, 28, and 90 days of production.

1.2. THESIS AIMS AND OBJECTIVES

Aim 1: To produce Alkali-Activated Pastes (AAPs) by the geo-polymerization reaction between volcanic tuff (white and green tuff collected from the Bayburt region in Turkey) and calcite with various alkaline activators and strengthening these pastes by steel and polypropylene fibers in specific proportions to increase the mechanical strength and durability of the mix.

1) **Objective:** To ensure completion of the pastes' final setting times to be produced within 1 hour at the latest.
2) **Objective:** To obtain the flexural strength at least 10 MPa in 90 days of AAPs samples production.
3) **Objective:** To obtain the compressive strength at least 25 MPa in 90 days of AAPs samples production.

Aim 2: To produce AAPs reinforced with steel and polypropylene fibers and determine the electromagnetic properties of these coating materials in the range of 100 MHz - 6000 MHz.

1) **Objective:** To provide high electromagnetic absorption and reflection features of an AAPs made with natural tuffs.
2) **Objective:** To produce a coating material that would be able to minimize electromagnetic pollution and its harmful effects on humans.

Aim 3: To develop a new tile types similar to ceramic materials using waste materials.

1) Objective: To produce an environmentally friendly tiles as the main powdered materials came from the waste.
2) Objective: To produce a new tile types that consumes a less embodied energy than the ceramic production does.

1.3. THESIS ARRANGEMENT

The remainder of the Thesis is arranged as follow:

Chapter 2: Background of the widely used materials to produce the AAMs.
Chapter 3: Describes the methodology used to produce and test the mechanical, physical, and electromagnetic properties of the AAPs in this thesis.
Chapter 4: Presents and discusses the test results.
Chapter 5: States the summary and the conclusions of this study based on the results. Finally, the reference list is presented.

PART 2

LITERATURE REVIEW

2.1. CONCRETE AND ENVIRONMENT

Annually, the production of cement is increasing by approximately 3% [46]. Nearly one ton of carbon dioxide (CO_2) is liberated into the atmosphere from the production of a ton of cement [47]. Portland cement production contributes to greenhouse gas emissions, which is estimated to be about 7% annually of the total greenhouse gas emissions to the earth's atmosphere [48]. Besides, cement is considered one of the most energy-intensive construction materials. Thus, the consumption of this material should be decreased and replaced gradually by an environmentally friendly material. Researchers have been trying to find an eco-friendly solution to this problem. Mehta (2002) [49] suggested minimizing carbon dioxide emissions by using less energy and fewer natural resources. Mehta characterized these short-term efforts as 'industrial ecology.' And the long-term aim is to decrease the impact of unwanted by-products of industry, which can be achieved by lowering the material consumption rate [49]. McCaffrey (2002) [46] also suggested that decreasing the amount of calcined material in cement and decreasing the number of buildings constructed using cement can reduce CO_2 emissions by cement industries.

2.2. HISTORY AND DEVELOPMENT OF AAMs

The first to published work related to AAMs was in 1908 by the German chemist Kühl [50]. Kühl studied the setting behavior of a binder produced by mixtures of basic blast furnace slag and alkaline components. However, this type of material did not receive any notable consideration only after decades. When Purdon in 1940, published a detailed study describing the interaction of blast furnace slags with various chemical

activators [10]. According to Purdon, the process was generated in two parts. In the first part, the liberation of silica aluminum and calcium hydroxide would take place. While in the second part, the formation of silica and alumina hydrates would start along with the regeneration of the alkali solution. From his study results, he concludes that the alkali hydroxides worked as catalysts. He proved his statement by leaching alkali hydroxides in the same quantity as granted in the original mix.

The major research progress regarding the AAMs for the next several decades started to grow by Glukhovsky [11]. Glukhovsky had investigated the binders used in ancient Egyptian and Roman constructions. He concluded from his investigation that those constructions constituted of Calcium aluminosilicate hydrates similar to those in Portland cement and crystalline phases of analcite, which is considered as a natural rock that would explain the durability of those binders. Stand on those investigations, Glukhovsky revealed a new type of binder and called it ‘‘soil-cement.’’ The word soil is used because the hardened binder seemed like a ground rock. Also, he called the corresponding concretes “soil silicates.” [51].

By the 1970s, Davidovits [52], developed and patented binders obtained from the alkali activation of calcined clay, which in 1979 he called this material ‘‘geopolymers’’. Since then, geopolymers term has been used widely for various types of alkali-aluminosilicate binders. Additionally, this name is now widely recognized as a generic expression for AAM systems. According to Davidovits, the geopolymer binder is produced by the early ancient Egyptians and Romans, and these materials helped them build their constructions [53]. Stands on the chemical and mineralogical investigations, Davidovits stated that the pyramid blocks are human-made binders of a mixture of limestone sand, calcium hydroxide, sodium carbonate, and water [53].
However, after increasing the studies regarding the AAMs, various terminologies were assigned to these materials depending on the research groups working on this material. And the most famous terminologies of AAMs are:

1) Soil Silicates.
2) Geopolymers.
3) Alkali-activated cement.

4) Alkaline Cements.
5) Geo-cements.

Research and investigation activities regarding the development of AAMs began to increase remarkably during the 1980s and 1990s. This field is now considered a highly active area for researchers. This material is being developed day by day, and this development includes scientific investigation efforts, deployment of commercial materials, and national and international standardization [54]. Table 2-1 summarizes important events in the historical timeline of the development of AAMs adapted from [47,55].

Table 2.1. History of the important events about AAMs [47,55].

Researchers	**Significance**	**Year**
Feret	Investigation on the slags used for cement	1939
Purdon	Investigation on alkali-slag combinations	1940
Glukhovsky	Theoretical investigation on the basis and development of alkaline cements	1959
Glukhovsky	"Alkaline cements" was preposed	1965
Davidovits	"Geopolymer" was preposed	1979
Malinowski	The Ancient aqueducts characterized	1979
Forss	slag-alkali-superplasticizer and F-cement Term used	1983
Langton and Roy	The Ancient building materials characterized	1984
Davidovits and Sawyer	Patent taken from "Pyrament" discovery	1985
Krivenko	R2O–RO–SiO2–H2O by his DSc thesis	1986
Malolepsy and Petri	Synthetic melilite slags as AAMs	1986
Malek et al.	Slag cement-low level radioactive wastes forms	1986
Davidovits	Compared between ancient and modern concretes	1987
Deja and Malolepsy	Proven of the Resistance to chlorides Acid	1989
Kaushal et al.	Formation of adiabatic cured nuclear waste from alkane mixtures	1989
Roy and Langton	Investigation on the analogs of ancient concretes	1989
Majundar et al.	C12A7– slag activation	1989
Talling and Brandstetr	AAS	1989
Wu et al.	Investigation on the activation of slag cement	1990
Roy et al.	Rapid setting time of alkali-activated cements	1991
Roy and Silsbee	An overview study on alkali-activated cements	1992
Palomo and Glasser	Investigation on calcined brown clay with metakaolin	1992
Roy and Malek	Investigation on Slag cement	1993

Table 2.1. (continue).

Glukhovsky	**Ancient, modern, and future concretes**	**1994**
Krivenko	Investigation on alkaline cements	1994
Wang and Scrivener	Investigation on Slag and alkali-activated microstructure	1995
Fernández-Jimenez and Puertas	Reaction of Alkali-Activated Slag (AAS) cement reaction kinetics	1997
Katz	Microstructure of Alkali-Activated Fly Ash (AAFA)	1998
Davidovits	Investigation on the Processes of mineral polymerization	1999
Gong and Yang	Alkali-activated red mud-slag cement	2000
Puertas	Alkali activation of fly ash-slag cement	2000
Bakharev	Alkali-activated slag concrete	2001-2002
Provis and Deventer	Nano crystallinity in 'geopolymers'	2005
Provis and Deventer	Investigation on structure, preparation, properties, and industrial applications of AAMs	2009
Lothenbach et al.	Influence of slag chemistry on the hydration of alkali-activated blast-furnace	2011
Provis and Deventer	Alkali-Activated Materials: State-of-the-Art Report	2014
BSI	Specification for Alkali-activated cementitious material (first major performance)	2016

2.3. ALKALI ACTIVATED MATERIALS AND GEOPOLYMERS (CHEMICAL PHASE)

Alkali-activated materials are a material formed by the aluminosilicate precursor activated by an alkaline activator to produce a material that hardens over time. The precursors used nowadays are by-products precursors. Those by-products are included recycled glass, Fly Ash (FA), Ground Granulated Blast Furnace Slag (GGBFS), Rice Husk Ash (RHA), and red mud. Commonly there are two terms used to describe these types of materials: geopolymers and alkali-activated materials. Both are chemically similar though each material is based on different types of aluminosilicate precursors and the precursors had a different content of Al and Ca as shown in Figure 2-1 [56]. From Figure 2-1, it can be observed that alkali-activated materials are a large group of materials, and the geopolymers are a subset of it. The geopolymers subset has the lowest Ca concentrations and the highest Al contents.

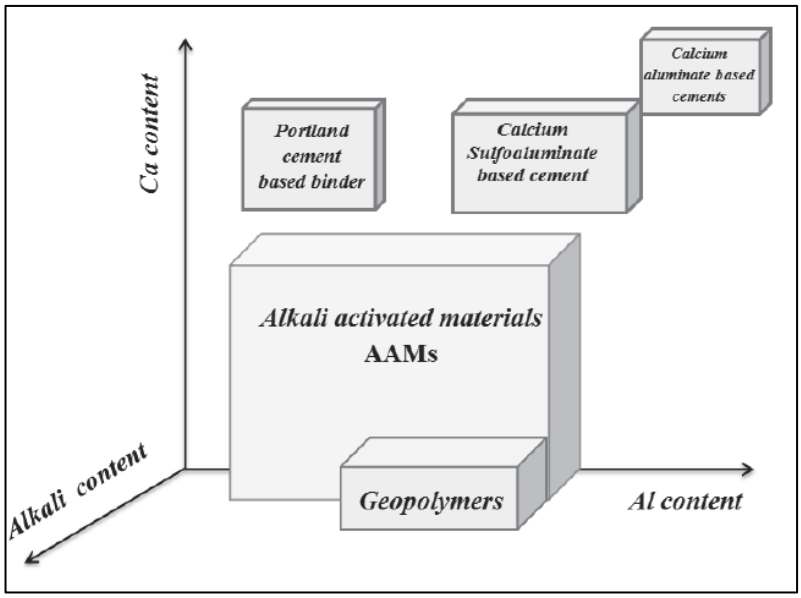

Figure 2.1. Classification of commonly used binders [56].

However, the hardening process of these types of materials required a geo-polymerization reaction [57]. The geo-polymerization reaction is described by Davidovits using the two-stage equation shown in Figure 2-2 below [57]. The chemical reaction between alumino-silicate oxides source such as (Si_2O_5, Al_2O_2) with alkali polysilicates (generally sodium or potassium silicate) yielding polymeric Si–O–Al bonds are required reaction for the geo-polymerization process. geo-polymerization reaction is described as an exothermic process that is carried out through oligomers. These oligomers give the actual system model for the three-dimensional macromolecular edifice [58]. One of many hardening mechanisms for this material involves the chemical reaction process of alumina-silicate oxides with alkalis and alkali–polysilicates that will yield polymeric Si–O–Al bonds with a (Si_2O_5, Al_2O_2)n formula. This would be accomplished by calcining alumina-silicate hydroxides (Si_2O_5, $Al_2(OH)_4$) throughout the reaction process of $2(Si_2O_5, Al_2(OH)_4) \rightarrow 2(Si_2O_5, Al_2\ O_2)n + 4H_2O$ or by condensation of SiO and Al_2O vapors as same as the reaction of 4SiO (vapor) + $2Al_2O$(vapor) + $4O_2 \rightarrow (Si_2O_5, Al_2O_2)n$ this would also provide condensed silica fume and corundum ($2SiO + O_2 \rightarrow 2SiO_2$ and $Al_2O+O_2 \rightarrow Al_2O_3$) [58].

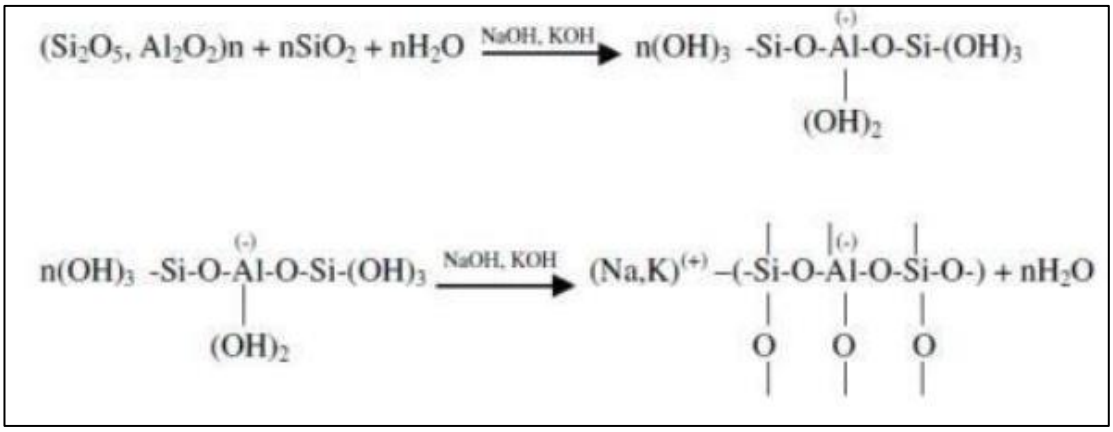

Figure 2.2. Two-stage equation describes the geo-polymerization reaction by Davidovits [57].

Three types of polysialates have been distinguished by Davidovits [58,59], those models are the Poly(sialate) type (-Si-O-Al-O), the Poly(sialate-siloxo) type (-Si-O-Al-O-Si-O), and the Poly(sialate-disiloxo) type (-Si-O-Al-O-Si-O). Figure 2-3 can describe Poly(sialates) models, according to Davidovits. Unlike different ordinary cement types, the geopolymer materials do not form calcium silicate- hydrate (C-S-H) for matrix formation of the bond's material and strength. However, it was formed to utilize the polycondensation of precursors that contains silica and alumina and a high alkali content to attain structural strength. Thus, geopolymer materials are sometimes referred to as alkali-activated aluminosilicate binders [60]. Though, Davidovits, the first producer for geopolymers, indicated that the term ‘alkali-activated’ could generate false ideas about geopolymer concrete and could create significant confusion. For instance, ‘Alkali-aggregate reaction (AAR)’ is a harmful effect on the concrete and could be confused with other terms such as ‘alkali-activated cement’ or ‘alkali-activated fly ash.’

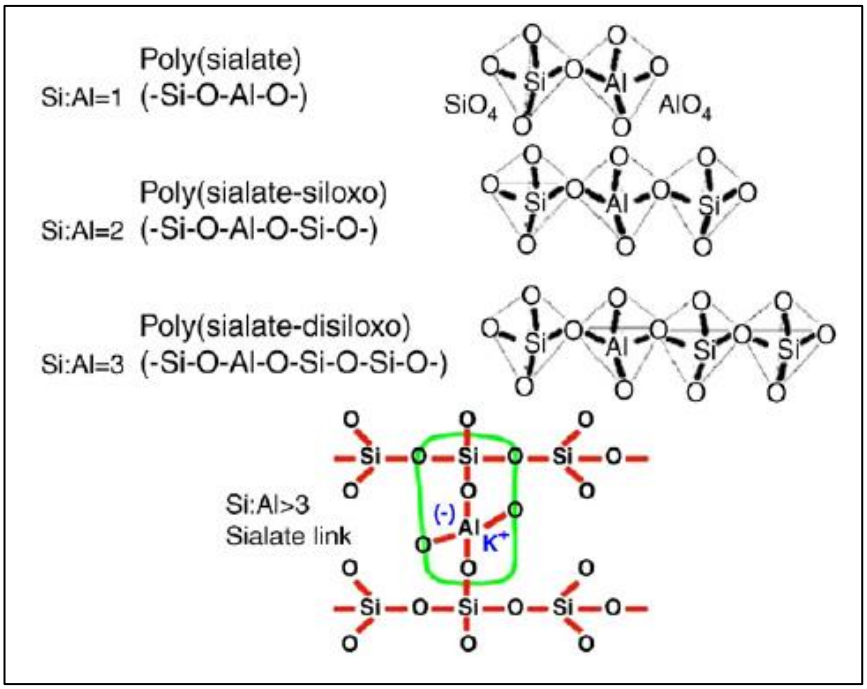

Figure 2.3. Poly(sialates) structures according to Davidovits [58].

Theoretically, we could use any raw material that contains reactive silica and aluminum to produce AAMs. However, the most used material to produce AAMs and studied widely by the researchers are blast furnace and fly ash.

Other materials such as metakaolin, kaolinitic clays, tuff, and red mud can be used to produce the AAMs, but they are less commonly used, and can produce different binding systems. However, based on the chemical composition of the materials used, binding systems can be classified into two systems calcium and silica enriched system (Ca + Si) and aluminosilicates dominated system (Si + Al) [55].

Generally, the matrix that would form from a material with a high Ca content such as GGBS will be a calcium-aluminate-silicate-hydrate (C-A-S-H) matrix with a lower Ca/Si ratio and a high Al incorporation [61]. While the system that would form from a material with a high Al content such as metakaolin would have sodium-aluminate-silicate-hydrate N-A-S-H type gels with a three-dimensional network as the major final product [62]. Each system exhibits unique behavior than the other regarding the setting and hardening processes, alkaline and curing demands, strength development, and the nature of the gel characteristics.

2.3.1. Alkali Activated High Calcium

Alkali activated high calcium are produced by the precursor rich with calcium. GGBS is the most used high calcium precursor. It is used due to the relatively high amounts of calcium and low aluminum contents in the glassy phase. The reaction process of slag to produce alkali-activated high calcium binders contains several stages. These stages include the destruction of the raw material and finally, end up with the condensation of the reaction products. Figure 2-4 describes the dissolution mechanism of glassy Ca-Si particles enriched phases similar to the reaction process alkali-activated slag. The additional bonds are not shown in this figure for clarity. Step A in Figure 2-4 describes that at the beginning stage and under alkalis in solution, ionic exchange of H^+ with Ca_2^+ and Na^+ appears between the slag particle surface and the solution. The removal of Ca_2^+ damages the original glassy structure and the Na^+ cation. However, because of the cation size difference, divalent cation's influence seems to be more significant. Step B describes the hydrolysis of Al-O-Si bonds. Step C presents the breakdown of the depolymerized glass network. Most of the slag's original bonds, especially the Ca-O and T-O ones, are being broken in this step. Moreover, the destruction of the entire glassy phase begins. Step D shows the release of Si and Al. After that, the Si-Al layer starts to appear near the slag particle's surface, and the reaction products are formed [63].

Other studies on alkaline activation of slag also indicated a similar reaction process as the process described above. For example, Fernandez et al. 1995 [64] suggested a four stages reaction process for this type of materials including the dissolution of the raw material particles, nucleation and growth of the initial products, interactions at the surfaces of the newly formed phases and the ongoing reaction at advanced times of curing . Wang and Scrivener 1995 [65] mad a study on the hydration products of alkali-activated slag. They suggested a similar hydration process as Portland cement, including dissolution and precipitation at an early-stage solid-state reaction at later ages. However, the real case of activation the slags exceeds this process, and it is more complicated than the illustrated route shown in Figure 2-4.

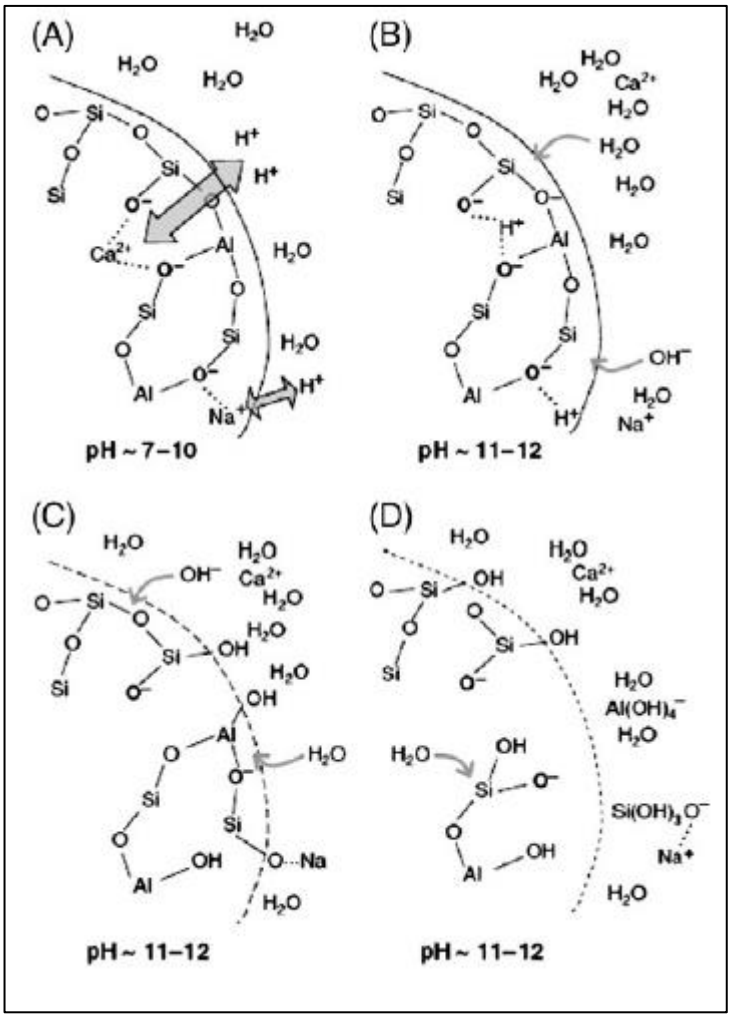

Figure 2.4. Dissolution mechanism of Ca-Si enriched phases [63].

2.3.2. Alkali Activated Aluminosilicates.

There are many sources' rich in aluminosilicates can provide an Alkali activated material based on aluminosilicates materials such as fly ash and metakaolin. Still, there are many differences between aluminosilicates sources, such as the particle shape and size, chemical composition, and glassy type. However, the main reactive phase in those materials is an important common character, and it is described as an amorphous aluminosilicate.

This type of reaction mainly consists of four stages [66]: destruction, coagulation, condensation, and crystallization. In the destruction stage, the destruction of the raw material to coagulation occurs; this will also include the breakdown of the Me-O and

T-O bonds in the origin material. The formation of Si-O-Na^+ new bonds that are stable in alkali solutions used makes this kind of reaction an irreversible reaction. Besides, it would work as the transport tool, which will help form a coagulated structure. This effect is considered similar to the one that happens on the Al-O-Si bond of starting material; under alkali attack, the aluminate forms $Al(OH)_4$ or $Al(OH)_6$. The second stage is referred to and describes the process of coagulation to condensation. In those stages, after the alkali attack starts to accumulate in the reaction, the silica and aluminum monomers in the solution forming a coagulated structure, which means the polycondensation occurs. The last stage of this reaction process is from condensation to crystallization. This stage happens when the solid phases are finally gradually generated and crystallized.

As shown in Figure 2-5, the raw material dissolves under alkali attack, and the aluminates and silicates are released as monomers. After that, the smaller molecule monomers accumulate together and develop larger ones. The silicate and aluminate tetrahedral start bonding together, developing rings with four tetrahedral units. At the early stage, Gel 1 is formed with around 1 Si/Al ratio that has relatively high aluminum content because of the Al release in the early terms of the reaction process. Bonds with Al-O are weaker; thus, it is more easily severed than Si-O bonds. More and more silica monomers are dissolved as the reaction process continues, and the gel 1 tends to transform into a more silica enriched gel (Gel 2 appears, and the Si/Al ratio is around 2). Finally, the polymerization occurs within the Gel 2, and large molecule reaction products are formed [66].

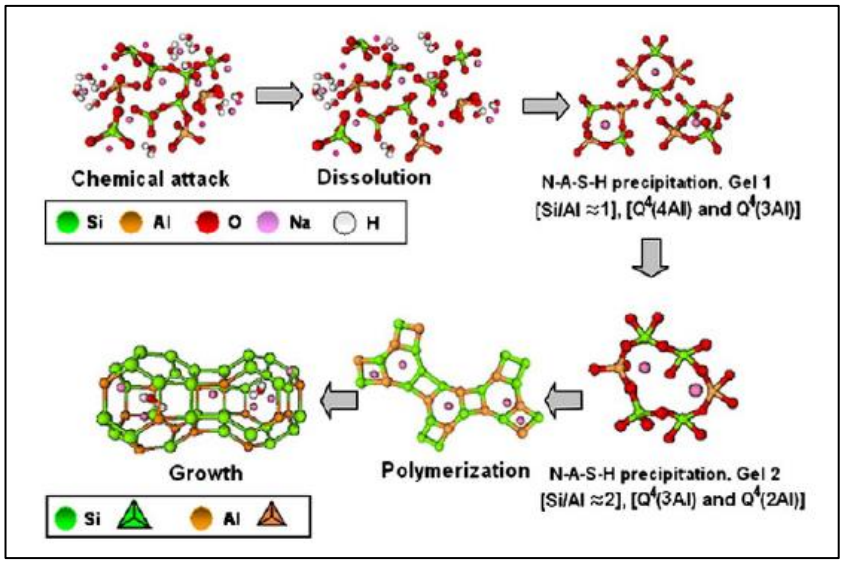

Figure 2.5. Modified descriptive model for activation of aluminosilicates [66].

2.4. POZZOLANA IN AAMs

Pozzolana can be divided depending on its source into two groups as artificial pozzolana and natural pozzolan. Artificial pozzolana comes from by-products industry. Artificial pozzolana is a widely used material in conventional concrete production. Fly ash and slag are the most famous types of artificial pozzolana. While Natural Pozzolana is the raw material that shows pozzolanic properties. The chemical composition, specific surface, and mineralogical structure play an important role in natural pozzolans' reactivity [15,67]. In general, the amount and structure of active phases in the amount of lime bound by pozzolan depends on the lime/pozzolan ratio of the mixture, SiO_2 content, and curing time. Various types of natural pozzolans can be used as cementation binders when an alkaline activator is added to them to produce AAMs. Metakaolin, trass, and tuff are examples of natural pozzolanic materials that are being used nowadays to produce AAMs. In this study, Tuff as a natural pozzolanic material is going to be used to produce the AAPs.

2.4.1. Trass

Trass is a natural raw material with a volcanic origin; It consists mainly of silica and aluminum oxide and contains lime traces. Trass alone does not have a hydraulic

binding feature. It requires lime to react and gives products with binding properties. The reactions that occur between silica and lime are known as a pozzolanic reaction. When trass is used as an additive, the lime that comes out due to the clinker's reaction with water enables the pozzolanic reaction to occur, and the trass becomes a binding agent. The natural pozzolans cause low permeability of additive compared to other cement types. Thus, it can make the new product of their reaction more resistant to chemical effects such as sulfate effect compared to OPC [68].

2.4.2. Tuff

Zeolite-rich volcanic tuffs have been used since prehistoric ages in construction because of it is availability. Mostly it is used as a dimension stone. Tuffs consist primarily of volcanic ash. Zeolitic tuffs are among the important raw materials of today's industry due to their chemical properties and crystal structures. Zeolitic tuffs are substances with small porous structure. The crystal structure and chemical properties of zeolites enable them to be evaluated in applications such as molecular sieve, selective adsorption, and catalytic use [68]. Zeolitic tuffs can be used in lightweight constructions. Besides, the lightweight building materials produced using zeolitic tuffs provide significant savings in the cooling and heating systems' initial investments due to their high thermal insulation properties.

Bayburt Tuff (BT), which is used in this study, is a volcanic tuff rich in silicon. BTs' main components are 68.9% SiO2, 12% Al2O3, 0.34% Fe2O3, and 3.85% CaO as they reported by Tekin (2016 and 2020) studies [15,16]. Other components are MgO, SO_3, Na_2O, K_2O. According to his research, the total SiO_2 + CaO in BT is> 70%, and BT is considered to be in the pozzolanic structure according to ASTM C618 [69] since the sum of SiO2 + Al2O3 + Fe2O3 is more than 70%.

2.5. ACTIVATORS

To form a binding material with Fly ash, slag, tuff, and other aluminosilicate materials, these materials need to be activated using alkalis. Alkaline activators used typically

for this process are caustic alkalis or alkaline salts. Activators can be classified into mainly six groups as reported by various studies [70,71] as following:

1) Alkalis, with MOH chemical formula.
2) Weak acid salts, with M_2CO_3, M_2SO_3, M_3PO_4, MF chemical formula.
3) Silicates, with $M_2O + nSiO_3$ chemical formula.
4) Aluminates, with $M_2O + nAl_2O_3$ chemical formula.
5) Alumina-silicates, with $M_2O + Al_2O_3 + (2\text{-}6)SiO_2$ chemical formula.
6) Strong acid salts, with M_2SO_4 chemical formula.

Where M represents the Metal (typically Sodium or potassium; however, Sodium-based is more economical)

2.5.1. Alkali Hydroxides and Alkali Silicates

Alkali hydroxides are composing of the hydroxide anion (OH^-) and alkali metal cation. As a metal cation, Sodium or potassium are used. Alkali hydroxides are the most widely used activators to activate the aluminosilicate materials to produce a bonding material. Special precautions should be taken when NaOH is used because the dilution releases a large amount of heat. The optimal alkalinity alkali-activated systems should be identified to produce the binding materials; otherwise, the reaction products' carbonation and leaching will be a concern [72].

Among the alkali silicates, Sodium silicate is the most common activator used to activate the aluminosilicate materials to produce a bonding material because of its availability, satisfaction results, and good price compared to other activators [71]. Sodium silicates have two forms that can be available commercially for them: liquid and solid forms. The liquid form is called water glass, as the commercial name of it. The viscosity is the major difference between potassium silicates and sodium silicates. Sodium silicate solutions have a higher viscosity than potassium silicate at the same silica modulus. Thus, potassium silicate can make the mixtures workable at a lower activator-to-binder ratio. However, potassium silicates are more expensive than Sodium silicate.

Among all of the activators, NaOH, Na_2CO_3, $Ca(OH)_2$, $Na2O.nSiO_2$, and Na_2SO_4 have the most economical chemical structure and wide usage area. Some potassium components are used in the laboratory. However, their potential applications are limited because of their availability and price. NaOH and Na_2SiO_3 were used as activators in this study.

2.5.2. Sodium Hydroxide (NaOH)

Sodium Hydroxide is one of the strongest bases, and it is used widely as a raw material in the chemical industry. It is not flammable and gives off heat when in contact with water. Caustic is a good disinfectant and differs commercially according to its purity [73].

2.5.3. Sodium Silicate (Na_2SiO_3)

Sodium silicate is the general name of the ingredients in the formula $Na_2O.nSiO_2$. Depending on the n coefficient, its properties and usage areas change. NaOH is added to a sodium silicate solution with a high modulus to produce a sodium silicate solution with a lower modulus. For a given modulus and concentration, the adjusted silicate solution can also be expected to have different types related directly to NaOH. A method has been proposed for producing alkali silicate with more than 1 module. In this method, organic solvents mixed with water are used to obtain hydrated silicate after dissolving the aqueous silicate in a solvent. This method allows direct glass water production with optimal modulus and concentration [74].

2.5.4. Dosage of activators

The dosage of the alkali activators can be expressed in various ways, such as molarities of the activator, oxides, or activator weight percentage and oxides molar ratios. According to the type and source of aluminosilicate material used and the type of activation solution, the optimum dosage can differ. Palomo et al. (1999) [60] suggested that the alkali cement's strength can be decreased with the increase of OH^- concentration in the system. For the KOH activator, It is possible to say that the

molarities ranges can be from 5M to 10M for the activation of natural minerals [75]. For the NaOH activator, many studies used it with different molarity ranges getting between 1M to 10M. The results of the studies showed that this amount of molarity could produce a satisfactory strength [15,73]. However, increasing the solutions' molarity can cause a faster setting time and significantly reduce the mix workability, making an adverse and undesirable effect.

2.6. REINFORCEMENT OF ALKALI-ACTIVATED MATERIALS WITH FIBERS

Using fibers as reinforcement for the construction material is not new. Fibers have been used as reinforcement for construction materials since ancient ages. In the past, horsehair has been used in mortar and straw in mud bricks. Fibers are usually used in brittle materials such as concrete to control cracking due to shrinkage. Fibers reduce the permeability of concrete and thus reduce the bleeding of water. Fibers are added to the mix for the long-term durability of the material. Using Polypropylene (PP) fiber for example, can improve the mechanical properties and enhances the durability properties [76]. And steel fibers can be used to retrofitting the reinforced concrete members and increase the durability of it [77]. Using glass fiber with AAMs can reduce the drying shrinkage behavior [26]. Besides, using fibers with construction materials can control electromagnetic waves' risk by absorbing it or reflecting it [34,41]. AAMs show brittle behavior and are susceptible to cracking like ordinary concrete [24]. Thus, using fibers with AAMs will limit this brittle behavior and shrinkage. In this study, PP and steel fibers were used as reinforcement for the AAMs produced in this study.

2.7. ELECTROMAGNETIC SPECTRUM RADIATION, AND WAVES

Electromagnetic Radiation (EMR) is a term that refers to the waves of the Electromagnetic Field (EMF) that is radiating through space and carrying electromagnetic radiant energy [78]. EMF field is the combination of an electric field and a magnetic field. EMR is generated through the moving of photons that carry the energy, and it behaves like waves and particles. The term Electromagnetic Spectrum

(EMS) is a related term to all frequencies of electromagnetic radiation. EMR includes Electromagnetic waves (EMW) of different frequencies. Different names indicate different frequencies since they have different sources and effects on matter. Gamma rays, X-rays, radio waves, infrared, visible light, microwaves, and ultraviolet are examples of different EMW names with different frequencies [78,79]. Electrically charged particles undergoing acceleration emitters the EMWs, and these EMWs could subsequently interact along with other charged particles and exerting force on them. Natural events or electronic devices can produce EMWs.

James Clerk Maxwell, who first unified fundamental electromagnetism laws, developed an Equation for understanding and exploiting EMWs' behavior [80]. Those Equations are mathematical expressions of Faraday's law, Gauss' law, and Ampere's law. According to Maxwell's equations, we can get that in free-space varying electrical field generates changes in magnetic fields or change in the magnetic field constitutes variations in electric fields. These electric and magnetic field variations are perpendicular to each other [81]. Analysis of Maxwell on the speed of variations leads Maxwell to think that EMWs should travel at the known speed of light. This thought was experimented with and strengthened by the studies of Heinrich Hertz. These findings lead to the famous Equation 2.1:

$$c = \lambda f \tag{2.1}$$

Where (c) is the speed of light and it is equal to $3{,}00 \times 10^8$ m/s, (f) is the frequency and (λ) is the wavelength. This formula's application to all frequencies gives the electromagnetic spectrum, which can be seen in Figure 2-6. In this study, the frequency of EMWs examined were from 100 MHz - 6000 MHz. This range were examined because it is the frequency for the most used daily devices like Bluetooth, mobile phones, microwaves, Wi-Fi, and TV. Figure 2-6 shows more weave generators have a frequency range from 100 MHz - 6000 MHz.

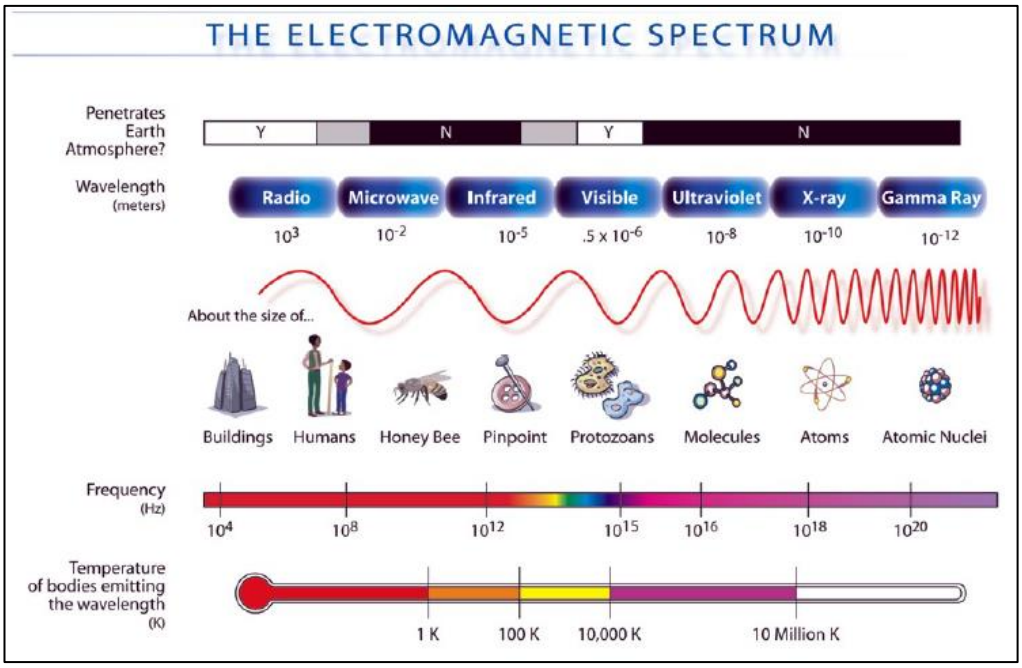

Figure 2.6. Electromagnetic spectrum [82].

In free-space, EMWs carry energy associated with the magnetic field and electric field. Photons carry this energy, and energy (E) of photons can is stated with equation 2.2, where (h) is Planck's constant and it is equal to 6,63 × 10^{-34} J.s.

$$E = hc/\lambda \tag{2.2}$$

This equation proves that EMWs with shorter wavelengths carry higher energy and/or EMWs with lower frequencies have lower energy.

2.8. INTERACTION OF EMWs WITH MATERIALS

The interaction of EMWs with materials is related to their properties. The material's density and structure, humidity and temperature in the surrounding environment, and porosity can change the material's dielectric properties for the microwave frequencies, millimeter-wave, and THz [83]. Also, the chemical composition and the thickness of the material, and electromagnetic interference affect the interaction of EMWs with materials [84]. The material's internal characteristic, which is known as the complex permittivity independent of the measurement technique, is accepted as an essential

value of material characterization for electrical engineering [85]. This characteristic can determine the radiation speed of the EMWs and the amount of stored energy by the material.

During the weave interaction through the material, some of the weaves are reflected, and some are transmitted. Thus, materials and EMWs interaction occur in three ways as absorption, reflection, and transmission [86]. The interaction between EMW and material is described in Figure 2-7 [87].

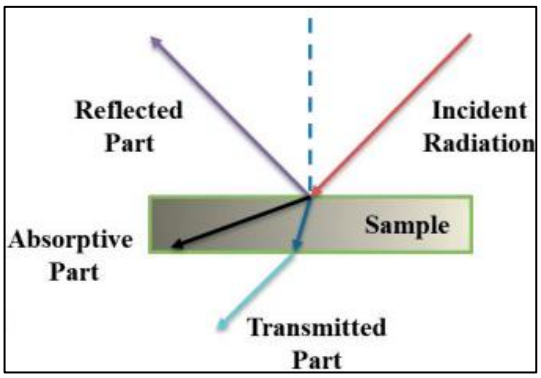

Figure 2.7. Interaction of EMW with material [87].

2.9. SHIELDING EFFECTIVENESS

The Shielding effectiveness (SE) for a material describes the ability of the material to prevent the transmission of EMWs from the outside to the inside or vice versa. SE is a measure of how strong a given material will attenuate EM energy in the form of magnetic and electric fields. The shielding effect of a material can be determined with major factors that affect it, such as the thickness of the material, its conductivity and permeability, and the incident wave frequency. The SE of a material depends on two main concepts: the reflection and absorption of EMWs by the material. Basically, reflection is the ability of a material to reflect the EMWs. EMW reflection can occur at the edge among any two media with wide discrepancies in their electrical or magnetic impedances. However, the skin depth of the material indicates the absorption effect. The skin depth is the penetration depth at which the strength of the field will

have decayed to 1/e of the surface current density. The SE parameter can be calculated with the Equation 2.3 below [88]:

$$SE = 20\log_{10}\left|\frac{H_i}{H_t}\right| \tag{2.3}$$

Where (Hi) is the electric and magnetic field's intensity at any point in the space where there are no shielding materials, (Ht) is the electric and magnetic field's intensity where there are shielding materials in the same place.

According to the shielding theory of Schelkunoff, for a shielding plate when it is infinite, and the direction of the incident wave is vertical, SE is equal to [89]:

$$SE = SE_A + SE_R + SE_M \tag{2.4}$$

Where SE_A is the absorption loss, SE_R is the reflection loss, and SE_M is the repetitious absorption loss. And the unit of SE will be in (dB). Figure 2-8 shows illustration of EMW's behavior inside and outside of shielding materials.

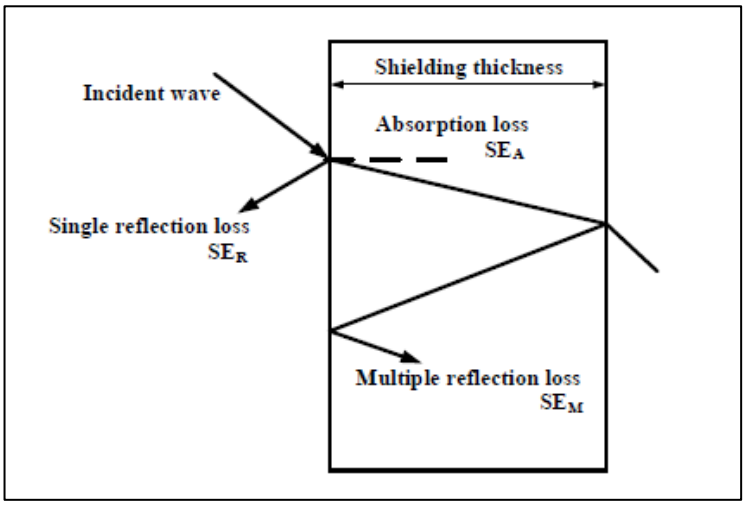

Figure 2.8. EMWs behavior inside and outside of shielding materials.

2.10. BENEFITS AND HAZARDS OF ELECTROMAGNETIC WAVES

EMWs have many benefits to humankind due to their applicability in many fields in our life. EMWs are applicable and compatible with many instruments and devices in our life nowadays. TV, cell phones, microwaves, and FM towers are all working with the help of EMWs, and they yield benefits to humanity. Though, those benefits came with some consequences. For example, using mobile phones could lead to some health hazards such as fatigue, dizziness, headache, tension, and sleep disturbance [90,91]. Besides, people living near antennas were suffering from a high risk of diseases such as: depression, hearing problems, irritability, visual disruptions, cardiovascular problems, and skin diseases [92]. Taye et al. [93] reported that there are some adverse effects of EMWs on honeybee colonies near the cell phone towers. Hocking et al. [94] reported that leukemia, tumors, and cancer were more in the people residing near to FM towers. In contrast, those living far away from the towers found fewer chances of diseases. Besides, he found that the children were more affected by leukemia's severe effects and tumors rather than adults living in the same spaces. Other effects of EMWs as reported from S. Batool et al. [95] study can include:

1) Effect on mammals and amphibians.
2) Effect on honeybees.
3) Effect on plants.
4) Effect on birds.
5) Effect on biotic systems.

2.11. EXTENSIVE LITERATURE REVIEW

Vlasceanu et al. (2020) [96] has developed new geopolymer composites with dielectric properties specially designed for radar antennas applications. For this, they examined in this study different mixtures based on two alkaline solutions and three metakaolin. The magnetite effect was studied by adding 1, 5, or 10 wt% of Fe_3O_4 in different mixtures. In addition, the effect of humidity is also highlighted. Dielectric investigations have been carried out between 2 and 3.3 GHz. The results showed that the metakaolin type does not affect dielectric properties, while the alkaline activation

solution's nature has a significant effect. The change in alkaline solution leaders to an increase in the permeability from 3.5 to 5.9. Increasing magnetite percentage up to 10% had a small influence on the polycondensation reaction and caused a slight increase in permittivity and permeability values.

Han-Seung Lee (2020) [97] investigated the effects of electromagnetic shielding performance on concrete with different thicknesses, concrete with adding 1 and 5 wt% carbon black, and 100 Micrometer thick Zn–Al metallic coating. The range of frequencies examined was between 0.85 to 1 GHz. The results showed that the maximum shielding value was 41.60 dB before the cutting with Zn–Al metallic coating. And after adding the Zn–Al metallic coating, the value increased approximately by 48 dB and reached 89.75 dB.

Dirikolu (2019) [71] produced alkali-activated pastes using tuffs from Bayburt/Turkey and marble waste and activated these binders with $NaOH+Na_2SiO_3$ or $Ca(OH)_2+Na_2SiO_3$ in specific ratios. Tests such as flexural and compressive strength, unit weight, and water absorption were performed. The results showed that the highest compressive strength was obtained as 19,7 MPa at 90 days of sample production from the group which produced with 100% White Tuff (WT) and activated with $Ca(OH)_2+Na_2SiO_3$. And the highest compressive strength was obtained as 37,8 MPa at 90 days of sample production from the group which produced with 100% Green Tuff (GT) and activated with $Ca(OH)_2+Na_2SiO_3$.

Manoj and Baboo (2019) [98] studied the effect of reinforcing the fly ash-based geopolymer concrete with polypropylene fiber. The length of the fiber used in this study was 12mm with a diameter of 0.032mm. The fiber was added to the mixes in seven weight fractions as (0.1%, 0.15%, 0.2%, 0.25%, 0.3%, 0.4% and 0.5%) by volume of concrete. The powdered materials were activated by a solution of 14M. This solution was produced with a combination of sodium hydroxide solution mixed with sodium silicate solution. The results showed that the incorporation of Polypropylene fiber to geopolymer concrete changes the failure pattern from brittle mode to ductile. Besides, the results showed that with the fiber reinforcement, the capillary porosity of hardened concrete could be reduced leading to increase the durability of the concrete.

Ding and Bai (2018) [99] investigated the fracture properties of steel fiber-reinforced slag-based geopolymer concrete/mortar (SGC/SGM). Steel fiber with a length of 13mm and a diameter of 212 μm was used in this study. And this fiber was added to the mixes by (1.0, 1.5, and 2.0%) volume of the fraction. The alkali activator liquid used was a combination of sodium silicate solution and sodium hydroxide. The water content and the mole ratio of SiO2 to Na2O of the sodium silicate solution were 59% (by mass) and 3.7, respectively. The results showed that the splitting tensile strength, fracture energy, and fracture toughness are significantly enhanced with fiber incorporation. The improvements of the strengths increase with the fiber volume contents for SGM, while SGC has an optimal fiber volume content of 1.5%. thus, the optimum fiber content differs from each mix type.

Ekinci (2017) [100] prepared geopolymer concretes with volcanic tuff procured from the Nevşehir region. Geopolymer concretes were produced in two different groups. The first group was activated by using the silica module 0.8 and 0.6, the second group using 10, 12, 14, and 16 M NaOH. Different curing temperatures and alkali/binder ratios were used. The effects of different proportions of nano-silica, micro silica, and styrene-butadiene latex additives on concretes giving the highest strength in both groups were investigated. The experimental results revealed that geopolymer concretes activated by using NaOH have higher compressive strength values than concretes activated using silica. SEM analysis and water absorption experiment results showed that micro silica's addition helped to form a compact structure.

Koppel et al. (2017) [101] examined the reflection and transmission properties of multiple types of construction materials at 2.4 GHz frequency. Two high-performance concrete plates with thickness of 13mm and densities of 1.975 g/cm^3 (round shape plate) and 2.093 g/cm^3 (panel shape) were two of the materials that were tested in this study. The water/cement ratios of the mixes were 0.2. The results showed that the least transmission was measured in the high-performance concrete plate (panel shape) where 34% and 35% of the wave were reflected. And for the round shape plate, the transmission was 71%, and 38% of the wave was reflected.

Bowen Guan et al. (2017) [102] investigated the effect of the utilization of natural magnetite in cement on the electromagnetic wave absorbing characteristic of the material. Cement (commercial name Poland cement, type 42.5 R), deionized water, and natural magnetite (Fe3O4) were utilized in this study. The materials were examined with a wave frequency range of 2.6–3.95 GHz. the results showed that the composites made with 15% magnetite had the best absorbing amount. The ultimate absorbing with a reflection loss of −28 dB at 3.7 GHz, and its absorbing bandwidth (<−10 dB) reaches 0.8 GHz.

Chi1 et al. (2017) [103] made a study to examine the effect of the drying shrinkage of the alkali-activated binder. Various contents and modulus ratios of alkali activators were produced to study their effect on the strength development and drying shrinkage of alkali-activated slag pastes. The results showed that the alkali-modulus ratio is the key factor influencing pH amount and drying shrinkage. The lower the alkali-modulus ratio is, led to a greater pH amount and leading to lower the drying shrinkage. Besides, they observed that increasing the amount of alkali-activators decreases the initial and final setting times. The maximum shrinkage at 28 days of production they found in their study was 0.765% and the minimum was 0.238%.

Navid Ranjbar et al. (2016) [104] made a study aimed to evaluate the short and long-term impacts of PP fiber reinforcement on fly ash-based geopolymer composites. PP fiber was added to the geopolymer paste in percentages of (0.5, 1, 2, 3, 4, and 5%) by fraction of volume. Sodium silicate (1.5gr water per milliliter at 20°C with a modulus ratio of 2.5) and sodium hydroxide in combination were used as activator solution solutions. Multiple physical and mechanical properties were applied to the fresh and hardened pastes. The results showed that the workability of the composites is reduced significantly by increasing the percentages of fiber. And the shrinkage could be controlled by increasing the fiber percentage. And the best percentage for controlling the shrinkage was 3%. Besides, they observed that the mechanical properties of the composites are governed by the strength development of the geopolymer matrix, and the strength of the composites without PP fiber was increased over time.

Lee et al. (2016) [105] made a study aimed to examine the electromagnetic shielding effectiveness of polypropylene/conductive (stainless steel) fiber composites. The stainless-steel fiber was added to the PP fiber at three percentages as 5wt%, 10wt%, and 20wt%. The thickness of the samples was about 2mm. The results showed that the maximum SF was provided from the composite with 20wt% stainless steel, and the SF was 43 dB.

Marlene A. Jenifer et al. (2015) [106] conducted an experimental study Amid to examine the impact of steel fibers' addition on split tensile strength, flexural strength, compression, and bond strength of hardened geopolymer concrete. They used in their mix Crimped stainless and crimped mild steel fibers of aspect ratio 60 with a volume fraction of 0.75%. From the results of their experiment, they observed that the addition of fibers in the mix leads to reduces crack propagation in geopolymer concrete and reaches a higher peak value. Besides, they observed that the fracture energy increase for geopolymer concrete as the compressive strength increased. The maximum compressive, tensile, and flexural strength they get was 51.78, 5.17, and 5.03 respectively.

A. Suriya Prakash et al. (2015) [107] conducted an experimental study aimed to examine the compressive strength, split tensile strength, and flexural strength of steel fiber-reinforced geopolymer concrete. Steel fibers were added to the mix in 0.5%, 1.0%, and 1.5% by volume fractions of concrete. The results obtained that the optimum percentage of steel fiber for their mix was 1%. And they found that adding 1% of steel fiber to the mix will increase the compressive and splitting tensile strength by 5% compared to conventional concrete.

Iqbal et al. (2015) [108] made a study aimed to investigate the effect adding micro steel fiber in different percentages to the properties of high strength steel fiber reinforced lightweight self-compacting Concrete (HSLSCC). The micro steel fiber content used was 0.5%, 0.75%. 1% and 1.25% volume fraction. The results showed that the splitting tensile strength increased around 18% with increase of steel fiber content by 0.75%. However, compressive strength tends to slightly decrease. It was

observed that there was 7% decrease in compressive strength with increase of steel fiber content from 0.5% to 1.25%.

Xingjun et al. (2015) [109] made an investigation aimed to examine the electromagnetic wave absorption properties and related mechanisms of foam concrete. Three samples of foam concrete with different thickness was made to examine the absorption properties. The dimensions of the samples were a size of 200×200 mm with a thickness of 10, 20, and 30 mm. the samples had 5 different filling ratios as 42.3 vol.%, 46.7 vol.%, 52.1 vol.%, and 62.4 vol.%. The results showed that the absorption property has a direct relation with the thickness and filling ratio of the sample. When the filling ratio is 52.1 vol.%, the peak reflectivity value reaches -20.6 dB at 5.5 GHz, and the bandwidth in which the reflection loss <-10 dB reaches as high as 10.7 GHz.
Fareed Ahmed Memon et al. (2011) [110] made an experimental study to examine the curing conditions effects on the compressive strength of self-compacting geopolymer concrete prepared by using fly ash in the mix as base material and a combination of sodium silicate plus sodium hydroxide as an alkaline activator. The results showed that the compressive strength of hardened concrete was significantly affected by curing time and curing temperature. Longer curing time leads to higher compressive strength. Besides, they observed that the highest compressive strength when the specimens were cured for a period of 96 hours; though, after 48 hours, the increase in strength was not significant. They found the highest compressive strength after 28 days of production, and it was approximately 54 MPa. Also, they observed that the increase in curing temperature from 60°C to 70°C leads to an increase in concrete strength. The compressive strength of self-compacting geopolymer concrete decreased when the curing temperature is exceeding 70°C.

Aire et al. (2011) [111] made a study aimed to evaluate the effectiveness of the PP fibers incorporation to concrete in controlling the plastic shrinkage and cracking. PP fibers were added to the mixes by (0, 0.1, 0.3, and 0.5%) fraction of volume. In addition to the plastic shrinkage test, slump and compressive strength tests were applied. From the results, it was observed that the addition of fibers decreased slightly slump values. However, the effect of fibers addition on unit weight and air content of concrete was negligible. Besides, the results showed that PP fibers reduced the extent of shrinkage

cracking, the number of cracks, and maximum crack widths. And by adding the lowest percentage of PP fiber in this study (0.1%) to the mixes, an average crack reduction of 60% was achieved.

Dai et al. (2009) [112] investigated the effects of curing time, the proportion of steel slag, and the sample thickness on radar absorbing properties in the frequency of 1–18 GHz. The results showed that the composites' absorption peak did not change at various proportions of steel slag and curing times. However, it changes to a lower frequency with the increase of thickness. They found that, with increasing thickness of the composite, absorption decreases from 23 dB to 7.5 dB in 1-8 GHz; but in 8-18 GHz, absorption first increases gradually to the maximum after those decreases.

Wen and Chung (2004) [34] examined the shielding effectiveness of steel fiber reinforced cement paste and mortar. The fiber was a stainless-steel fiber with diameter was 8 μm with 6 mm length. The cement used was Portland cement (Type I). And the water/cement ratio was equal to 0.40 for the pastes and mortars. From the results, they obtained maximum shielding effectiveness of 70 dB at 1.5 GHz in cement paste that contains 0.72 vol.% stainless steel fiber.

Cao and Chung (2004) [113] made a study aimed to examine the effect of using the fly ash in cement pastes as an admixture on the electromagnetic shielding effectiveness. Portland cement (Type I) was used to produce the paste. Fly ash (Class F) was added to the cement pastes as a replacement for the cement by 5 percentages as 0:100, 15:85, 50:50, 85:15, and 100:0. And the water/powdered ratio was 0.35. The results showed that the shielding effectiveness from 4 to 8 dB at 1 GHz was observed by adding the fly ash to the pastes. In addition, they noted that Fe_2O_3 in the fly ash had the contribution to increase the shielding effect.

Puertas et al. (2003) [114] made a study on the effect of addition of PP fiber on geopolymer concrete. In their study, different types of source materials such as slag, fly ash and slag/fly ash combination were used. The PP fiber was added to the mixes by percentages of 0.5% and 1% by volume of mortar. The results showed that the addition of 0.5% and 1% PP fiber did not affect the compressive strength of slag based

geopolymer concrete at 2- and 28-day. Though, in fly ash based geopolymer concrete the 2-day compressive strength was increased due to increase of PP fiber contents but a slight reduction was observed at 28 days in the same composite. In the case of combined slag/fly ash based geopolymer concrete, insignificant increase in compressive strength was noticed by increasing the PP fibers from 0.5% to 1.0% at both ages.

PART 3

MATERIALS AND METHODS

3.1. MATERIALS

3.1.1. Natural Tuffs

Natural Tuffs are used in this study as the main material that will be activated to produce the AAPs. Natural Tuffs are collected from the Bayburt region in Turkey and named as Bayburt Stone. Tuffs are among the industrial raw material resources widely used in that region. Its easy processing and lightness are frequently used as a building stone, especially in historical monument repair and mosque construction.

Tuffs are mostly yellowish-cream and cream in color. However, in some places, they are quite fractured and disintegrated. In some places, the tuff was completely green due to zeolitization and chloritization. Secondary small pore appearances have emerged in the fine-grained tuffs due to the chlorite mineral's washing due to precipitation and the alteration of the chlorite mineral [115]. There are three types of tuffs in the Bayburt region white, yellow, and green tuffs. White Tuff (WT) and Green Tuff (GT) were used in the study.

3.1.1.1. White Tuff (WT)

White Tuff (WT) has dacitic composition vitric tuff, and there is a matrix of volcanic material in the rock and quartz, plagioclase, biotite, and rock fragments in the matrix [116]. In the analyzes carried out in the mineralogy and petrography laboratory of the General Directorate of Mineral Research and Exploration, WT has a porphyritic texture, composed of alkali feldspar, quartz, zeolite, and opaque minerals, and has a

zeolite form clinoptilolite and heulandite-like structures. This stone has a yellowish gray fine-textured and named zeolitic tuff. Figure 3-1 shows the WT after griding.

Figure 3.1. White tuff.

Chemical properties of WT are given in Table 3-1, physical and mechanical properties are given in Table 3-2, and XRD analysis of WT is given in Figure 3-2.

Table 3.1. Chemical composition of WT, GT, and Calcite.

Oxides	**WT**	**GT**	**Calcite**
SiO_2	68.92	49.92	<0.1
Al_2O_3	11.96	10.25	-
Fe_2O_3	0.34	6.00	<0.005
CaO	3.85	13.10	95-99
MgO	1.29	2.57	<0.2
SO_3	0.21	0.26	-
Na_2O	0.23	1.45	-
K_2O	2.38	1.82	-
Total Alkali	1.8	2.65	-
Total	99.31	99.41	99.21
K.K.	10.13	14.04	-

According to the XRD analysis in Figure 3-2, quartz and feldspar minerals were observed as fractured and angular in places in the highly amorphous and rich zeolite mineral paste. Flow texture and volcanic glassy parts were also seen in the structure in thin sections. Intense quartz and zeolite minerals are also seen in the SEM images shown in Figure 3-3.

Table 3.2. Physical Properties of WT and GT.

Property	WT	GT
Specific gravity (as a stone block)	2.37	2.74
Hardness (Mohs)	4-5	3-4
Apparent porosity (%)	20.6	13.3
Compressive strength (MPa)	44.1	96.8
Impact strength (MPa)	0.8	3.7
Flexural strength (MPa)	12.3	22.9
Average Abrasion Resistance (cm3/50cm2)	25	26.4

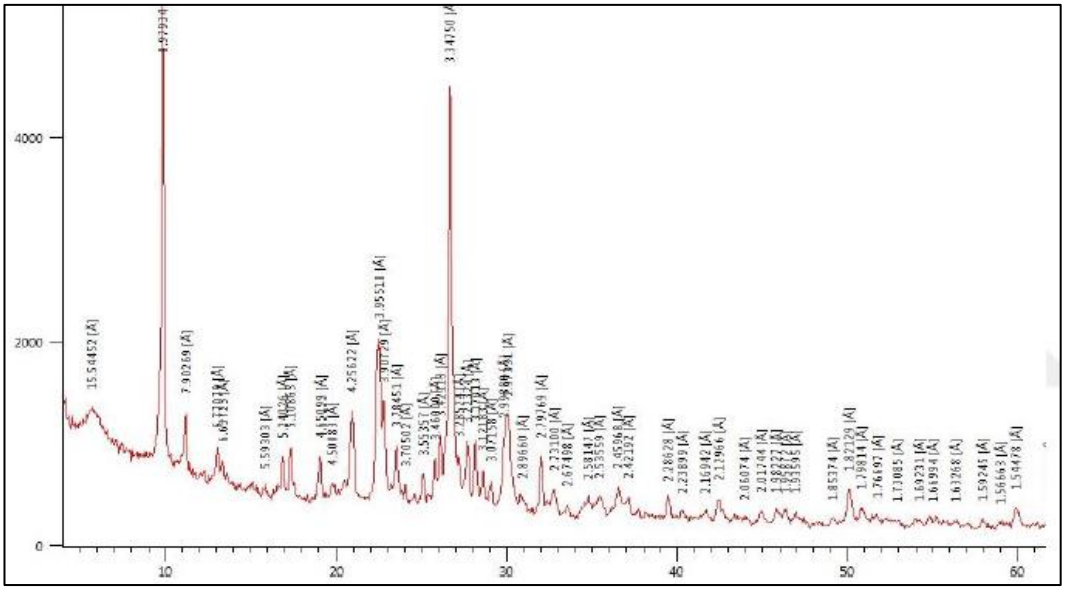

Figure 3.2. XRD analysis of WT [71].

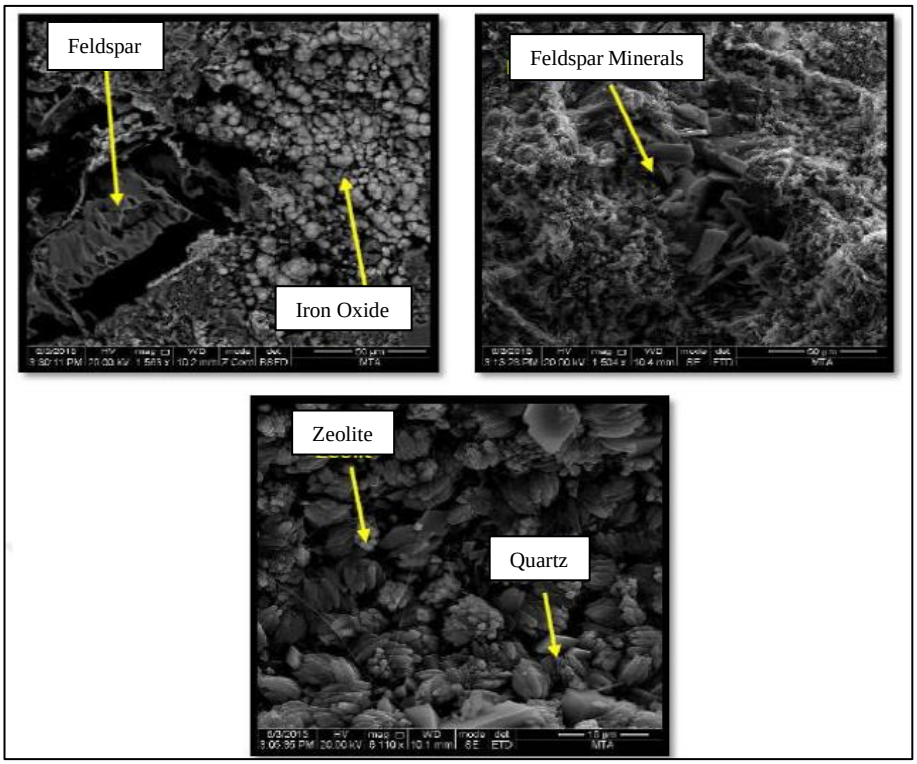

Figure 3.3. SEM images of WT [71].

3.1.1.2. Green Tuff (GT)

Green Tuff (GT) tensile and compressive strength values are different from WT. GT is a rhyolitic tuff and there is a matrix of volcanic materials in the rock, quartz, plagioclase, trass, and chloritized biotite minerals in this matrix [117]. GT density is low, and its water absorption rate is high. The abrasion and bending resistance is considered better than the other tuff types from the Bayburt region [116]. Figure 3-4 shows the GT after griding. Chemical properties of GT are given in Table 3-1, physical and mechanical properties are given in Table 3-2 and mineralogical properties are given in Figure 3-5.

Figure 3.4 Green tuff.

According to the analyzes performed on GT in the mineralogy and petrography laboratory of the General Directorate of Mineral Research and Exploration: GT has a grayish-green color and fine-grained macroscopic structure. GT texture is porphyritic and contains quartz, biotite, plagioclase, opaque minerals, zeolite, and alkaline feldspar. In typical tuff textured rock, dispersed phenocrysts are observed in the paste. The paste is almost entirely composed of zeolite crystals and biotite minerals have been observed in inflow textures.

According to the XRD analysis given in Figure 3-5, intense zeolite, quartz, mica group, and feldspar minerals were seen. This information is supported by the SEM images given in Figure 3-6.

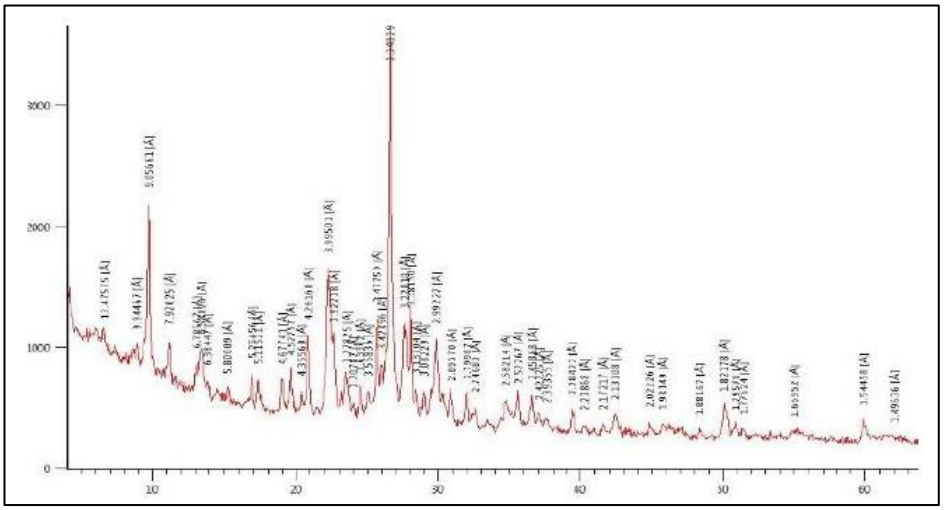

Figure 3.5. XRD analysis of GT [71].

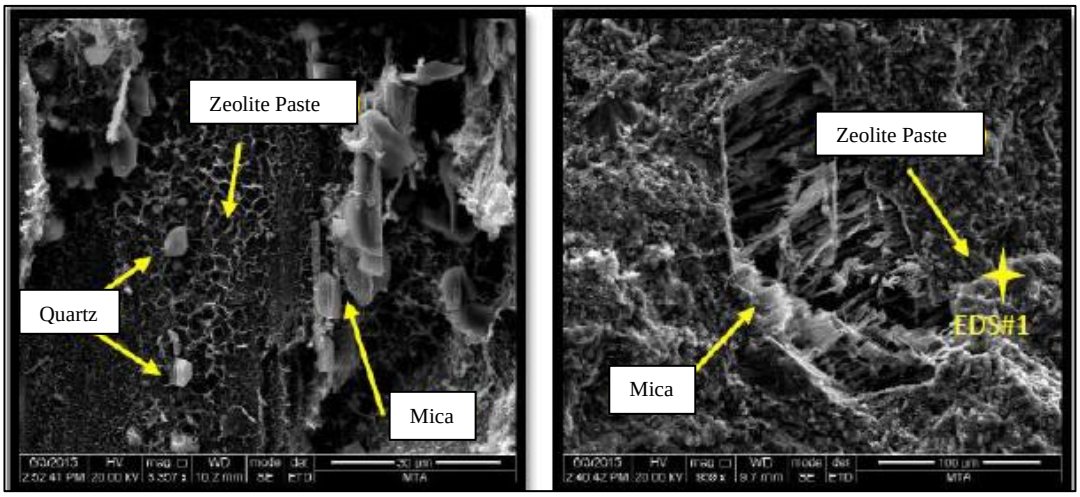

Figure 3.6. SEM images of GT [71].

3.1.1.3. Bayburt Tuff Supply and Grinding

In this study, volcanic tuff in powder forms were used as aluminosilicate sources to produce the AAMs. Two types of volcanic tuff Wastes (WT and GT) collected from the Bayburt region in Turkey were used. Laboratory crusher used to crush the WT and GT and reduce the particle diameter to approximately Dmax: 20 mm. Then, each of these materials was groundied to be D90: 100 microns in a horizontal axis ball mill. The grain distribution and specific surface analyses were carried out using Mastersizer 3000 (Malvern) particle size analyzer. Specific surface, specific gravity, and the fineness of the materials are given in Table 3-3.

Table 3.3. Specific gravity and Specific surface data of WT, GT, and Calcite.

Raw materials	**Specific gravity (g/cm^3)**	**Specific surface area (cm^2/g)**	**Fineness (Sieve analysis µm)**		
			D_{90}	**D_{50}**	**D_{10}**
WT	2.43	11237	61.3	16.6	3.94
GT	2.61	8420	83.0	26.4	9.82
Calcite	2.71	2645	100	35	3.5

3.1.2. Calcite

Calcite is in carbonate rocks and the most stable polymorph of calcium carbonate ($CaCO_3$). It has different crystallized structures (rhomboid, scalenohedral) and colorless transparent. It is easy to grind, and the powder form is white in color. Its hardness is 3 according to the Mohs scale, and its density is around 2.6-2.7. Chemical properties of calcite are given in Table 3-1.

3.1.3. Water and Activators

Tap water was used in this study. NaOH with at least 99.9% purity was used in solid form. The liquid form of Na_2SiO_3 was used in this study. The chemical and physical properties of Na_2SiO_3 are given in Table 3-4.

Table 3.4. The chemical and physical properties of Na_2SiO_3.

Property	**Amount**
Density (g / cm^3)	1.396 – 1.418
Na2O (wt%)	11.3 – 12.9
SiO2 (wt%)	22.6 – 25.8
Module (SiO_2/ Na_2O)	1/2

3.1.4. Polypropylene and Steel Fibers

Polypropylene (PP) and Steel fibers were used in this study with the technical properties that are shown in Table 3-5. Figure 3-7a shows the PP fibers used in this study and Figure 3-7b shows the steel fibers.

Table 3.5. Technical properties of polypropylene and steel fiber.

Properties	**Polypropylene**	**Steel**
Tensile strength (MPa)	350	3000
Modulus of elasticity (GPa)	3,5	200
Softening temperature (°C)	140	1083
Specific gravity (g/cm^3)	0,81	7.87
Fiber diameter (micron)	300	150
Fiber length (mm)	12	6
Slenderness (length/diameter)	12	87
Electrical conductivity (ohm-cm)	-	100%

Figure 3.7. a) Polypropylene fibers and b) Steel fibers.

3.2. TEST PROCEDURES

This section is divided into two parts. The first part describes the flow table test procedure for fresh state AAPs and the second part describes the hardened reinforced AAPs tests' procedure; mainly, flexural and compressive strength tests, water absorption test, shrinkage test, and electromagnetic properties examination.

3.2.1. Flow Table Test Procedure for Fresh State AAPs

Workability was measured by using flow table equipment shown in Figure 3-8. The flow table was hand-driven linked with a rounded table of 252 mm diameter. And a rounded mould with 61 mm inner top diameter, 95 mm inner bottom diameter, and 50 mm height. Table and mould are both made of brass.

Flow table test was performed according to ASTM C1437 standards [118]. Flow table test was conducted on fresh pastes taken from the mixer for all experimental batches prepared in this study. This test was conducted by pouring the paste into the mould until it totally filled to the top of the it. After that, the mould is removed, and the paste starts to spread at the same time 25 blows within 15s are applied to the table by the

equipment's hand. After that, the spreading diameter is measured from 4 sides, and the average value is taken as the spreading value, as shown in Figure 3-8a-b.

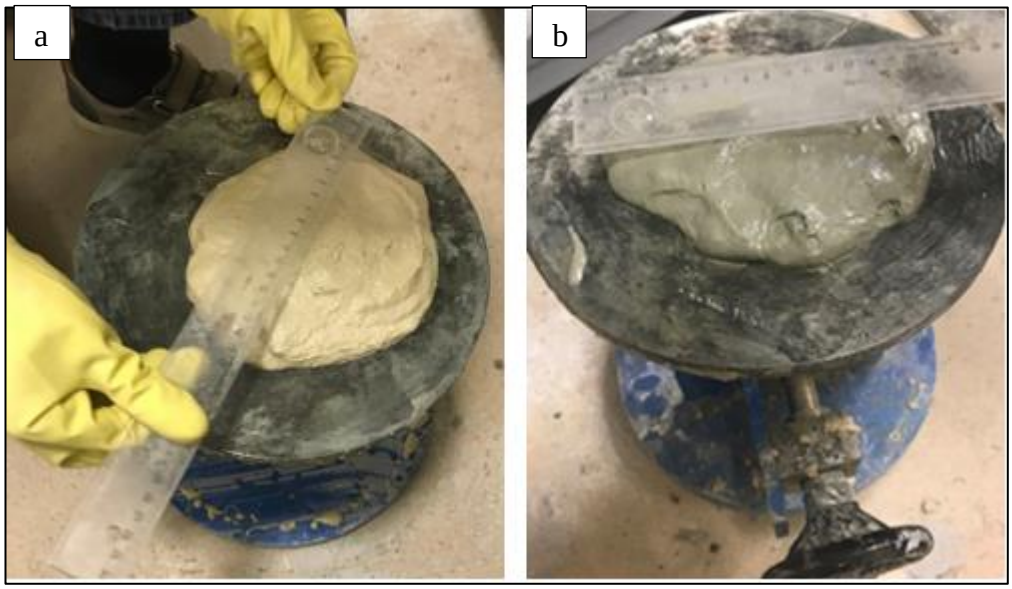

Figure 3.8. a) Measuring the spreading diameter of an AAP made with WT. b) Measuring the spreading diameter of an AAP made with GT.

3.2.2. Hardened reinforced AAPs Tests

3.2.2.1. Flexural and Compressive Strength Tests

Flexure Strength (FS) test was conducted on samples with the dimension of 40×40×160 mm according to ASTM C348-18 [119]. Axial compression test was performed on 40mm cube samples (the two cubes left after preforming the flexural strength test on the sample) according to ASTM C109/109M-16a [120]. Figure 3-9a shows sample during compressive strength (CS) test and Figure 3-9a shows sample during FS test.

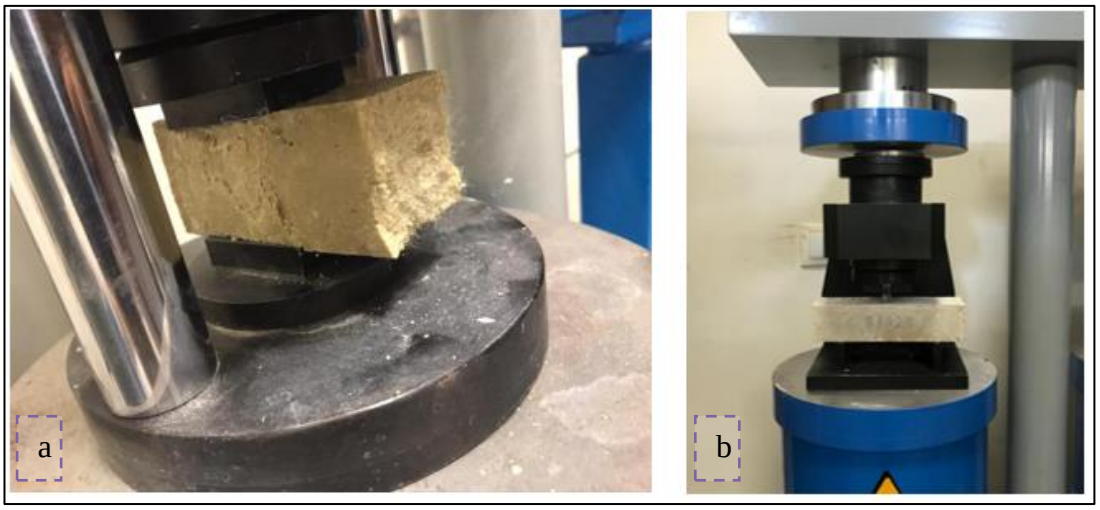

Figure 3.9. Compressive and Flexural Strength tests.

First, the samples were weighed to calculate the unit weight (UW). Then the FS test was performed. At the end of the test, two cubes are left, and the CS test was performed on them. Experiments were carried out on the samples after 2, 28, 90, 180 days of production. Each sample gives 1 FS result and 2 CS results, and the average of the compressive strength results was taken.

The FS of the samples was found by Equation (3.1) and the CS by Equation (3.2).

$$\sigma e = \frac{3PL}{2b\,d^2} \tag{3.1}$$

$$fc = \frac{P}{A_C} \tag{3.2}$$

Where:

$\boldsymbol{\sigma e}$: Flexural strength.
L: Distance between the two carrying pointes of the sample.
b: Cross-section short side length.
d: Cross-section long side length
$\boldsymbol{fc}$: Compressive strength.
P: The ultimate load read at the moment of breaking the sample.
$\mathbf{A_c}$: Surface area of the sample exposed to the applied load.

3.2.2.2. Water Absorption Test

Dry density, water absorption, and apparent porosity of the samples were measured according to the Archimedes method in code, ASTM C20 [121]. Tests were performed for all series after 28 and 90 days of production.

Water absorption test equipment consists mainly of weight balance and oven. The samples taken from the curing conditions were submerged by water for 24 hours as shown in Figure 3-10a. After 24 hours, the samples were taken from the water and the surface was dried with a towel Figure 3-10b, then the saturated dry surface (M_1) and their weight in water (M_2) were weighed. Figure 3-10d and Figure 3-10e illustrate the measuring of the sample weight with a dry surface and inside the water. After that, the samples were kept in the oven for another 24 hours in a 100 ±5 $°C$ as shown in Figure 3-10f and its dry weight (M_0) was measured after taking it from the oven Figure 3-10g. Water absorption ratio, specific gravity, and the apparent porosity were calculated with Equation (3.3), Equation (3.4), and Equation (3.5) respectively. Figure 3-10c shows water absorption test equipment's. After taking the samples from the oven, flexural and compressive strength tests were done on the samples.

$$W(\%) = \frac{M_1 - M_0}{M_0} \text{ x } 100 \tag{3.3}$$

$$\delta = \frac{M_0}{M_0 - M_2} \tag{3.4}$$

$$Pg = \frac{W * M_0}{M_1 - M_2} \tag{3.5}$$

Where,

W: Water absorption rate.
Pg: Apparent porosity.
δ: Specific gravity.
M_0: Dry weight (after taking the sample out of the oven).
M_1: Water-saturated dry surface weight.
M_2: Weight in water.

Figure 3.10. Water absorption test.

3.2.2.3. Shrinkage Test

The shrinkage test was conducted on samples with the dimension of 40×40×160 mm according to ASTM C596 – 18 [122]. Shrinkage Measuring Device equipment used in this study is shown in Figure 3-11.

The shrinkage test has been done several times for each batch within 180 days of samples' production. The test is divided into two steps. The first step is taking the sample's length (Ls) after the demoulding with the digital caliper shown in Figure 3-11a (this step is done for one time after the demoulding). The second step is done on

every test day. It starts with placing the stainless-steel reference shown in Figure 3-11b in the shrinkage device and rotate it carefully to ensure it is placed appropriately as shown in Figure 3-11c. After that, the reading is taken from the digital watch on the device as the reference length (Lr). After that, one sample is placed in the device as shown in Figure 3-11d, and the same procedure done to the reference is applied, and the length of the sample is taken (Ls1).

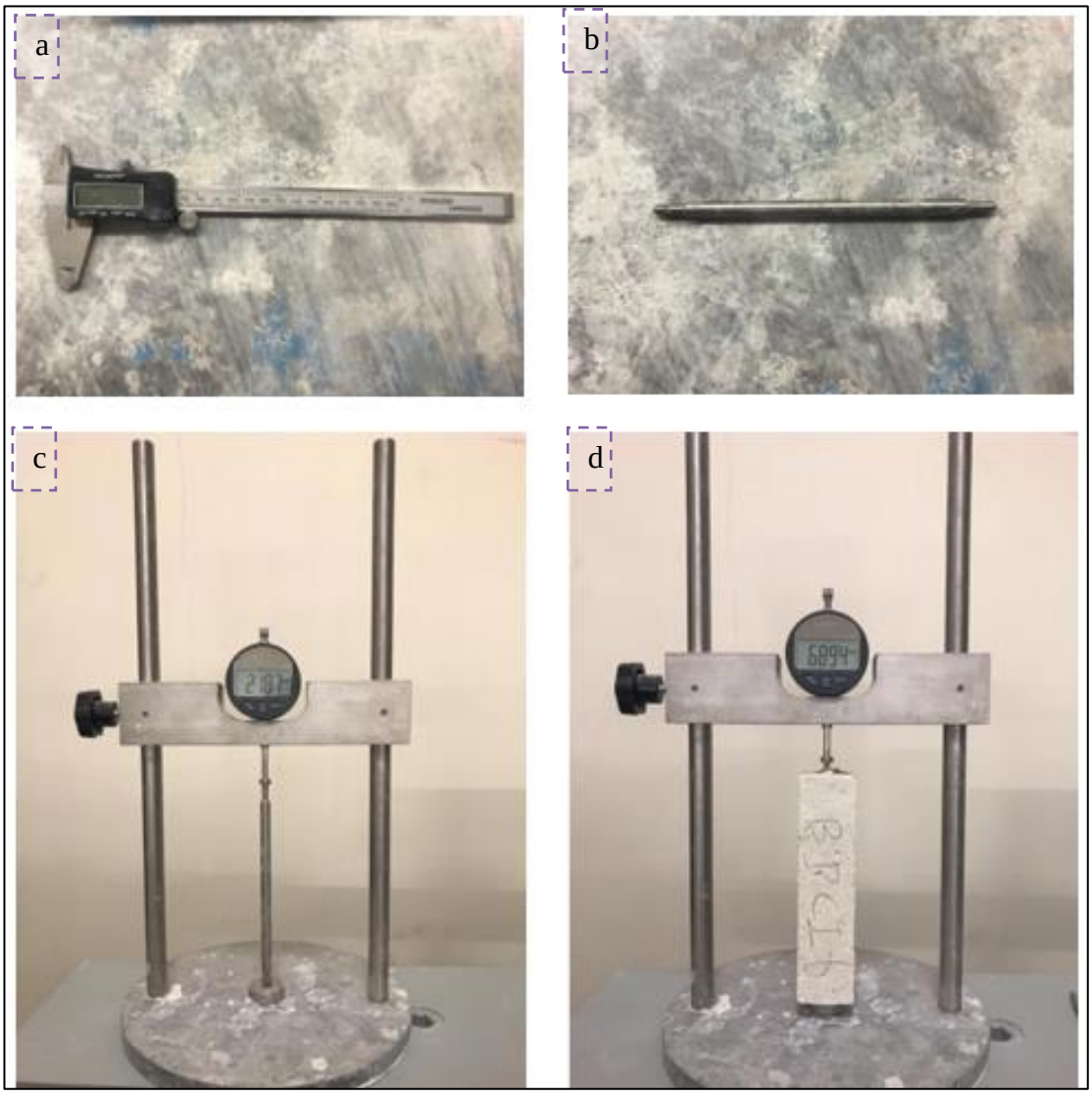

Figure 3.11. Shrinkage measuring device equipment.

The shrinkage is found by dividing the difference between two sample lengths taken from the shrinkage device divided by the sample length taken by the digital caliper

after demoulding. After that, a calibration is done by calculating the difference between two references readings as shown in Equation (3.6).

$$\text{Shrinkage } (\%) = \frac{((Ls1-Ls2)-(Lr1-Lr2))*100}{Ls} \quad (3.6)$$

Where,

Ls: is the sample length measure by the digital caliper.
Ls1: is the first reading took for the sample by the shrinkage device.
Ls2: is the reading took for the sample by the shrinkage device at different testing days.
Lr1: is the first reading took for the reference by the shrinkage device.
Lr1: is the reading took for the reference by the shrinkage device at different testing days.

3.2.2.4. Electromagnetic Properties Examination

The electromagnetic examination was carried out on tiles with average dimensions of 300x300x10 mm produced specially for each batch. For the determination of the materials' electromagnetic properties, the same installation of equipment shown in Figure 3-12 has been applied and the procedure of the examination is described in the next section. However, this procedure is done inside a $1m^3$ detached non-reflective room (Faraday cage) to ensure more accurate results.

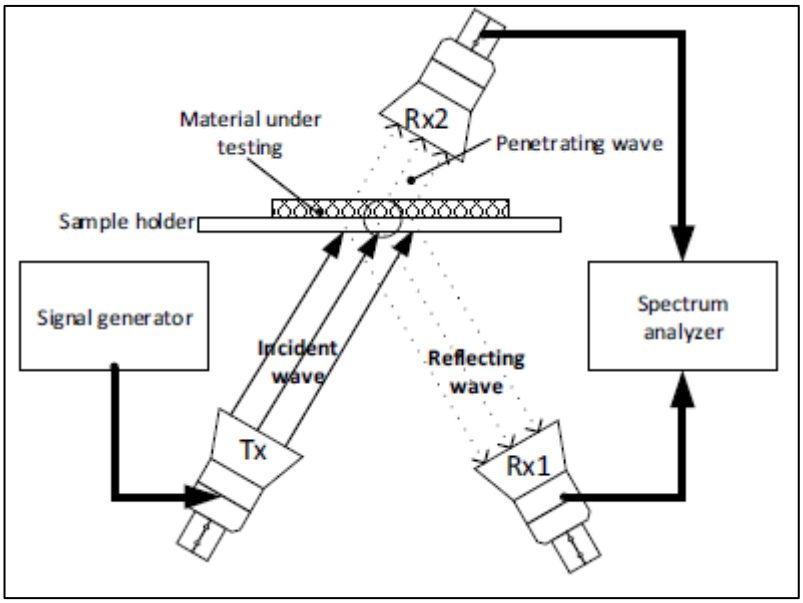

Figure 3.12. Electromagnetic Properties Examination [101].

The equipment and software used in this study are shown in Figure 3-15, and they are including:

- DFG 4060 RF wave generator (wave generator).
- Two spectrum analyzer type HF 60105 spectrum analyzer (spectrum analyzer).
- Faraday cage.
- Laptop.
- MCS Spectrum Analyzer software.

3.2.2.4.1. Examination Procedure

For examining the electromagnetic properties, DFG 4060 RF wave generator (wave generator) and spectrum HF 60105 spectrum analyzer (spectrum analyzer) were used in the measurements. The frequency range of the spectrum analyzer is between 900 MHz and 9.4 GHz. The measurement frequencies range applied for the samples were from 900 MHz to 6 GHz. The wave generator and the two spectrum analyzer's antennas are directional antennas and they installed inside the Faraday cage as shown in the Figure below. The wave generator, on the other hand, was connected to the

computer with a USB cable. First, the wave generator is installed on one side of the sample. Then, one spectrum analyzer installed from one side of the sample to receive the absorbed wave inside the sample after the weave generation. The other spectrum analyzer is installed from the opposite side of the sample to receive the reflected wave from the sample after the weave generation. The collected data are presented on the laptop by the MCS real-time spectrum analyzer software in the dB unit. Electromagnetic absorption and reflection features were measured after 90 days of production. The installation of the equipment used is described in Figure 3-13.

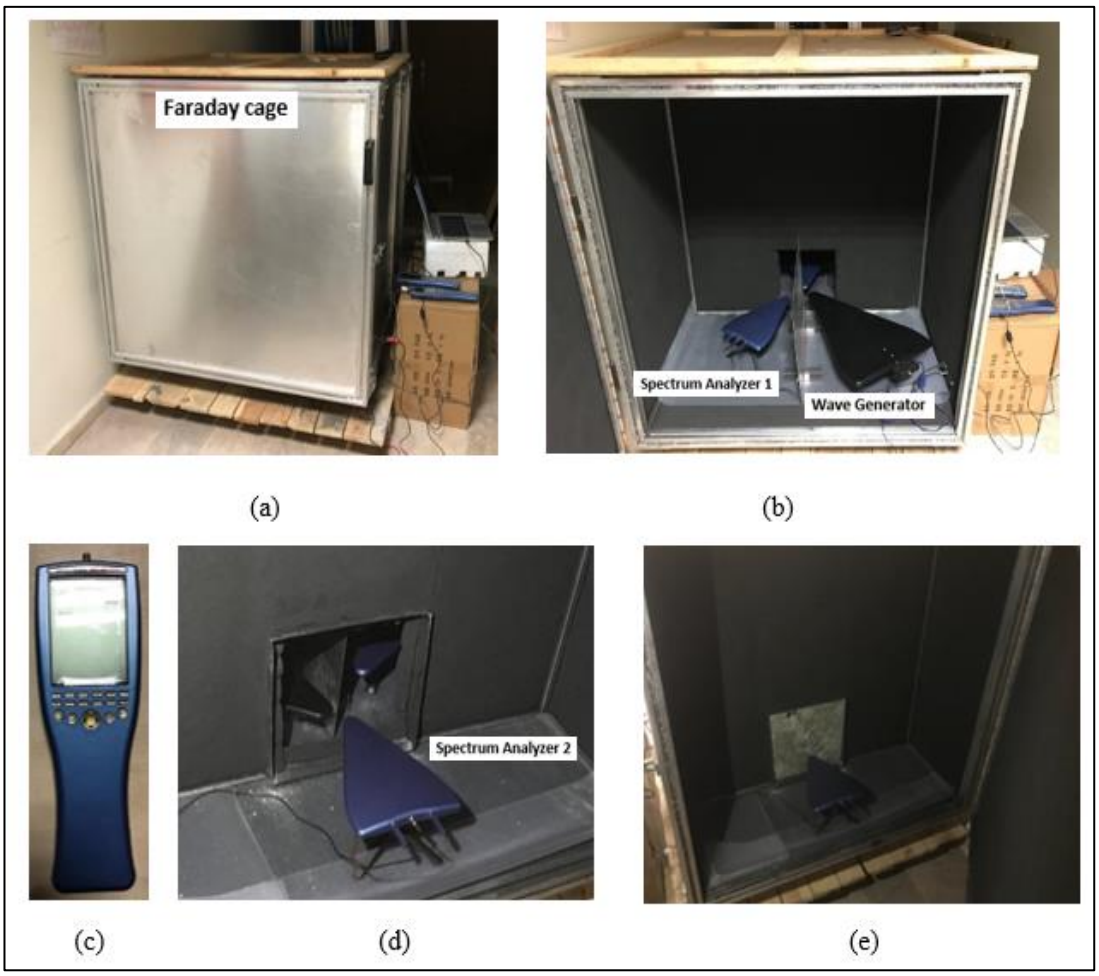

Figure 3.13. Equipment used to measure electromagnetic properties: a) Faraday cage, b) wave generator and spectrum analyzer (1), c) spectrum analyzer, d) spectrum analyzer (2), and e) sample place inside the Faraday cage.

3.3. MIXTURE PROPORTIONS AND PRODUCTION

One series were produced in this study. This series contain 2 groups (the first group is batches made with the WT and the second group is batches made with the GT, and each group contains several batches. A combination of NaOH and Na_2SiO_3 was used as an activator for both groups. The series is designated depending on the activators and binders' types as following:

N Series: WT or GT + (calcite or without calcite) + ((%70 Na_2SiO_3 and %30 Water) + (NaOH)).

1) **Group 1:** WT+ (calcite or without calcite) + ((%70 Na_2SiO_3 and %30 Water) + (NaOH)).
    - WT+ (calcite) + ((%70 Na2SiO3 and %30 Water) + (NaOH)).
    - WT+ (without calcite) + ((%70 Na_2SiO_3 and %30 Water) + (NaOH)).
2) **Group 2:** GT+ (calcite or without calcite) + ((%70 Na_2SiO_3 and %30 Water) + (NaOH)).
    - GT+ (calcite) + ((%70 Na2SiO3 and %30 Water) + (NaOH)).
    - GT+ (without calcite) + ((%70 Na_2SiO_3 and %30 Water) + (NaOH)).

3.3.1. N Series

A total of 20 different batches of alkali-activated composites were produced in the N series. PP and Steel fibers were added to the composite mixes in 0%, 1%, 2%, and 3% by volume of composites. The mixtures were activated using sodium hydroxide and sodium silicate (the solution contained %70 Na_2SiO_3 and %30 water before adding the NaOH) combinations with 6 M, 8 M, and 10 M activator solutions (the temperature of solutions was 55±2 ^{0}C) and had a Solution/Powder (S/P) ratio of 0.6 for batches produced with 6 M solution and 0.8 for batches produced with 8 M and 10 M solutions. The batches made with WT were activated with 8M solution. And the batches made with GT were activated with 6M solution. 6M activator solution were used with the batches made with GT to maintain an appropriate setting time. Otherwise, and because

of the different in the chemical composition between WT and GT, the mixes made with GT will set fast and the fresh pastes cannot be poured into the moulds. The mixture proportions of the N series batches are presented in Table 3-6. Labelling of samples in Table 3-6 as follows: W and G refer to WT and GT respectively, P refers to polypropylene fiber, S refers to steel fiber, N refers to the N series, the first number at the end of the labels refer to the percentage of fiber by the volume of the composite, and the second number (if there is) shows that the calcite powder was not added to the mix and this number is always zero.

Table 3.6. Mix proportions of N Series batches (by weight).

NO	**Batch**	**Component amount by weight (%)**				**Fiber (by volume). (%)**	**NaOH + water solution**			**S/P**
-	**-**	**Wt**	**GT**	**Calcite**	**Solution**	**-**	**6M**	**8M**	**10M**	**-**
1	WN0-0	55.50	-	0.00	44.50	0			+	0,8
2	WN0	32.52	-	30.03	37.44	0		+		0.6
3	WPN1	32.41	-	29.92	37.31	1		+		0.6
4	WPN2	32.29	-	29.82	37.17	2		+		0,6
5	WPN3	32.17	-	29.70	37.03	3		+		0,6
6	WPN3-0	54.87	-	0.00	43.99	3			+	0,8
7	WSN1	31.26	-	28.87	35.98	1		+		0,6
8	WSN2	30.07	-	27.77	34.62	2		+		0,6
9	WSN3	28.95	-	26.73	33.33	3		+		0,6
10	WSN3-0	49.02	-	0.00	39.30	3			+	0,8
11	GN0-0	-	55.50	0.00	44.50	0			+	0,8
12	GN0	-	32.52	30.03	37.44	0	+			0,6
13	GPN1	-	32.41	29.93	37.31	1	+			0,6
14	GPN2	-	32.29	29.82	37.18	2	+			0,6
15	GPN3	-	32.18	29.71	37.04	3	+			0,6
16	GPN3-0	-	54.89	0.00	44.01	3			+	0,8
17	GSN1	-	31.43	29.02	36.18	1	+			0,6
18	GSN2	-	30.23	27.91	34.80	2	+			0,6
19	GSN3	-	28.89	26.68	33.26	3	+			0,6
20	GSN3-0	-	49.16	0.00	39.42	3			+	0,8

3.3.1.1. Mixing procedure, Casting of samples and Curing

Mixing was carried out in two stages for the patches activated with sodium hydroxide and sodium silicate (70% Na_2SiO_3 and 30% Water) combinations in the N series.

The first stage was mixing the alkali-activated solution with the WT or GT by a spatula until it became a homogenous mix. After that, the fibers (PP or steel) are added to the mix and mixed until it became a homogenous mix again.

The second stage is adding the calcite to the homogenous mixture and mixing it with the Hobart mixer at slow speed for 30 seconds (for batches without calcite, slow speed mixing is not applied). And then, the mixing will continue with rapid speed for 60 seconds.

Fresh mixtures were casted into stainless steel moulds with a volume of 40×40×160 mm and 300×300×10 mm and vibrated for 60 seconds (the vibration step did not apply for the batches reinforced with steel fiber to avoid the segregation between the fiber and the matrix as this fiber have high density comparing to the other component of the mix). After that, the composite samples were kept at room temperature of 24 ± 2 ℃ and 35 ± 10% relative humidity before and after demoulding for curing. This mixing and curing technique were adopted from the prior study on NaOH and Na_2SiO_3 activated AAMs containing calcite and Bayburt stone [67].

PART 4

RESULTS AND DISCUSSION

The results and discussion part is divided into five sections. The sections are illustrating the results of fresh paste test and hardened paste tests applied on two groups of batches. The first group is batches made with WT + (calcite or without calcite) and the second group is batches made with GT + (calcite or without calcite). The section is arranged as:

- Setting Time and Flow Table Test results and discussion,
- Flexural and Compressive Strength Tests results and discussion.
- Water Absorption, Specific Gravity, and Apparent Porosity results and discussion.
- Shrinkage results and discussion.
- Electromagnetic properties results and discussion.

4.1. HARDENING TIME AND FLOW TABLE TEST

Flow table test results of all the batches in the N series were represented by the spreading diameter in cm unit. Table 4-1 shows the results of hardening time, and flow table test results of the N series. Figure 4-1 illustrates the spreading diameter of the N series batches made with WT. Figure 4-2 illustrates the spreading diameter of the N series batches made with GT. In this section, the results of the batches made with WT are discussed firstly. Then the results of the batches made with GT are discussed. However, hardening time and flow table test results of the batches made with WT and GT are not compared with each other due to the molarity difference between the mixes made with WT and GT.

Table 4.1. Hardening time, and flow table test results of the N series.

Group 1			Group 2		
Batch	Spreading Diameter (cm)	Hardening time	Batch	Spreading Diameter (cm)	Hardening time
WN0-0	20.75	43 days	GN0-0	25	31 days
WN0	25	1.5 hours ± 5 min	GN0	25	1 hour ± 5 min
WPN1	22	1.5 hours ± 5 min	GPN1	25	1 hour ± 5 min
WPN2	18	1.5 hours ± 5 min	GPN2	19.5	1 hour ± 5 min
WPN3	15	1.5 hours ± 5 min	GPN3	15.75	1 hour ± 5 min
WPN3-0	15.75	57 days	GPN3-0	23	31 days
WSN1	25	1.5 hours ± 5 min	GSN1	25	1 hour ± 5 min
WSN2	25	1.5 hours ± 5 min	GSN2	25	1 hour ± 5 min
WSN3	25	1.5 hours ± 5 min	GSN3	25	1 hour ± 5 min
WSN3-0	20	57 days	GSN3-0	25	29 days

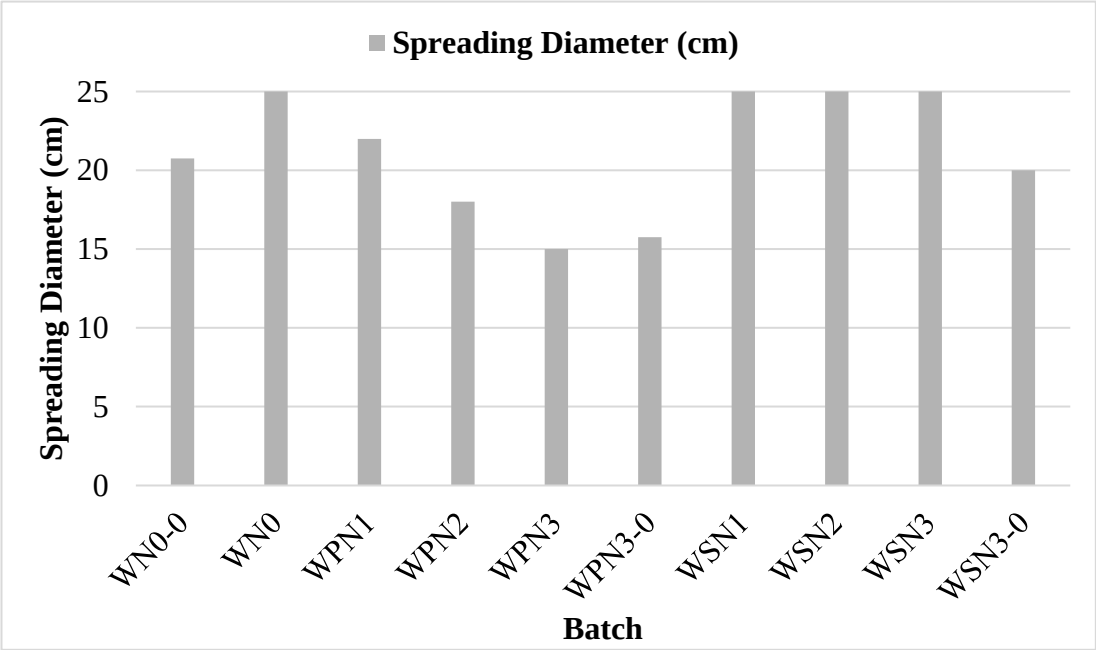

Figure 4.1. The spreading diameter of the N series batches made with WT.

The results of Table 4-1 and Figure 4-1 are discussed below:

- Increasing the PP fiber percentage led to a decrease in the spreading diameter of the batches made with (WT + calcite) and reinforced with PP fiber. The spreading diameter percentages of WN0, WPN1, WPN2, and WPN3 is 99.21%, 87.30%, 71.43%, and 59.52%, respectively. Thus, PP fiber had a major effect on decreasing the workability of the composites. This refers to the

well distribution of PP fiber inside the composites' matrix due to the low density of this fiber comparing to the other components inside the matrix.

- Increasing the steel fiber percentage did not have any effect on the spreading diameter of the batches made with (WT + calcite) and reinforced with steel fiber. The spreading diameter percentages of WN0, WSN1, WSN2, and WSN3 were the same, and it was 99.21%. This happened due to the density difference between steel fiber and the other matrix components. Steel fiber is considered to be denser; thus, the fiber settled at the middle of the table during the flow table test, and the segregation has appeared between the matrix and the fiber.
- Reinforcing the batches made with only WT with PP and steel fibers led to a decrease in the spreading diameter percentage by -24.10% for the WPN3-0 batch and -3.61% for the WSN3-0 batch comparing to the batch without any reinforcement (WN0-0). Thus, PP fiber reinforcement led to a decrease in the workability, and reinforcement with the steel fiber had no major effect on the workability for the same reasons discussed in the previous two points.
- The hardening time for batches made with (WT+ calcite) was 1.5 hours. However, the hardening time for batches made with WT only was more than 28 days. This happened due to the difference in S/P between the batches with and without calcite. The S/P ratio for the batches without calcite was 0.8 and for the batches with calcite was 0.6. Increasing the S/P ratio led to an increase in the hardening time. Besides, adding the calcite into the mixes enhanced the geo-polymerization reaction and accelerate it as the calcite mainly consists of CaO structures that could be entered the reaction as a Ca source and could be activated by the activator solution.

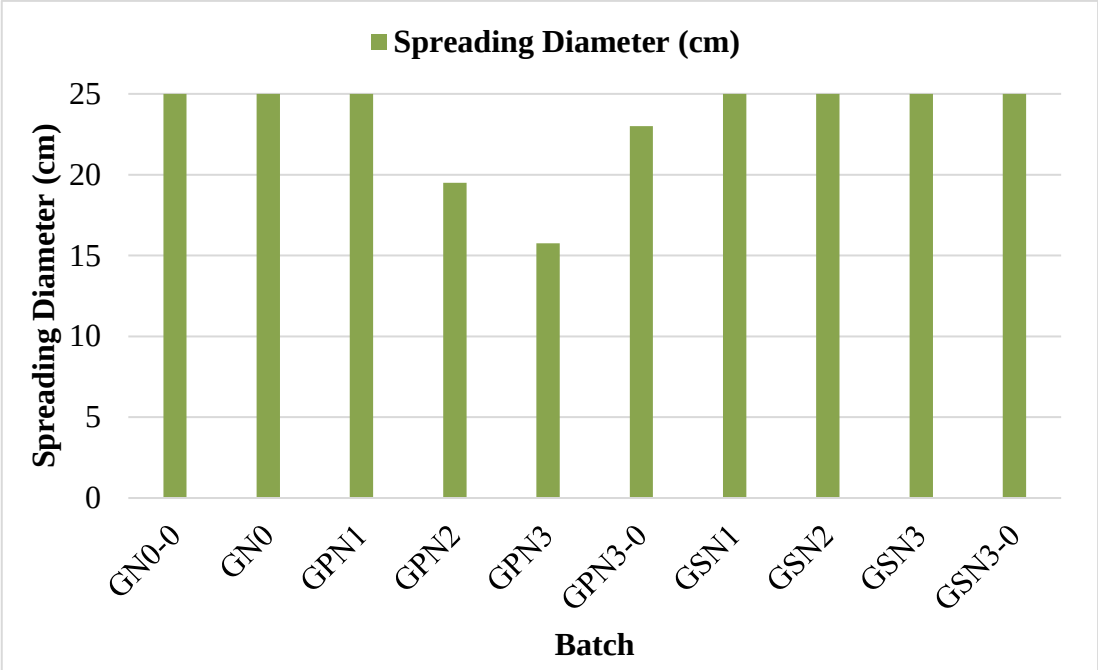

Figure 4.2. The spreading diameter o**f** the N series batches from made with GT.

The results of Table 4-1 and Figure 4-2 are discussed below:

- Increasing the PP fiber percentage led to a decrease in the spreading diameter of the batches made with (GT + calcite) and reinforced with PP fiber. The spreading diameter percentages of GN0, GPN1, GPN2, and GPN3 is 99.21%, 99.21%, 77.38%, and 62.50%, respectively. Thus, PP fiber had a major effect on decreasing the workability of the composites. This refers to the well distribution of PP fiber inside the composites' matrix due to the low density of this fiber comparing to the other components inside the matrix.
- Increasing the steel fiber percentage did not have any effect on the spreading diameter of the batches made with (GT + calcite) and reinforced with steel fiber. The spreading diameter percentages of GN0, GSN1, GSN2, and GSN3 were the same, and it was 99.21%. This happened due to the density difference between steel fiber and the other matrix components. Steel fiber is considered to be denser; thus, the fiber settled at the middle of the table during the flow table test, and the segregation has appeared between the matrix and the fiber.
- Reinforcing the batches made with only GT with PP and steel fibers led to a decrease in the spreading diameter percentage by -8% for the GPN3-0 batch

and 0% for the GSN3-0 batch comparing to the batch without any reinforcement (GN0-0). Thus, PP fiber reinforcement led to a decrease in the workability, and reinforcement with the steel fiber had no major effect on the workability for the same reasons discussed in the previous two points.

- The hardening time for batches made with (GT+ calcite) was 1 hour. However, the hardening time for batches made with GT only was more than 28 days. This happened due to the difference in S/P between the batches with and without calcite. The S/P ratio for the batches without calcite was 0.8 and for the batches with calcite was 0.6. Increasing the S/P ratio led to an increase in the hardening time. Besides, adding the calcite into the mixes enhanced the geo-polymerization reaction and accelerate it as the calcite mainly consists of CaO structures that could be entered the reaction as a Ca source and could be activated by the activator solution.

4.2. FLEXURAL AND COMPRESSIVE STRENGTH TESTS

Flexural and compressive strength tests were applied for all the batches in the N series at 2, 28, 90, and 180 days of production. Table 4-2 shows the results of Flexural Strength (FS), Compressive Strength (CS), flexural strength/compressive strength percentage (FS/CS (%)) and Unit Weight (UW) of the N series. For each type of fiber and tuff, two graphs were made to explain the flexural and compressive strength tests results for more clearer comparison. The figures from Figure 4-3, Figure 4-4, Figure 4-7, Figure 4-8, Figure 4-10, Figure 4-11, Figure 4-14, and Figure 4-15 illustrate the results of flexural and compressive strength of all the batches in the N series. The results are discussed in this section as:

- Flexural strength, compressive strength, and the unit weight results of the batches made with WT and reinforced with PP fiber.
- Flexural strength, compressive strength, and the unit weight results of the batches made with WT and reinforced with steel fiber.
- Flexural strength, compressive strength, and the unit weight results of the batches made with GT and reinforced with PP fiber.

- Flexural strength, compressive strength, and the unit weight results of the batches made with GT and reinforced with steel fiber.

However, the strengths and unit weight results of the batches made with WT and GT are not compared with each other due to the molarity difference between the mixes made with WT and GT.

Table 4.2. Flexural Strength (FS), Compressive Strength (CS), FS/CS (%) and Unit Weight (UW) results of the N series.

Group 1						Group 2					
Batch	**Day**	**FS**	**CS**	**FS/CS (%)**	**UW**	**Batch**	**Day**	**FS**	**CS**	**FS/CS (%)**	**UW**
	2	-	-	-	-		2	-	-	-	-
	28	-	-	-	-		28	-	-	-	-
WN0-0	90	5.63	15.06	37.36	1.85	GN0-0	90	3.79	5.42	69.93	1.85
	180	6.51	16.00	40.69	1.80		180	7.17	20.29	35.31	1.85
	2	2.89	18.60	15.56	1.82		2	3.56	6.43	55.33	1.91
	28	7.15	21.45	33.32	1.81		28	5.14	13.79	37.28	1.84
WN0	90	5.82	22.70	25.66	1.77	GN0	90	2.52	4.83	52.23	1.81
	180	3.83	13.28	28.84	180		180	2.38	7.72	30.83	1.71
	2	1.83	16.49	11.13	1.80		2	3.69	1.35	274.09	1.90
	28	7.72	25.66	30.08	1.77		28	4.53	5.70	79.43	1.67
WPN1	90	10.32	29.72	34.73	1.77	GPN1	90	3.17	7.12	44.52	1.64
	180	5.84	21.41	27.28	1.67		180	4.87	12.10	40.25	1.56
	2	2.73	14.23	19.17	1.77		2	5.15	9.24	55.77	1.87
	28	7.40	25.66	28.84	1.71		28	8.90	20.71	42.99	1.79
WPN2	90	9.47	30.72	30.82	1.71	GPN2	90	6.76	15.32	44.13	1.68
	180	11.75	26.66	44.07	1.77		180	10.12	20.05	50.49	1.64
	2	1.99	13.18	15.13	1.79		2	6.73	9.45	71.22	1.87
WPN3	28	8.23	23.06	35.69	1.71		28	10.43	21.23	49.16	1.80
	90	10.99	27.44	40.06	1.71	GPN3	90	11.70	15.12	77.38	1.62
	180	12.52	28.66	43.68	1.66		180	15.30	19.33	79.15	1.60
	2	-	-	-	-		2	-	-	-	-
	28	-	-	-	-		28	-	-	-	-
WPN3-0	90	4.73	1.66	284.94	1.59	GPN3-0	90	6.76	9.07	74.53	1.76
	180	6.50	8.67	75.01	1.80		180	9.84	18.95	51.91	1.72
	2	2.15	18.12	11.85	1.95		2	5.89	11.74	50.15	2.07
	28	6.98	24.79	28.16	1.95		28	11.57	24.53	47.18	2.05
WSN1	90	8.55	24.75	34.54	1.88	GSN1	90	2.67	4.34	61.52	1.68
	180	4.20	18.96	22.15	1.88		180	2.84	8.34	34.07	1.69
	2	5.87	19.51	30.06	1.95		2	6.43	11.31	56.87	2.07
	28	7.50	24.53	30.58	1.95		28	7.45	22.48	33.14	2.04
WSN2	90	6.07	25.45	23.84	1.88	GSN2	90	3.74	11.11	33.68	1.90
	180	5.07	23.63	21.46	1.88		180	3.17	9.74	32.49	1.80
WSN3	2	6.07	18.94	32.04	2.01	GSN3	2	8.05	12.43	64.79	2.22
	28	9.53	28.69	33.23	1.95		28	8.08	25.74	31.39	2.26
WSN3	90	8.51	29.02	29.34	1.96	GSN3	90	3.34	12.62	26.47	1.96
	180	4.73	29.68	15.94	1.91		180	2.90	10.70	27.06	1.92
	2	-	-	-	-		2	-	-	-	-
	28	-	-	-	-		28	-	-	-	-
WSN3-0	90	5.04	2.85	177.15	1.99	GSN3-0	90	6.79	12.30	55.20	2.04
	180	9.84	13.96	70.49	1.84		180	7.23	14.35	50.35	2.05

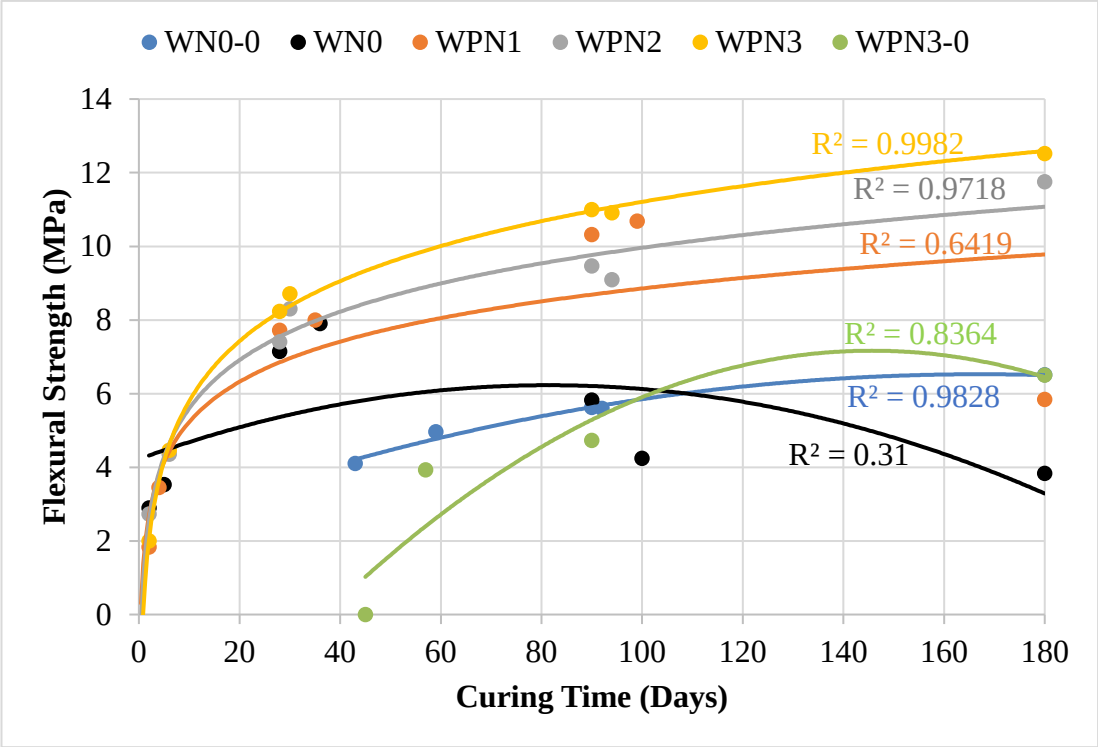

Figure 4.3. Flexural strength of the N series batches made with WT and reinforced with PP fibe.

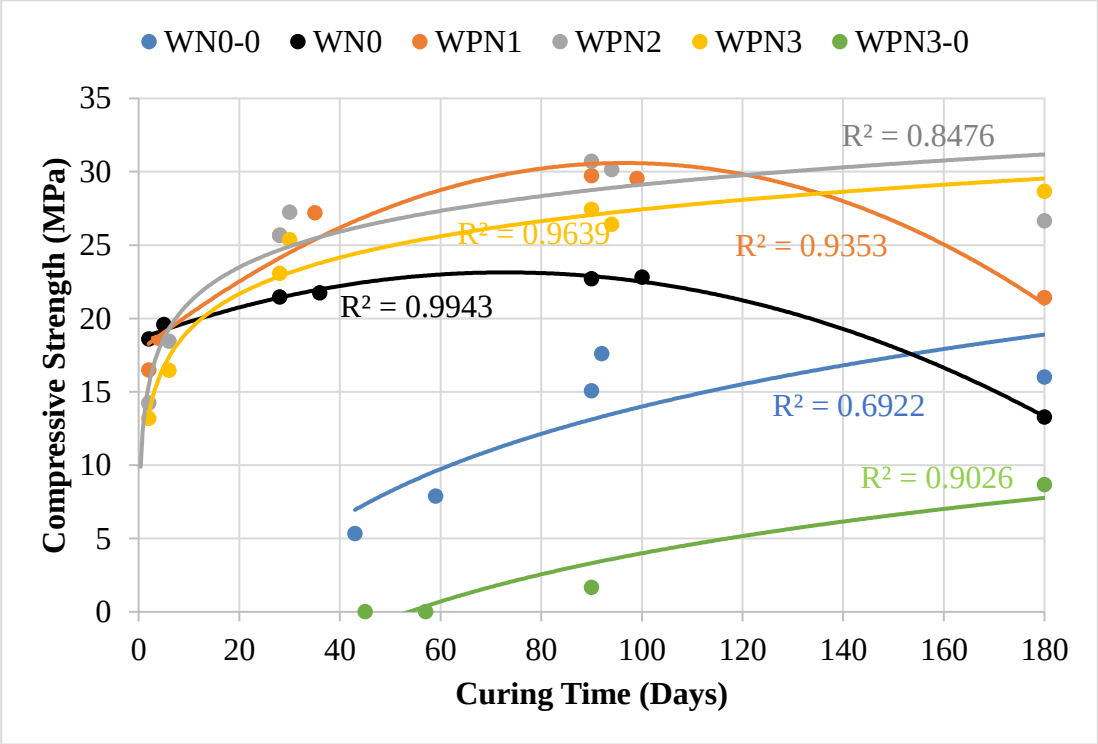

Figure 4.4. Compressive strength of the N series batches made with WT and reinforced with PP fiber.

Figure 4-3 illustrates the flexural strength results of the N series batches made with WT and reinforced with PP fiber. And Figure 4-4 illustrates the compressive strength of the N series batches made with WT and reinforced with PP fiber. The results of Table 4-2, Figure 4-3, and Figure 4-4 are discussed below:

- The unit weight of the batches WN0, WPN1, WPN2 and WPN3 were decreased by -2.97%, -1.44%, -3.26%, and -4.36%, respectively when the batches were tested on the 90th day of production comparing to the same samples when they were tested at the 2nd day of production. The unit weight of the batches was decreased by time due to the continuity of the geo-polymerization reaction that led to the hydration process of the liquid and consuming the alkali liquid. Besides, Increasing the PP fiber content led to decrease the unit weight of the sample as the PP fiber took a space from the volume of the mould. And this decrease reached to -3.29% with WPN2 batch comparing to WN0 batch. However, this decrease was not significant. Due to this the unit weight effects on the strength were not significant.
- The unit weight of WN0-0 and WPN3-0 batches were 1.85 and 1.59, respectively when they were tested at the 90th day of production. Reinforcing with the PP fiber led to decrease the unit weight of the sample as the PP fiber took a space from the volume of the mould. The unit weight for these batches effected the strength significantly. Leading to provide WN0-0 batch a higher flexural and compressive strength comparing to WPN3-0 because it has a higher unit weight.
- The flexural strength of the batch with 0% reinforcement (WN0) was enhanced by 101.55% when it was tested on the 90th day of production comparing to the same batch when it was tested at the 2nd day of production. And the maximum 90 days flexural strength enhanced with the PP fiber reinforcement. The enhancement of the strength was 77.35%, 62.68%, and 88.86% with reinforcing the batches with 1% (WPN1), 2% (WPN2), and 3% (WPN3) PP fiber, respectively comparing to the batch without fiber (WN0). The matrix of the batches and the PP fiber worked well on the 90th day of production, leading to an increase in the flexural strength with the fiber reinforcement, as the failure behavior goes to the ductility behavior as shown in Figure 4-5a. Besides, this

refers to the continuity of the geo-polymerization reaction leading the matrix to be more compatible with the fiber due to its hardening by time over the fiber.

- The compressive strength of the batch with 0% reinforcement (WN0) was enhanced by 22.06% when it was tested on the 90th day of production comparing to the same batch when it was tested at the 2nd day of production. And the maximum 90 days compressive strength enhanced with the PP fiber reinforcement. The enhancement of the strength was 30.91%, 35.32%, and 20.86% with reinforcing the batches with 1% (WPN1), 2% (WPN2), and 3% (WPN3) PP fiber, respectively comparing to the batch without fiber (WN0). Reinforcing the batches with PP fiber led to increase the compressive strength at 90 days as the matrix and the PP fiber were combatable together due to the well distribution of the PP fiber in the matrix as shown in Figure 4-5b. Besides, this refers to the continuity of the geo-polymerization reaction leading the matrix to be more compatible with the fiber due to its hardening by time over the fiber.
- Reinforcing the batches made without calcite with 3% PP fiber (WPN3-0 batch) led to a decrease in the maximum 90 days flexural and compressive strength by -15.91% and -88.98%, respectively comparing to the batch without PP fiber reinforcement (WN3-0 batch). This refers to the decrease in the unit weight of the sample when it was reinforced with PP fiber, as the PP fiber took space from the volume of the mould.
- The carbonation of the matrix was one of the critical reasons that led to a decrease in the flexural and compressive strengths of the batches made with WT. All the batches in the N series and made with WT faced the carbonation leaching effect as the carbonation mainly leaches from the matrix. The carbonation leads to fill the voids inside the matrix and accelerates the hydration process which will lead to a high shrinkage of the samples. Besides, the low humidity inside the lab led to an increase in the carbonation and hydration of the liquid and the shrinkage increased due to that. The carbonation appeared at the matrices mainly due to the high Ca and sodium particles inside the WT and calcite structures. Besides, over time the carbonation of the matrices is increased leading to damage to the samples more and more. Figure 4-6a show the carbonation of a sample made with WT at the 1st week of

production and Figure 4-6b shows the carbonation of the same sample at the 90th day of production.

- The FS/CS (%) for all the batches made with WT and reinforced with PP fiber increased over time with increasing the strengths. Besides, increasing the PP fiber percentage led to increase the FS/CS (%).
- Batches without calcite did not show an early flexural or compressive strength as they were not set. As the S/P ratio of the batches without calcite were lower than the batches with calcite and the absence of the CaO which is mainly comes from calcite and accelerate the reaction did not cooperate with the reaction.
- The flexural strength of the batch made with calcite and 0% reinforcement (WN0) was decreased by -34.25% when it was tested on the 180th day of production comparing to the same batch when it was tested at the 90th day of production. And the compressive strength of the same batch was decreased by -41.51% when it was tested on the 180th day of production comparing to the same batch when it was tested at the 90th day of production. This refers to the calcite addition and the carbonation leaching from it. Calcite enhanced the initial strength however the strength did not maintain by time. Besides, the strength of all the batches made with WT and calcite decreased over time as the matrix lost it strength.
- The flexural strength of the batch made without calcite and 0% reinforcement (WN0) was increased by 15.73% when it was tested on the 180th day of production comparing to the same batch when it was tested at the 90th day of production. And the compressive strength of the same batch was increased by 6.26% when it was tested on the 180th day of production comparing to the same batch when it was tested at the 90th day of production. The maintenance of the strength appeared as this batch had a low carbonation as the calcite was not added to the mix. Besides, the strengths of all the batches made with only WT increased over time as the matrix gained strength.
- Figure 0.5. a) WPN2 batch after the failure from the flexural strength test. b) the distribution of the PP fiber inside the WPN2 batch.
- Figure 0.6. a) WPN2 batch after the failure from the flexural strength test. b) the distribution of the PP fiber inside the WPN2 batch.

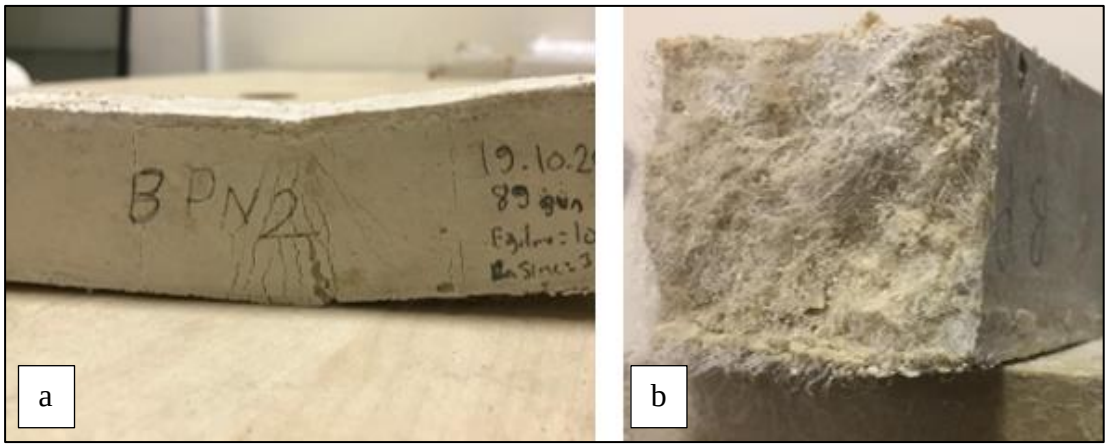

Figure 4.5. a) WPN2 batch after the failure from the flexural strength test. b) the distribution of the PP fiber inside the WPN2 batch.

Figure 4.6. a) BPN1 batch at the first week of production. b) BPN1 batch on the 90th day of production.

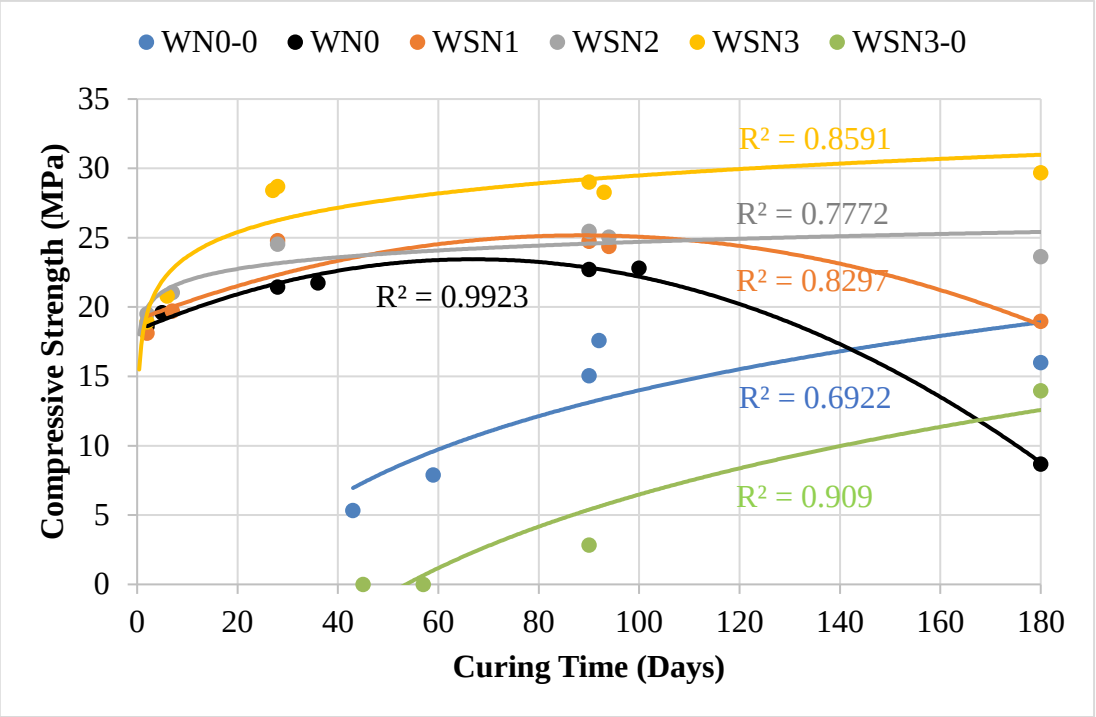

Figure 4.7. Flexural strength of the N series batches made with WT and reinforced with steel fiber.

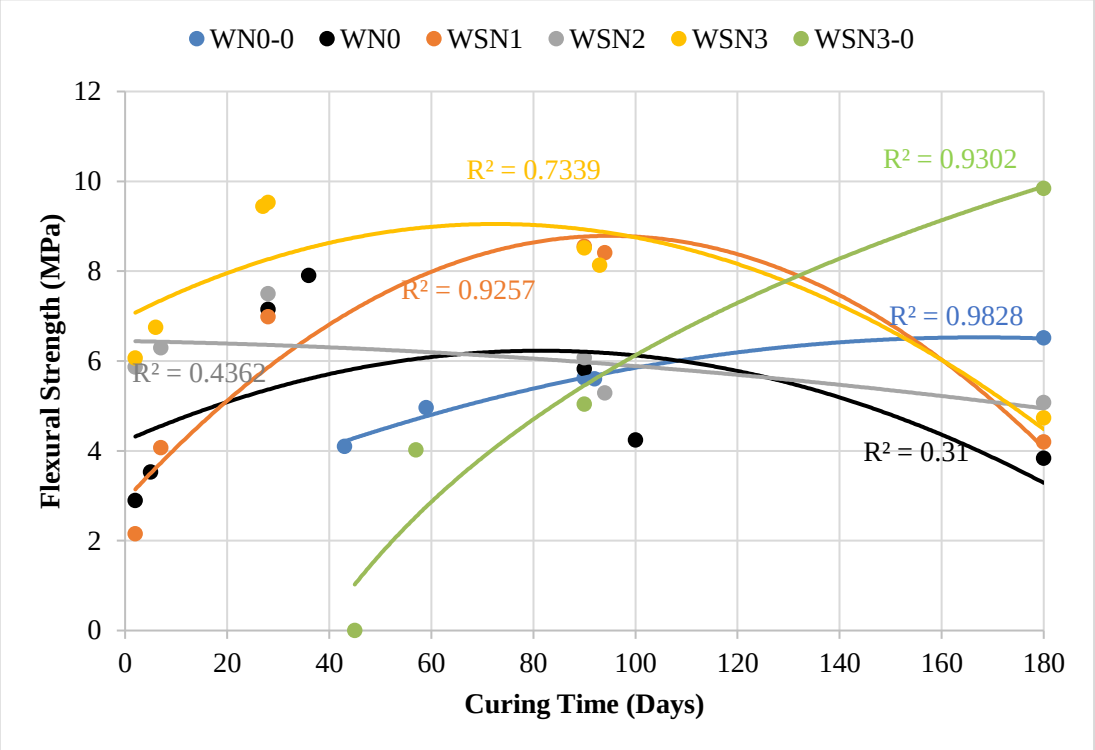

Figure 4.8. Compressive strength of the N series batches made with WT and reinforced with steel fiber.

Figure 4-7 illustrates the flexural strength results of the N series batches made with WT and reinforced with steel fiber. And Figure 4-8 illustrates the compressive strength of the N series batches made with WT and reinforced with steel fiber. Table 4-2, Figure 4-7, and Figure 4-8 are discussed below:

- The unit weight of the batches WN0, WSN1, WSN2 and WSN3 were decreased by -2.97%, -3.91%, -3.91%, and -2.49%, respectively when the batches were tested on the 90th day of production comparing to the same samples when they were tested at the 2nd day of production. The unit weight of the batches was decreased by time due to the continuity of the geo-polymerization reaction that led to the hydration process of the liquid and consuming the alkali liquid. Increasing the steel fiber content led to increase the unit weight of the sample as this fiber has a high mass comparing to the other components of the matrix. And this increase reached to 10.73% with WSN3 batch at the 90th day of production comparing to WN0 batch. This increase effected the strength positively and led WSN3 batch to get the highest compressive and flexural strength comparing WN0, WSN1, and WSN2.
- The unit weight of WN0-0 and WSN3-0 batches were 1.85 and 1.99, respectively when they were tested at the 90th day of production. Reinforcing with the steel fiber led to increase the unit weight of the sample as the steel have a high unit weight comparing to the other components of the matrix. Still, the strength of the WN0-0 batch was higher than WSN3-0 batch as the steel fiber settled at the bottom of the samples due to its high unit weight comparing to the other components of the matrix.
- The flexural strength of the batch with 0% reinforcement (WN0) was enhanced by 101.55% when it was tested on the 90th day of production comparing to the same batch when it was tested at the 2nd day of production. And the maximum 90 days flexural strength enhanced with the steel fiber reinforcement. The enhancement of the strength was 46.87%, 4.27%, and 46.29% with reinforcing the batches with 1% (WSN1), 2% (WSN2), and 3% (WSN3) steel fiber, respectively comparing to the batch without fiber (WN0). Increasing the steel fiber percentage led to increase the flexural strength as the fiber worked well with the matrix due to the ability of this fiber to bend with the load. The failure

behavior seen to be one crack from the middle with angle of 45^{o} mainly from shear as shown in Figure 4-9a. Besides, this refers to the continuity of the geo-polymerization reaction leading the matrix to be more compatible with the fiber due to its hardening by time over the fiber.

- The compressive strength of the batch with 0% reinforcement (WN0) was enhanced by 22.06% when it was tested on the 90th day of production comparing to the same batch when it was tested at the 2nd day of production. And the maximum 90 days compressive strength enhanced with the steel fiber reinforcement. The enhancement of the strength was 9.03%, 12.13%, and 27.84% with reinforcing the batches with 1% (WSN1), 2% (WSN2), and 3% (WSN3) steel fiber, respectively comparing to the batch without fiber (WN0). Reinforcing the batches with the steel fiber led to increasing the compressive strength due to the continuity of the geo-polymerization reaction over time leading the matrix to be more compatible with the fiber due to its hardening by time over the fiber.
- Reinforcing the batches made without calcite with 3% steel fiber (WSN3-0 batch) led to a decrease in the maximum 90 days flexural and compressive strength by -10.40% and -81.11%, respectively comparing to the batch without steel fiber reinforcement (WN3-0 batch). The strength decreased, as the fiber had a poor distribution inside the mix due to the big difference between the density of the steel fiber and the other components, steel fiber is considered to be denser, so it grouped together at various places as shown in Figure 4-9b.
- The carbonation of the matrix was one of the critical reasons that led to a decrease in the flexural and compressive strengths of the batches made with WT. All the batches in the N series and made with WT faced the carbonation leaching effect as the carbonation mainly leaches from the matrix. The carbonation leads to fill the voids inside the matrix and accelerates the hydration process which will lead to a high shrinkage of the samples. Besides, the low humidity inside the lab led to an increase in the carbonation and hydration of the liquid and the shrinkage increased due to that. The carbonation appeared at the matrices mainly due to the high Ca and sodium particles inside the WT and calcite structures. Besides, over time the carbonation of the matrices is increased leading to damage to the samples more and more. Figure

4-6a show the carbonation of a sample made with WT at the 1st week of production and Figure 4-6b shows the carbonation of the same sample at the 90th day of production.

- The FS/CS (%) for all the batches made with WT and reinforced with steel fiber increased over time with increasing the strengths. Besides, increasing the steel fiber percentage led to increase the FS/CS (%).
- Batches without calcite did not show an early flexural or compressive strength as they were not set. As the S/P ratio of the batches without calcite were lower than the batches with calcite and the absence of the CaO which is mainly comes from calcite and accelerate the reaction did not cooperate with the reaction.
- The flexural strength of the batch made with calcite and 0% reinforcement (WN0) was decreased by -34.25% when it was tested on the 180th day of production comparing to the same batch when it was tested at the 90th day of production. And the compressive strength of the same batch was decreased by -41.51% when it was tested on the 180th day of production comparing to the same batch when it was tested at the 90th day of production. This refers to the calcite addition and the carbonation leaching from it. Calcite enhanced the initial strength however the strength did not maintain by time. Besides, the strength of all the batches made with WT and calcite decreased over time as the matrix lost it strength.
- The flexural strength of the batch made without calcite and 0% reinforcement (WN0) was increased by 15.73% when it was tested on the 180th day of production comparing to the same batch when it was tested at the 90th day of production. And the compressive strength of the same batch was increased by 6.26% when it was tested on the 180th day of production comparing to the same batch when it was tested at the 90th day of production. The maintenance of the strength appeared as this batch had a low carbonation as the calcite was not added to the mix. Besides, the strengths of all the batches made with only WT increased over time as the matrix gained strength.

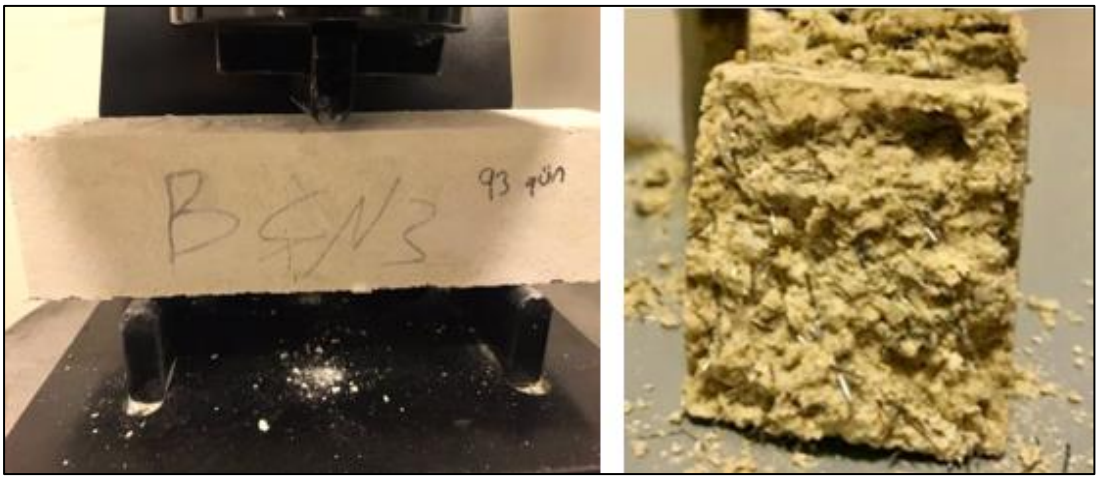

Figure 4.9. a) WSN3 batch after the failure from the flexural strength test. b) the distribution of the steel fiber inside the WSN3-0 batch.

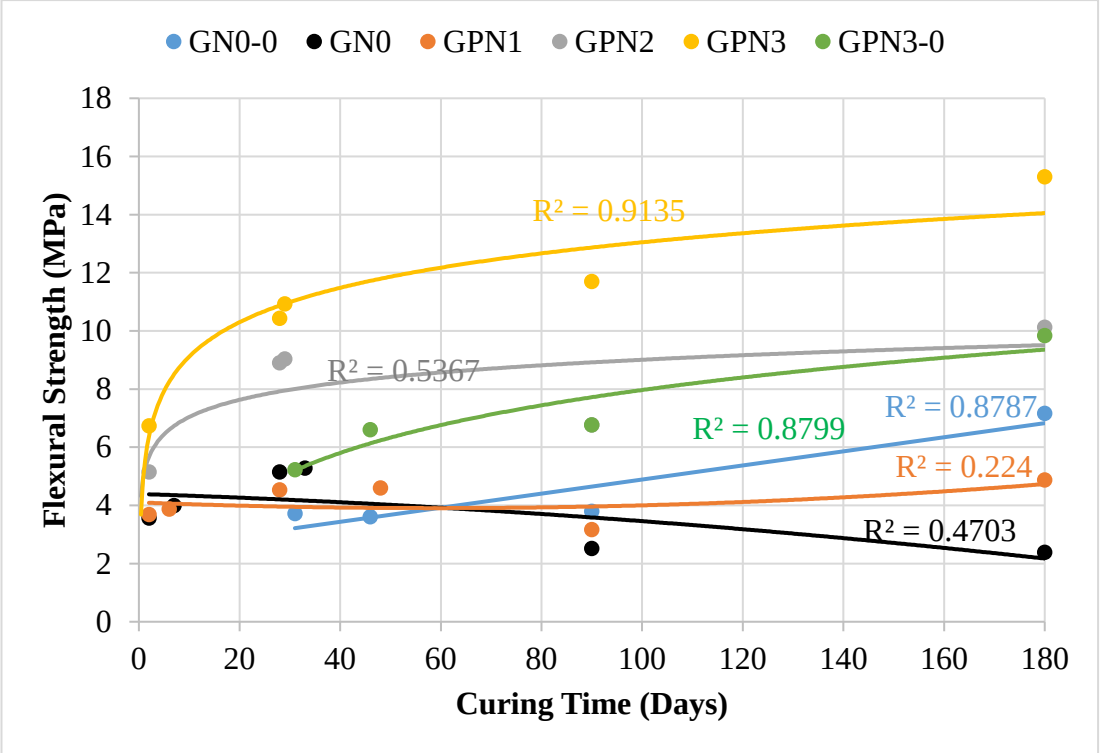

Figure 4.10. Flexural strength of the N series batches made with GT and reinforced with PP fiber.

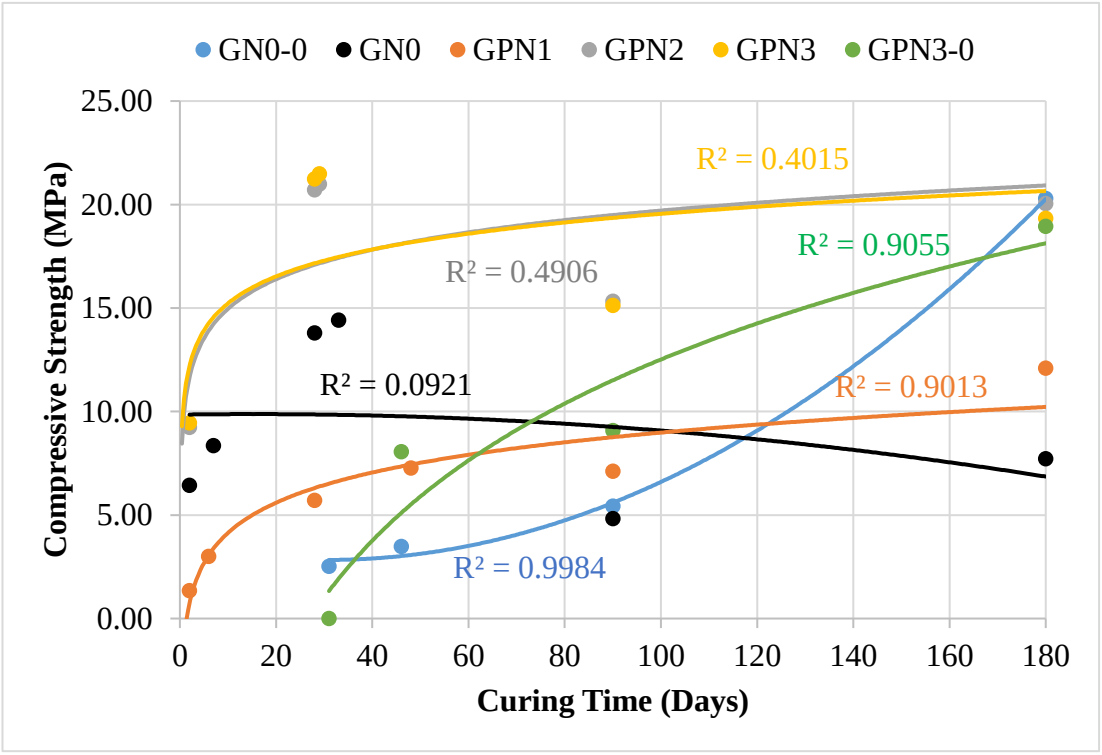

Figure 4.11. Compressive strength of the N series batches made with GT and reinforced with PP fiber.

Figure 4-10 illustrates the flexural strength results of the N series batches made with GT and reinforced with PP fiber. And Figure 4-11 illustrates the compressive strength of the N series batches made with GT and reinforced with PP fiber. Table 4-2, Figure 4-10, and Figure 4-11 are discussed below:

- The unit weight of the batches GN0, GPN1, GPN2 and GPN3 were decreased by -5.27%, -13.63%, -9.75%, and -13.42%, respectively when the batches were tested on the 90th day of production comparing to the same samples when they were tested at the 2nd day of production. The unit weight of the batches was decreased by time due to the continuity of the geo-polymerization reaction that led to the hydration process of the liquid and consuming the alkali liquid. Besides, Increasing the PP fiber content led to decrease the unit weight of the sample as the PP fiber took a space from the volume of the mould. And this decrease reached to -10.36% with GPN3 batch at the 90th day of production comparing to GN0 batch. This decrease effected the strength positively and led

GPN3 batch to get the highest compressive and flexural strength comparing GN0, GPN1, and GPN2.

- The unit weight of GN0-0 and GPN3-0 batches were 1.85 and 1.76, respectively when they were tested at the 90th day of production. Reinforcing with the PP fiber led to decrease the unit weight of the sample as the PP fiber took a space from the volume of the mould. However, GPN3-0 batch showed a higher strength than GN0-0 batch due to the well distribution of the PP fiber in the matrix.
- The flexural strength of the batch with 0% reinforcement (GN0) was decreased by -29.21% when it was tested on the 90th day of production comparing to the same batch when it was tested at the 2nd day of production. This gives an indication that the matrix of the batches made with GT is weakened by time and has low durability. However, the maximum 90 days flexural strength enhanced with the PP fiber reinforcement. The enhancement of the strength was 25.79%, 168.25%, and 364.29% with reinforcing the batches with 1% (GPN1), 2% (GPN2), and 3% (GPN3) PP fiber, respectively comparing to the batch without fiber (GN0). The matrix of the batches and the PP fiber worked well at 90 days due to the well distribution of this fiber, leading to an increase in the flexural strength with the fiber reinforcement as the failure behavior goes to the ductility behavior as shown in Figure 4-12a-b.
- The compressive strength of the batch with 0% reinforcement (GN0) was decreased by -24.96% when it was tested on the 90th day of production comparing to the same batch when it was tested at the 2nd day of production. This gives an indication that the matrix of the batches made with GT is weakened by time and has low durability. And the maximum 90 days compressive strength enhanced with the PP fiber reinforcement. The enhancement of the strength was 47.41%, 217.18%, and 213.04% with reinforcing the batches with 1% (GPN1), 2% (GPN2), and 3% (GPN3) PP fiber, respectively comparing to the batch without fiber (GN0). Reinforcing the batches with PP fiber led to increase the compressive strength at 90 days as the matrix and the PP fiber were combatable together due to the well distribution of the PP fiber in the matrix leading to a cohesive matrix as shown in Figure 4-12b. Besides, the strength increased due the continuity of the geo-

polymerization reaction leading the matrix to be more compatible with the fiber due to its hardening by time over the fiber.

- Reinforcing the batches made without calcite with 3% PP fiber (GPN3-0 batch) led to an increase in the maximum 90 days flexural and compressive strength by 78.36% and 67.34%, respectively comparing to the batch without PP fiber reinforcement (GN0-0 batch). The strength increased due the continuity of the geo-polymerization reaction leading the matrix to be more compatible with the fiber due to its hardening by time over the fiber.
- The carbonation of the matrix was one of the critical reasons that led to a decrease in the flexural and compressive strengths of the batches made with GT. All the batches in the N series and made with GT faced the carbonation leaching effect as the carbonation mainly leaches from the matrix. The carbonation leads to fill the voids inside the matrix and accelerates the hydration process which will lead to a high shrinkage of the samples. Besides, the low humidity inside the lab led to an increase in the carbonation and hydration of the liquid and the shrinkage increased due to that. The carbonation appeared at the matrices mainly due to the high Ca and sodium particles inside the GT and calcite structures. Besides, over time the carbonation of the matrices is increased leading to damage to the samples more and more. Figure 4-13a show the carbonation of a sample made with GT at the 1st week of production and Figure 4-13b shows the carbonation of the same sample at the 90th day of production.
- The FS/CS (%) for all the batches made with GT and reinforced with PP fiber increased over time when the strength increased, and decreased when the strength was decreased. Besides, increasing the PP fiber percentage led to increase the FS/CS (%).
- Batches without calcite did not show an early flexural or compressive strength as they were not set. As the S/P ratio of the batches without calcite were lower than the batches with calcite and the absence of the CaO which is mainly comes from calcite and accelerate the reaction did not cooperate with the reaction.
- The flexural strength of the batch made with calcite and 0% reinforcement (GN0) was decreased by -5.56% when it was tested on the 180th day of production comparing to the same batch when it was tested at the 90th day of

production. And the overall compressive strength is decreasing over time. This refers to the calcite addition and the carbonation leaching from it. Calcite enhanced the initial strength however the strength did not maintain by time. Besides, the strengths of all the batches made with GT and calcite decreased over time as the matrix lost it strength.

- The flexural strength of the batch made without calcite and 0% reinforcement (GN0) was increased by 89.05% when it was tested on the 180th day of production comparing to the same batch when it was tested at the 90th day of production. And the compressive strength of the same batch was increased by 274.35% when it was tested on the 180th day of production comparing to the same batch when it was tested at the 90th day of production. The maintenance of the strength appeared as this batch had a low carbonation as the calcite was not added to the mix. Besides, the strength of all the batches made with only GT increased over time as the matrix gained strength.

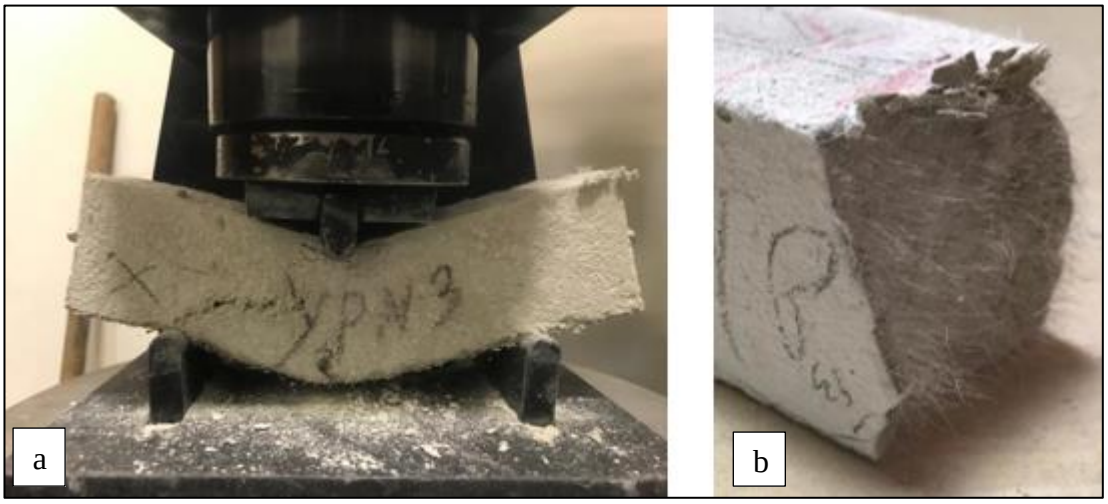

Figure 4.7. a) GPN3 batch after the failure from the flexural strength test. b) the distribution of the PP fiber inside the GPN3 batch.

Figure 4.8. GPN1 batch at the first week of production. b) GPN1 batch on the 90th day of production.

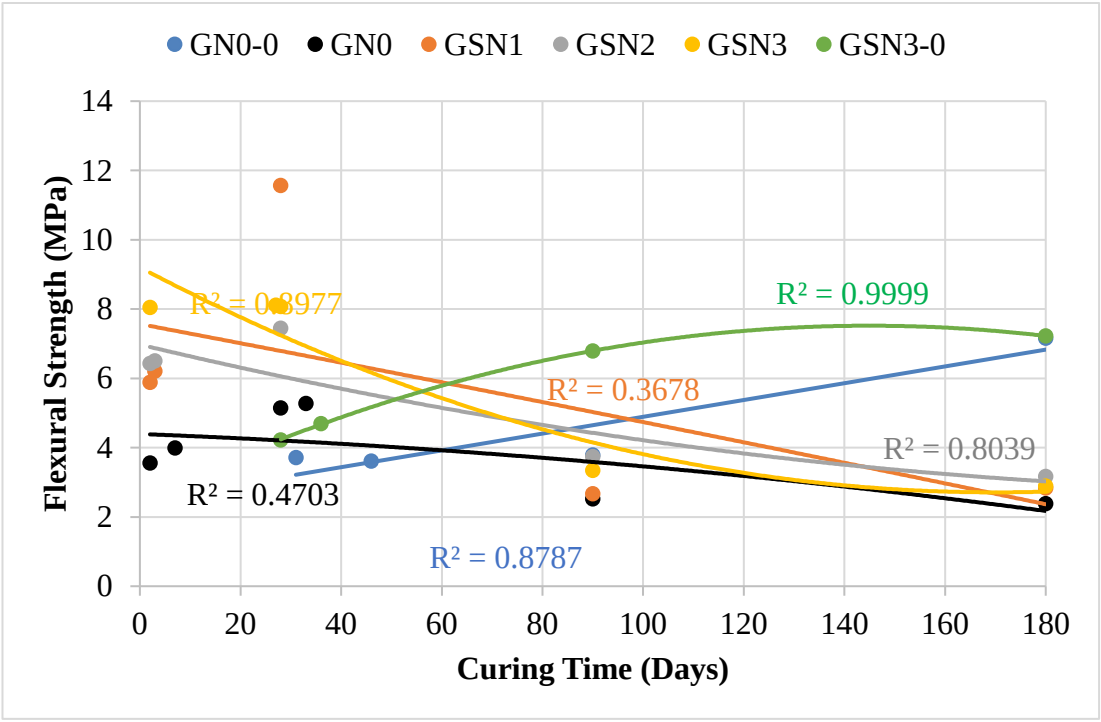

Figure 4.9. Flexural strength of the N series batches made with GT and reinforced with steel fiber.

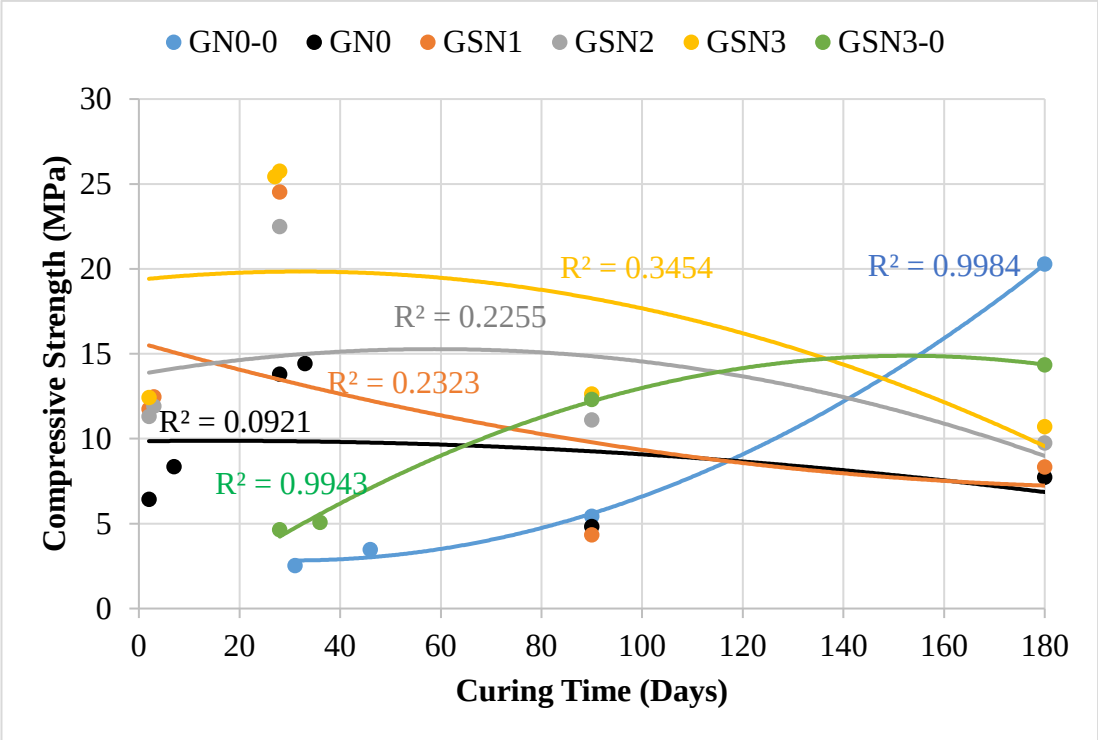

Figure 4.10. Compressive strength of the N series batches made with GT and reinforced with steel fiber.

Figure 4-14 illustrates the flexural strength results of the N series batches made with GT and reinforced with steel fiber. And Figure 4-15 illustrates the compressive strength of the N series batches made with GT and reinforced with steel fiber. Table 4-2, Figure 4-14, and Figure 4-15 are discussed below:

- The unit weight of the batches GN0, GSN1, GSN2 and GSN3 were decreased by -5.27%, -18.74%, -8.43%, and -11.63%, respectively when the batches were tested on the 90th day of production comparing to the same samples when they were tested at the 2nd day of production. The unit weight of the batches was decreased by time due to the continuity of the geo-polymerization reaction that led to the hydration process of the liquid and consuming the alkali liquid. Increasing the steel fiber content led to increase the unit weight of the sample as this fiber has a high mass comparing to the other components of the matrix. And this increase reached to 8.50% with GSN3 batch at the 90th day of production comparing to GN0 batch. This increase effected the compressive strength positively and led GSN3 batch to get the highest compressive

comparing GN0, GSN1, and GSN2. However, the flexural strength did not have a notable effect as this fiber have a poor distribution inside the matrix as shown in Figure 4-16b.

- The unit weight of GN0-0 and GSN3-0 batches were 1.85 and 2.04, respectively when they were tested at the 90th day of production. Reinforcing with the steel fiber led to increase the unit weight of the sample as the steel have a high unit weight comparing to the other components of the matrix.
- The flexural strength of the batch with 0% reinforcement (GN0) was decreased by -29.21% when it was tested on the 90th day of production comparing to the same batch when it was tested at the 2nd day of production. This gives an indication that the matrix of the batches made with GT is weakened by time and has low durability. However, the maximum 90 days flexural strength enhanced with the steel fiber reinforcement. The enhancement of the strength was 5.95%, 48.41%, and 32.54% with reinforcing the batches with 1% (GSN1), 2% (GSN2), and 3% (GSN3) steel fiber, respectively comparing to the batch without fiber (GN0). Increasing the steel fiber percentage led to increase the flexural strength as the fiber worked well with the matrix due to the ability of this fiber to bend with the load. The failure behavior seen to be one crack from the middle with angle of 45^{o} mainly from shear as shown in Figure 4-16a. Besides, the strength increased due the continuity of the geo-polymerization reaction leading the matrix to be more compatible with the fiber due to its hardening by time over the fiber.
- The compressive strength of the batch with 0% reinforcement (GN0) was decreased by -29.21% when it was tested on the 90th day of production comparing to the same batch when it was tested at the 2nd day of production. This gives an indication that the matrix of the batches made with GT is weakened by time and has low durability. However, the maximum 90 days compressive strength enhanced with the steel fiber reinforcement. The enhancement of the strength was 129.92% and 161.28% with reinforcing the batches with 2% (GSN2) and 3% (GSN3) steel fiber, respectively comparing to the batch without fiber (GN0). However, 1% steel fiber did not show a positive effect on increasing the compressive strength, as steel fiber generally have a poor distribution inside the matrix as shown in Figure 4-16b. Generally,

increasing the steel fiber percentage led to increase the flexural strength as the fiber worked well with the matrix due to the ability of this fiber to bend with the load. The failure behavior seen to be one crack from the middle with angle of 45^{o} mainly from shear as shown in Figure 4-16a. Besides, the strength increased due the continuity of the geo-polymerization reaction leading the matrix to be more compatible with the fiber due to its hardening by time over the fiber.

- Reinforcing the batches made without calcite with 3% steel fiber (GSN3-0 batch) led to an increase in the maximum 90 days flexural and compressive strength by 67.34% and 126.94%, respectively comparing to the batch without steel fiber reinforcement (GN0-0 batch). The strength increased due the continuity of the geo-polymerization reaction leading the matrix to be more compatible with the fiber due to its hardening by time over the fiber.
- The carbonation of the matrix was one of the critical reasons that led to a decrease in the flexural and compressive strengths of the batches made with GT. All the batches in the N series and made with GT faced the carbonation leaching effect as the carbonation mainly leaches from the matrix. The carbonation leads to fill the voids inside the matrix and accelerates the hydration process which will lead to a high shrinkage of the samples. Besides, the low humidity inside the lab led to an increase in the carbonation and hydration of the liquid and the shrinkage increased due to that. The carbonation appeared at the matrices mainly due to the high Ca and sodium particles inside the GT and calcite structures. Besides, over time the carbonation of the matrices is increased leading to damage to the samples more and more. Figure 4-13a show the carbonation of a sample made with GT at the 1st week of production and Figure 4-13b shows the carbonation of the same sample at the 90th day of production.
- The FS/CS (%) for all the batches made with GT and reinforced with steel fiber increased over time when the strength increased, and decreased when the strength was decreased. Besides, increasing the steel fiber percentage led to increase the FS/CS (%).
- Batches without calcite did not show an early flexural or compressive strength as they were not set. As the S/P ratio of the batches without calcite were lower

than the batches with calcite and the absence of the CaO which is mainly comes from calcite and accelerate the reaction did not cooperate with the reaction.

- The flexural strength of the batch made with calcite and 0% reinforcement (GN0) was decreased by -5.56% when it was tested on the 180th day of production comparing to the same batch when it was tested at the 90th day of production. And the overall compressive strength is decreasing over time. This refers to the calcite addition and the carbonation leaching from it. Calcite enhanced the initial strength however the strength did not maintain by time. Besides, the strengths of all the batches made with GT and calcite decreased over time as the matrix lost it strength.
- The flexural strength of the batch made without calcite and 0% reinforcement (GN0) was increased by 89.05% when it was tested on the 180th day of production comparing to the same batch when it was tested at the 90th day of production. And the compressive strength of the same batch was increased by 274.35% when it was tested on the 180th day of production comparing to the same batch when it was tested at the 90th day of production. The maintenance of the strength appeared as this batch had a low carbonation as the calcite was not added to the mix. Besides, the strength of all the batches made with only GT increased over time as the matrix gained strength.

Figure 4.11. a) GSN2 batch after the failure from the flexural strength test. b) the distribution of the PP fiber inside the GSN2 batch.

4.3. WATER ABSORPTION, SPECIFIC GRAVITY, AND APPARENT POROSITY

Water absorption test were performed to all of the samples at 28, and 90 days of production. However, all of the batches in the N series did not show any resistance to water at 28 days of production as the geo-polymerization reaction was not fast enough to reach the final polymerization product that resist water. Table 4-3 shows the results of the water absorption, specific gravity, and apparent porosity of the N series at 90 days of production. Figure 4-17 and Figure 4-18 illustrates the Specific gravity, and apparent porosity results of the N series batches at 90 days of production. In this section, the results of the batches made with WT are discussed firstly. Then the results of the batches made with GT are discussed. However, water absorption, specific gravity, and apparent porosity results of the batches made with WT and GT are not

compared with each other due to the molarity difference between the mixes made with WT and GT.

Table 4.3. Water absorption, specific gravity, and apparent porosity results of the N series at 90 days of production.

	Batch	Water absorption (%)	Specific gravity	Apparent porosity (%)
Group 1	**WN0-0**	16.54	2.00	24.87
	WN0	19.91	1.97	28.18
	WPN1	24.31	2.05	33.28
	WPN2	27.80	2.11	36.98
	WPN3	24.51	2.08	33.79
	WPN3-0	46.81	2.08	49.31
	WSN1	0.00	0.00	0.00
	WSN2	17.49	2.32	28.85
	WSN3	0.00	0.00	0.00
	WSN3-0	38.94	2.58	50.09
Group 2	**GN0-0**	29.17	2.34	40.53
	GN0	0.00	0.00	0.00
	GPN1	34.14	2.23	43.19
	GPN2	22.08	2.10	31.69
	GPN3	23.44	2.17	33.68
	GPN3-0	29.88	2.12	38.76
	GSN1	0.00	0.00	0.00
	GSN2	0.00	0.00	0.00
	GSN3	0.00	0.00	0.00
	GSN3-0	26.54	2.66	41.35

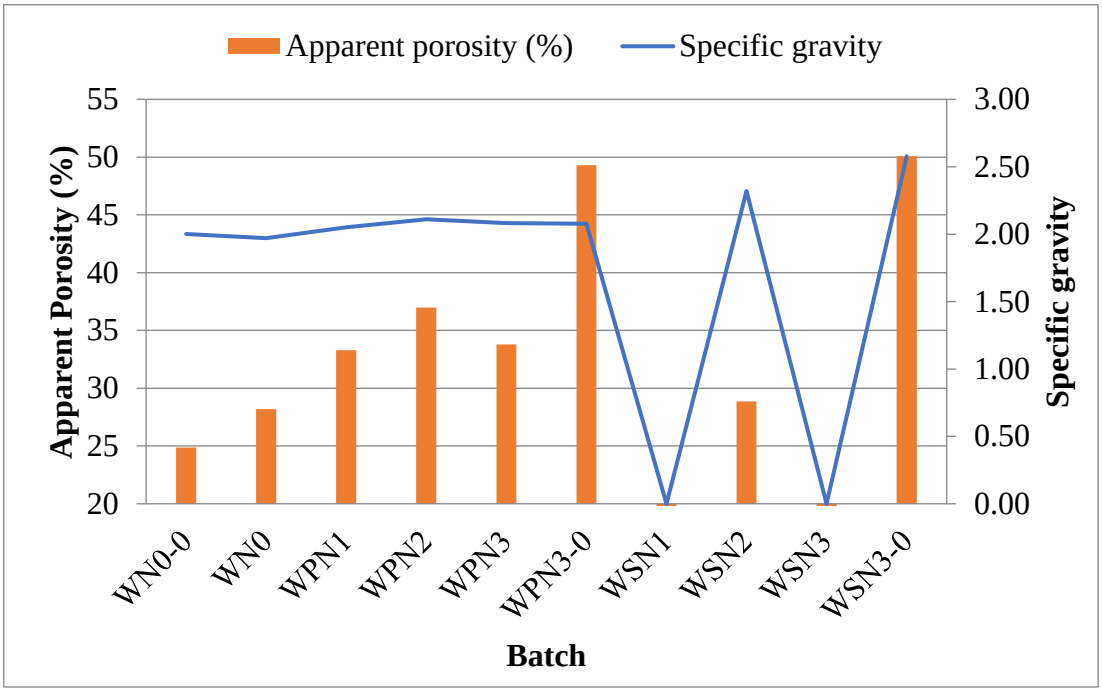

Figure 4.12. Specific gravity, and apparent porosity results of the N series batches made with WT at 90 days of production.

Figure 4-17 shows the specific gravity, and apparent porosity results of the N series batches made with WT at 90 days of production. Table 4-3 and Figure 4-17 are discussed below:

- The water absorption results for the batches made with (WT + calcite) and reinforced with PP fiber with percentages of 1% (WPN1), 2% (WPN2), and 3% (WPN3) was increased by 24.31%, 27.80%, and 24.51%, respectively comparing to the batch without PP fiber reinforcement (WN0). This seemed since reinforcing with PP fiber leads to make extra pores inside the matrix as the porosity of batches reinforced with PP fiber with percentages of 1% (WPN1), 2% (WPN2), and 3% (WPN3) was increased by 18.09%, 31.23%, and 19.90%, respectively comparing to the batch without PP fiber reinforcement (WN0).

- For the batches reinforced with steel fiber, only WSN2 batch resisted the water and the water absorption of it was 17.49%. this refers to the poor distribution of the steel fiber inside the matrix, leading to make the matrix less cohesive.
- The specific gravity of the batches made with (WT + calcite) and reinforced with PP fiber with percentages of 1% (WPN1), 2% (WPN2), and 3% (WPN3) was increased by 4.13%, 7.13%, and 5.70%, respectively comparing to the batch without PP fiber reinforcement (WN0). And for the only batch reinforced with steel fiber and resisted the water (WSN2), the specific gravity of this batch increased by 17.69% comparing to the batch without PP fiber reinforcement (WN0). Steel fiber had an effect on the specific gravity as this fiber has a high specific gravity. On the other hand, PP fiber did not have a major effect on the specific gravity as the percentage of the PP fiber by the volume of the composite is low and the specific gravity of this fiber is low comparing to the other components of the mix.
- The water absorption results for the batches made with only WT and reinforced with 3% PP fiber (WPN3-0) and 3% steel fiber (WSN3-0) were increased by 182.98% and 135.39%, respectively comparing to the batch without fiber reinforcement (WN0-0). This seemed since reinforcing the batches with PP and steel fibers leads to make extra pores inside the matrix as the porosity of batches increased by 98.25% for WPN3-0 batch and 101.39% for WSN3-0 batch comparing to the batch without fiber reinforcement (WN0-0). Besides, the specific gravity increased by 3.84% for WPN3-0 batch and 28.79% for WSN3-0 batch comparing to the batch without fiber reinforcement (WN0-0) for the same reason described in the previous point.

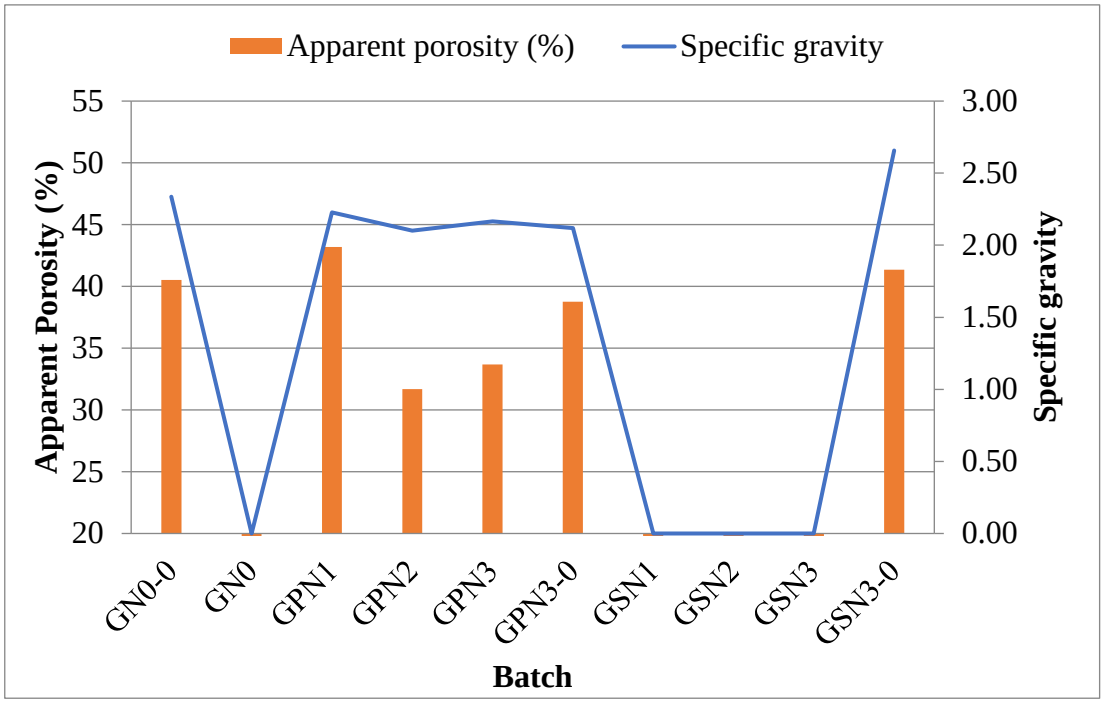

Figure 4.18. Specific gravity, and apparent porosity results of the N series made with GT after 90 days of production.

Figure 4-18 shows the specific gravity, and apparent porosity results of the N series batches made with GT at 90 days of production. Table 4-3 and Figure 4-18 are discussed below:

- The water absorption results for the batches made with (GT + calcite) and reinforced with PP fiber were between 22.08% and 34.14%. GPN2 batches showed the lowest value, and the GPN1 batch showed the highest value. And for the batches reinforced with steel fiber, all of the batches did not resist the water as the main resistance of water comes from the matrix and the matrix did not resist the water as seen from the WN0 batch. This seemed since PP fiber has a low density comparing to the steel fiber, thus it mixed and distributed well in the matrix leading to make the mix cohesive. However, due to the high density of steel fiber, the fiber did not distribute well in the matrix and grouped at separate parts inside the matrix leading to a non-cohesive matrix.
- The specific gravity of the batches made with (GT + calcite) and reinforced with PP fiber was between 2.10 and 2.23. GPN2 batches showed the lowest value, and GPN1 batch showed the highest value. PP fiber did not have a major

effect on the specific gravity as the percentage of the PP fiber by the volume of the composite is low and the specific gravity of this fiber is low comparing to the other components of the mix.

- The apparent porosity of the samples made with GT and reinforced with PP fiber was between 31.69% and 43.19%. GPN2 batches showed the lowest value, and GPN1 batch showed the highest value. Batches with a low apparent porosity had higher strength.
- The water absorption results for the batches made with only GT and reinforced with 3% PP fiber (GPN3-0) and 3% steel fiber (GSN3-0) were increased by 2.44% for GPN3-0 batch and decreased by -9.01% for GSN3-0 batch comparing to the batch without fiber reinforcement (GN0-0). However, the apparent porosity and specific gravity of GPN3-0 and GSN3-0 did not change and affect much comparing to the batch without any reinforcement GN0-0.

4.4. SHRINKAGE

The shrinkage test was performed on the batches several times within 180 days of the samples' production. The first test was performed after taking the sample from the mould and the last at 180 days of production. Figures from Figure 4-19, Figure 4-21, Figure 4-23, and Figure 4-25 illustrates the shrinkage results of the N series. In this section, the results are discussed as:

- The shrinkage results of the batches made with WT and reinforced with PP fiber.
- The shrinkage results of the batches made with WT and reinforced with steel fiber.
- The shrinkage results of the batches made with GT and reinforced with PP fiber.
- The shrinkage results of the batches made with GT and reinforced with steel fiber.

The shrinkage results of the batches made with WT and GT are not compared with each other due to the molarity difference between the mixes made with WT and GT.

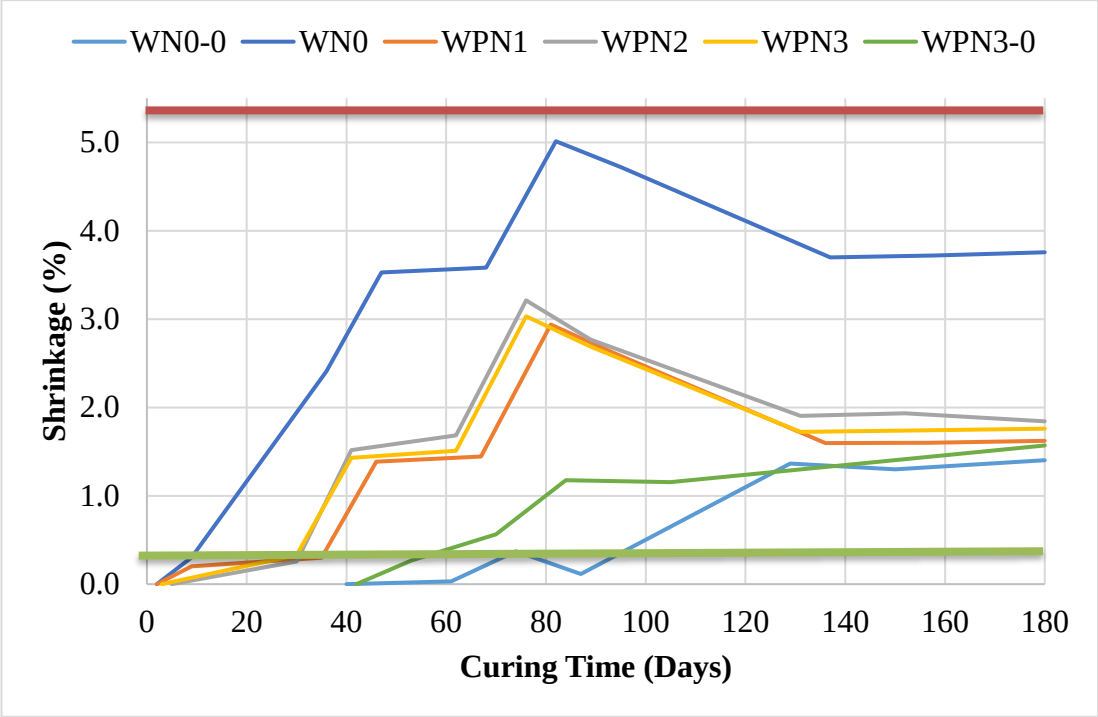

Figure 4.19. Shrinkage results of the N series batches made with WT and reinforced with PP fiber.

Figure 4-19 illustrates the shrinkage results of the N series batches made with WT and reinforced with PP fiber. The red and green lines in Figure 4-19 represent the starting of cracks and geometry deformation of the batches, respectively. Figure 4-19 results are discussed below:

- For the batches made with (WT + calcite), the maximum shrinkage appeared with WN0 batch that is not reinforced with PP fiber, and the maximum shrinkage was approximately 5%. However, reinforcing the batches with PP fiber led to decrease the shrinkage as this fiber could reduce the crake's width and the maximum shrinkage decreased approximately 2% when 1% of PP fiber is added (WPN1 batch).
- The carbonation leaching was one of the main reasons that led to increase the shrinkage as described in the flexural and compressive strengths section. Besides, the humidity inside the lab was low and led to accelerate the hydration

of the liquid inside the matrix, due to this the shrinkage was increased over time.

- Although the shrinkage reached more than 3% for the batches, the cracks did not appear at the surface as shown in Figure 4-20a. However, the samples deformed over time as shown in Figure 4-20b. The geometry deformation starts when the shrinkage reaches approximately 0.3% for all the batches made with WT.
- For the batches made with only WT, reinforcing the batches with 3% PP fiber (WPN3-0) led to an increase in the maximum shrinkage approximately by 0.8% compared to the batch without any reinforcement (WN0-0). Thus, the matrix without calcite had defined the shrinkage limits instead of the PP fiber.
- The shrinkage amount approximately remained constant for all the batches between the 90th and 180th days of production. This refers to the appearance of the final AAMs final products due to ending of the geo-polymerization reaction.

Figure 4.13. a) the surface of WN0-0 batch at the 90th day of production. b) the deformation of WN0-0 batch at the 90th day of production.

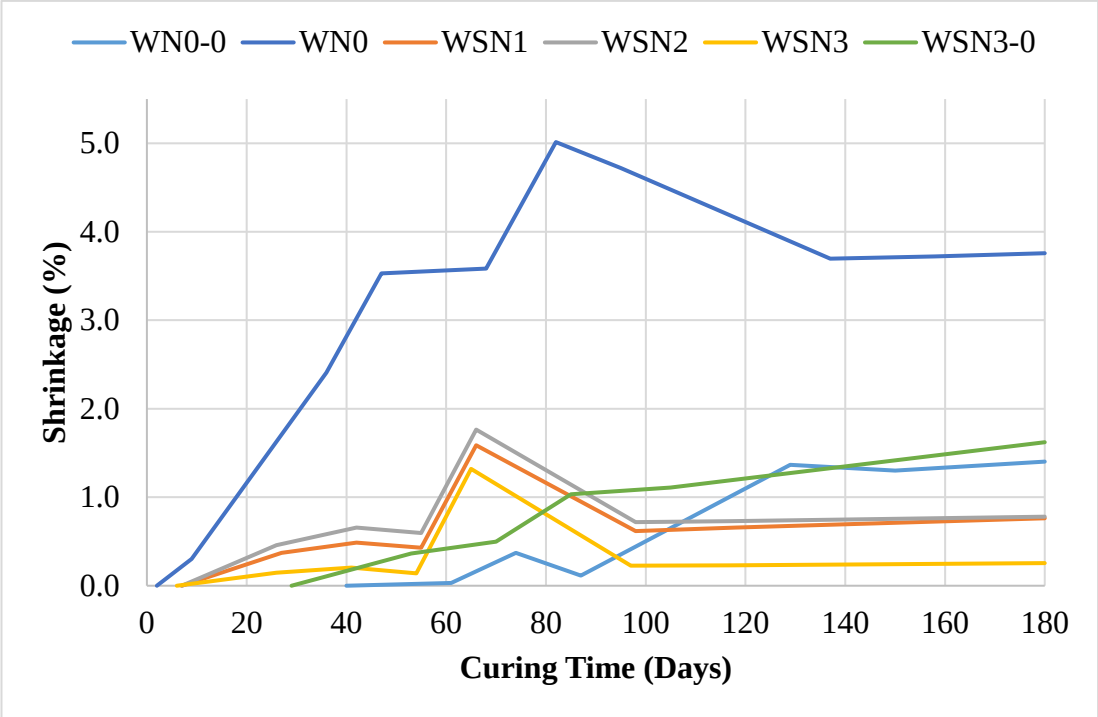

Figure 4.14. Shrinkage results of the N series batches made with WT and reinforced with steel fiber.

Figure 4-21 illustrates the shrinkage results of the N series batches made with WT and reinforced with steel fiber. The red and green lines in Figure 4-21 represent the starting of cracks and geometry deformation of the batches, respectively. Figure 4-21 results are discussed below:

- For the batches made with (WT + calcite), the maximum shrinkage appeared with WN0 batch that is not reinforced with steel fiber. And the maximum shrinkage was approximately 5%. However, reinforcing the batches with steel fiber led to decrease the shrinkage as this fiber could reduce the crake's width and the maximum shrinkage decreased approximately 3.6% when 3% of steel fiber is added (WSN3 batch).
- The carbonation leaching was one of the main reasons that led to increase the shrinkage as described in the flexural and compressive strengths section. Besides, the humidity inside the lab was low and led to accelerate the hydration of the liquid inside the matrix, due to this the shrinkage was increased over time.

- The geometry deformation appeared on all the batches made with WT and reinforced with steel fiber as shown in Figure 4-22a. The geometry deformation starts when the shrinkage reaches approximately 0.3% for all the batches made with WT. And, the cracks appeared on the surface as shown in Figure 4-22b when the shrinkage reaches approximately 0.5% for all the batches made with WT and reinforced with steel fiber.
- For the batches made with only WT, reinforcing the batches with 3% steel fiber (WSN3-0) led to an increase in the maximum shrinkage approxmatliy by 0.6% compared to the batch without any reinforcement (WN0-0). Thus, the matrix without calcite had defined the shrinkage limits instead of the PP fiber.
- The shrinkage amount approximately remained constant for all the batches between the 90th and 180th days of production. This refers to the appearance of the final AAMs final products due to ending of the geo-polymerization reaction.

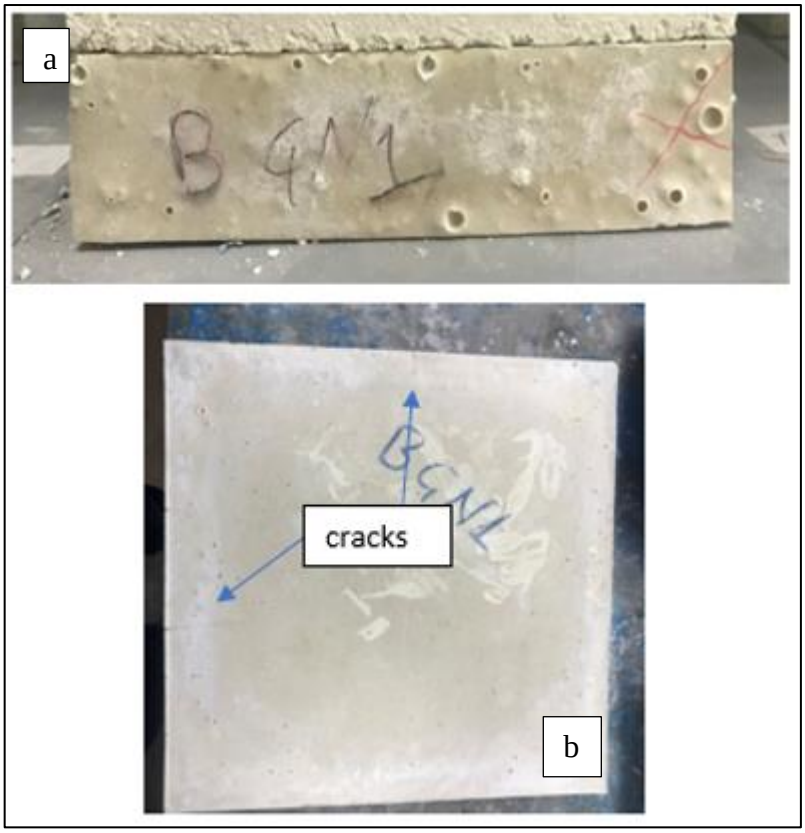

Figure 4.15. a) WSN1 batch's deformation at 90th day of production. b) the cracks on WSN1 batch at the 90th day of production.

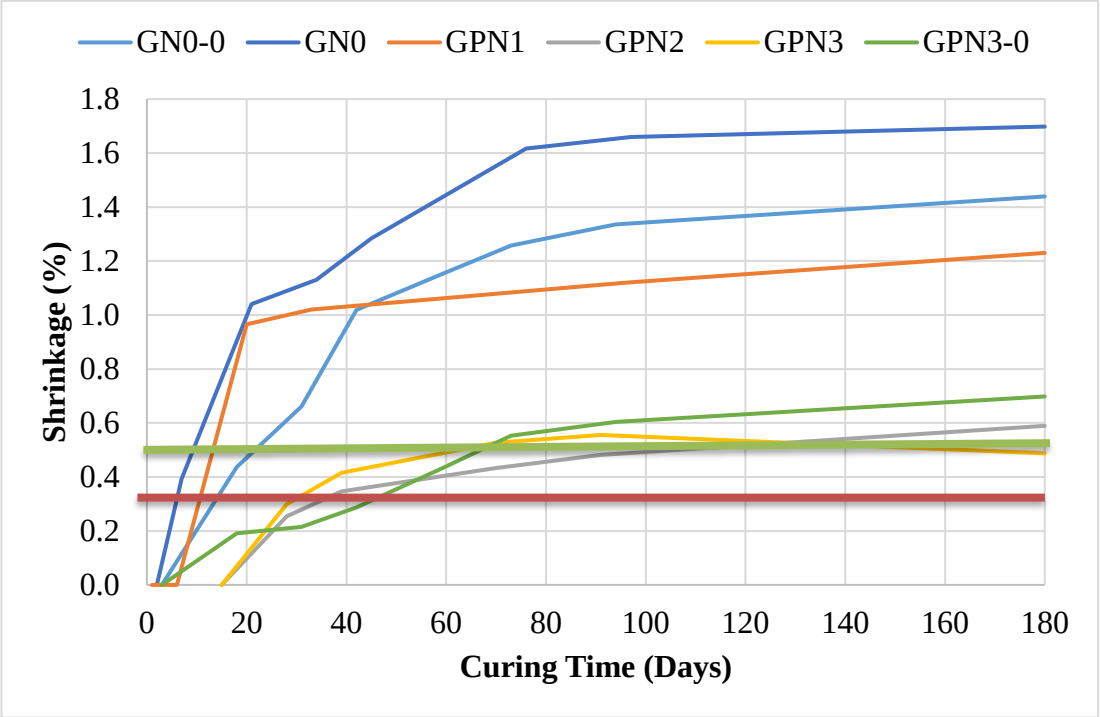

Figure 4.16. Shrinkage results of the N series batches made with GT and reinforced with PP fiber.

Figure 4-23 illustrates the shrinkage results of the N series batches made with GT and reinforced with PP fiber. The red and green lines in Figure 4-23 represent the starting of cracks and geometry deformation of the batches, respectively. Figure 4-23 results are discussed below:

- For the batches made with (WT + calcite), the maximum shrinkage appeared with GN0 batch that is not reinforced with PP fiber, and the maximum shrinkage was approximately 1.64%. However, reinforcing the batches with PP fiber led to decrease the shrinkage as this fiber could reduce the crake's width and the maximum shrinkage decreased approximately 1.2% when 2% of PP fiber is added (GPN2).
- The carbonation leaching was one of the main reasons that led to increase the shrinkage as described in the flexural and compressive strengths section. Besides, the humidity inside the lab was low and led to accelerate the hydration of the liquid inside the matrix, due to this the shrinkage was increased over time.

- The cracks appeared on the surface as shown in Figure 4-24a when the shrinkage reaches approximately 0.3% for all the batches made with GT and reinforced with PP fiber. And the geometry deformation appeared on all the batches made with GT and reinforced with PP fiber as shown in Figure 4-24b. The geometry deformation starts when the shrinkage reaches approximately 0.5% for all the batches made with GT.
- For the batches made with only GT, reinforcing the batches with 3% PP fiber (WPN3-0) led to a decrease in the maximum shrinkage (for the same reason from the 1st point) approxmatliy by 0.7% compared to the batch without any reinforcement (GN0-0).
- The shrinkage amount approximately remained constant for all the batches between the 90th and 180th days of production. This refers to the appearance of the final AAMs final products due to ending of the geo-polymerization reaction.

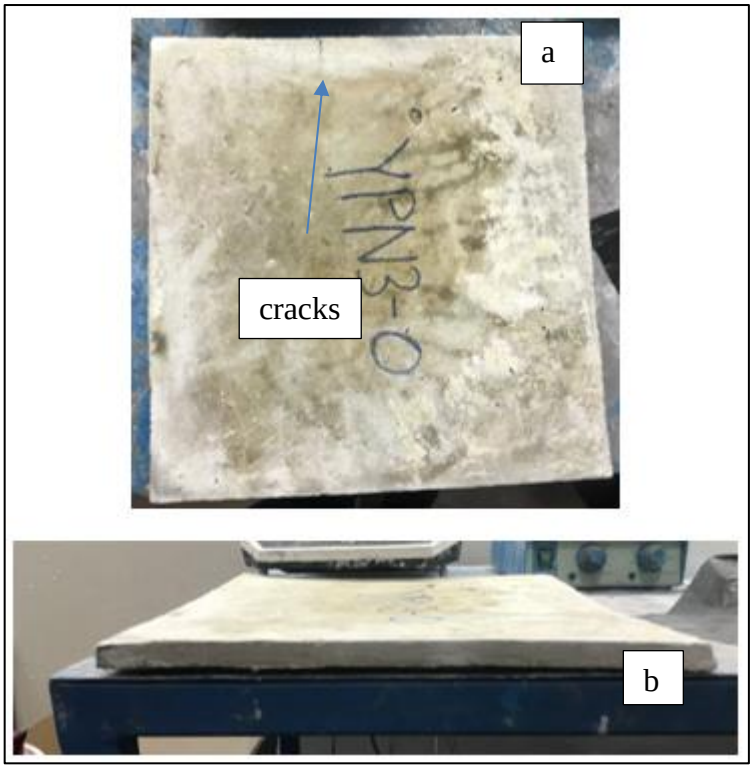

Figure 4.17. a) the cracks on GPN3-0 batch at the 90th day of production. a) GPN3-0 batch's deformation at 90th day of production.

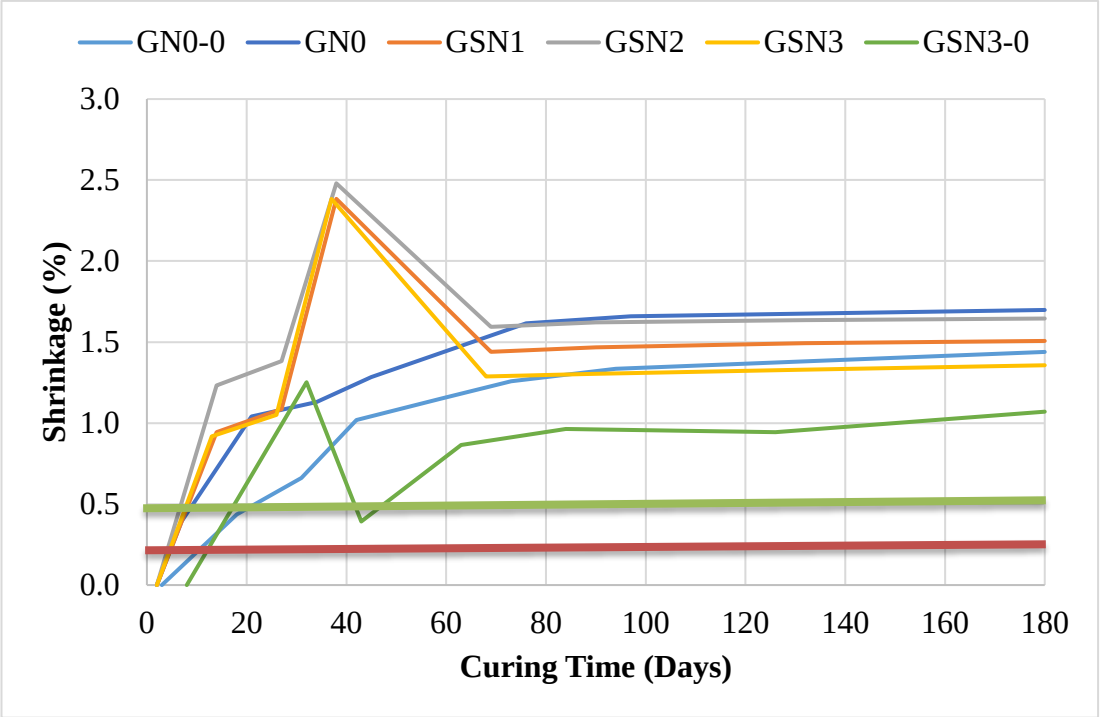

Figure 4.18. Shrinkage results of the N series batches made with GT and reinforced with steel fiber.

Figure 4-25 illustrates the shrinkage results of the N series batches made with GT and reinforced with steel fiber. The red and green lines in Figure 4-25 represent the starting of cracks and geometry deformation of the batches, respectively. Figure 4-25 results are discussed below:

- For the batches made with (WT + calcite), the maximum shrinkage appeared with GSN2 batch, and the maximum shrinkage was approximately 2.5%. reinforcing the batches made with GT led to increase the shrinkage.
- The carbonation leaching was one of the main reasons that led to increase the shrinkage as described in the flexural and compressive strengths section. Besides, the humidity inside the lab was low and led to accelerate the hydration of the liquid inside the matrix, due to this the shrinkage was increased over time.
- The cracks appeared on the surface as shown in Figure 4-26a when the shrinkage reaches approximately 0.2% for all the batches made with GT and reinforced with steel fiber. And the geometry deformation appeared on all the batches made with GT and reinforced with steel fiber as shown in Figure 4-

26b. The geometry deformation starts when the shrinkage reaches approximately 0.5% for all the batches made with GT.

- For the batches made with only GT, reinforcing the batches with 3% steel fiber (WSN3-0) led to a decrease in the maximum shrinkage (for the same reason from the 1st point) approxmatliy by 0.3% compared to the batch without any reinforcement (GN0-0).
- The shrinkage amount approximately remained constant for all the batches between the 90th and 180th days of production. This refers to the appearance of the final AAMs final products due to ending of the geo-polymerization reaction.

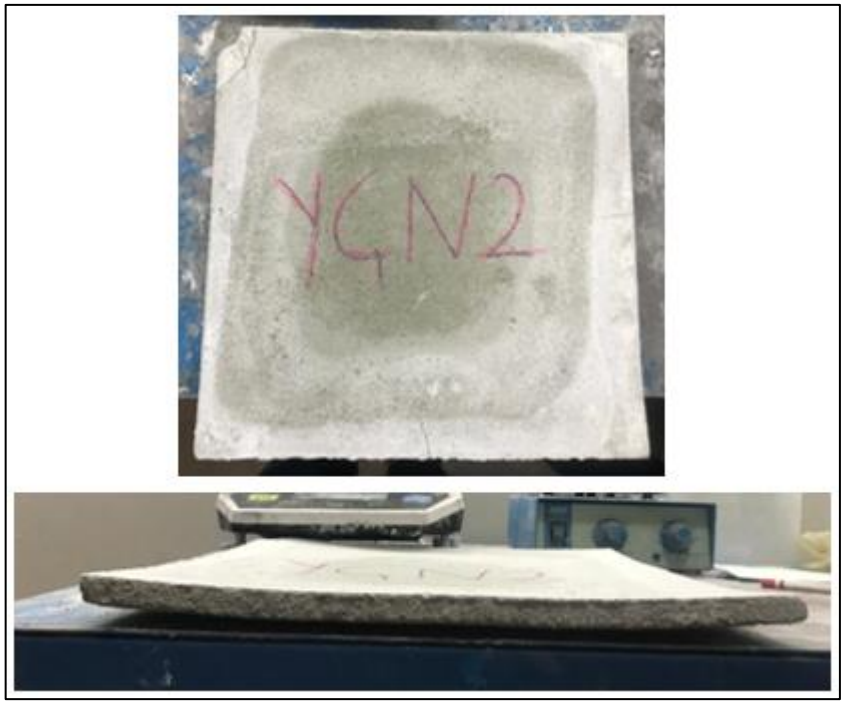

Figure 4.19. a) the cracks on GSN2 batch at the 90th day of production. a) GSN2 batch's deformation at 90th day of production.

4.5. ELECTROMAGNETIC PROPERTIES

Electromagnetic absorption and reflection features for all the batches in the N series were measured between the 28th and 56th days of production. For each type of fiber and tuff, two graphs were made to illustrate the absorption and reflection features. Figure 4-27, Figure 4-29, Figure 4-31, Figure 4-33, Figure 4-35, Figure 4-36, Figure

4-37, and Figure 4-38 are illustrating the results of absorption and reflection features of all the batches from the N series. Each figure shows the (reflection or absorption) values of a composite made with (WT or GT) reinforced with (PP fiber, steel fiber, or without any reinforcement). The evaluation and discussion of the electromagnetic properties start with the absorption values of all the batches from the N series. Then the reflection values of all the batches from the N series are evaluated and discased. The evaluation and discussion of the electromagnetic properties' values manly are focus on the ability of blocking the frequencies of 900 MHz (Mobiles frequencies), 1800 MHz (Mobiles frequencies), 2400 MHz (Bluetooth and Wi-Fi frequencies), and 5000 MHz (Wi-Fi frequencies) by absorbing or reflecting them considering the minim amount should be provided in dB to block those waves is -20 dB. After discussing each feature value (reflection or absorption) for all the batches from the N series, a comparison between the batches made with WT and GT, batches reinforced with PP and steel fiber, and batches made with and without calcite is presented. A comparison between the electromagnetic features of WT and GT was done in this section, as the molarity of the mixes do not affect the electromagnetic features.

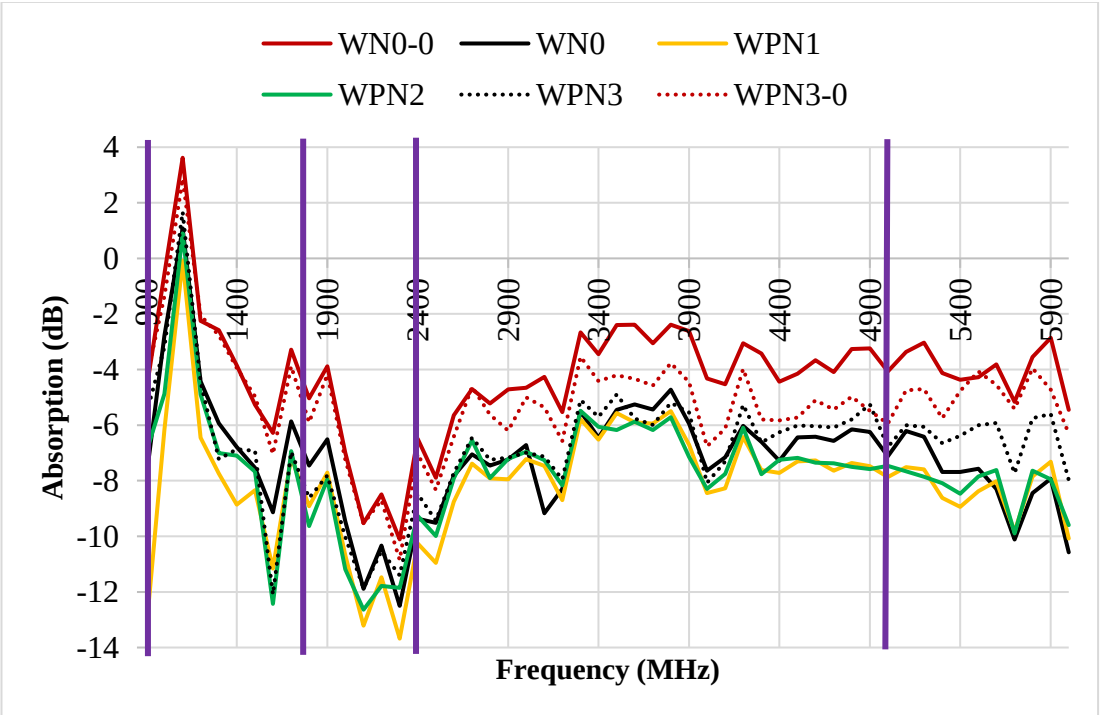

Figure 4.20. Absorption behavior of the N series batches made with WT and reinforced with PP fiber.

Figure 4.28. a) WPN1 tile at the 50th day of production, b) WPN2 tile, c) WPN3 tile at the 50th day of production.

Figure 4-27 illustrates the absorption behavior of the N series batches made with WT and reinforced with PP fiber. Figure 4-28 shows WPN1, WPN2, and WPN3 tiles. Figure 4-27 results are discussed below:

- The wave absorption amount of WN0-0, WN0, WPN1, WPN2, WPN3, and WPN3-0 batches at 900 MHz frequency were -4.72 dB, -7.84 dB, -13.3 dB, -6.96 dB, -5.59 dB, and -4.33 dB, respectively. WPN1 absorbed the highest amount of waves and increased the wave absorption by -5.46 dB comparing to the batch without PP fiber reinforcement (WN0). This refers to the assessment of this fiber to reduce the shrinkage of the samples leading to reduce cracks and permeability. However, increasing the PP fiber content led to a decrease in the absorption amount, as this fiber could transmit the waves because PP fiber has no electric-conductive behavior. Thus, the matrix of the samples was the main definer of the waves' absorption behavior. For the batches with and without calcite, WN0 and WPN3 batches absorbed -3.12 dB and -1.37 dB more than the WN0-0 and WPN3-0 batches, respectively. This refers to the high amount of CaO inside WN0 and WPN3 batches comparing to the amount of CaO inside WN0-0 and WPN3-0 batches. CaO is mainly provided to the batches from calcite, as CaO the main chemical component of the calcite. Thus, CaO had a positive effect on enhancing the wave absorption amount. However, as none of the batches mentioned above could absorb -20 dB at 900 MHz frequency, those batches are going to fail in blocking the wave produced by mobiles frequencies.

- The wave absorption amount of WN0-0, WN0, WPN1, WPN2, WPN3, and WPN3-0 batches at 1800 MHz frequency were -5.03 dB, -7.45 dB, -8.92 dB, -9.63 dB, -8.62 dB, and -5.9 dB, respectively. WPN2 absorbed the highest amount of waves and increased the wave absorption by -2.18 dB comparing to the batch without PP fiber reinforcement (WN0). This refers to the assessment of this fiber to reduce the shrinkage of the samples leading to reduce cracks and permeability. However, increasing the PP fiber content did not show a notable effect on the wave absorption, as this fiber could transmit the waves because PP fiber has no electric-conductive behavior. Thus, the matrix of the samples was the main definer of the waves' absorption behavior. For the batches with and without calcite, WN0 and WPN3 batches absorbed -2.42 dB and -2.72 dB more than the WN0-0 and WPN3-0 batches, respectively. This refers to the high amount of CaO inside WN0 and WPN3 batches comparing to the amount of CaO inside WN0-0 and WPN3-0 batches. CaO is mainly provided to the batches from calcite, as CaO the main chemical component of the calcite. Thus, CaO had a positive effect on enhancing the wave absorption amount. However, as none of the batches mentioned above could absorb -20 dB at 1800 MHz frequency, those batches are going to fail in blocking the wave produced by mobiles frequencies.
- The wave absorption amount of WN0-0, WN0, WPN1, WPN2, WPN3, and WPN3-0 batches at 2400 MHz frequency were -6.49 dB, -9.37 dB, -10.25 dB, -9.26 dB, -8.47 dB, and -7.03 dB, respectively. WPN1 absorbed the highest amount of waves and increased the wave absorption by -0.88 dB comparing to the batch without PP fiber reinforcement (WN0). This refers to the assessment of this fiber to reduce the shrinkage of the samples leading to reduce cracks and permeability. However, increasing the PP fiber content led to a decrease in the absorption amount, as this fiber could transmit the waves because PP fiber has no electric-conductive behavior. Thus, the matrix of the samples was the main definer of the waves' absorption behavior. For the batches with and without calcite, WN0 and WPN3 batches absorbed -2.88 dB and -1.44 dB more than the WN0-0 and WPN3-0 batches, respectively. This refers to the high amount of CaO inside WN0 and WPN3 batches comparing to the amount of CaO inside WN0-0 and WPN3-0 batches. CaO is mainly provided to the

batches from calcite, as CaO the main chemical component of the calcite. Thus, CaO had a positive effect on enhancing the wave absorption amount. However, as none of the batches mentioned above could absorb -20 dB at 2400 MHz frequency, those batches are going to fail in blocking the wave produced by Bluetooth and Wi-Fi frequencies.

- The wave absorption amount of WN0-0, WN0, WPN1, WPN2, WPN3, and WPN3-0 batches at 5000 MHz frequency were -4.07 dB, -7.12 dB, -7.87 dB, -7.46 dB, -6.79 dB, and -5.95 dB, respectively. WPN1 absorbed the highest amount of waves and increased the wave absorption by -0.75 dB comparing to the batch without PP fiber reinforcement (WN0). This refers to the assessment of this fiber to reduce the shrinkage of the samples leading to reduce cracks and permeability. However, increasing the PP fiber content did not show a notable effect on the wave absorption, as this fiber could transmit the waves because PP fiber has no electric-conductive behavior. Thus, the matrix of the samples was the main definer of the waves' absorption behavior. For the batches with and without calcite, WN0 and WPN3 batches absorbed -3.05 dB and -0.84 dB more than the WN0-0 and WPN3-0 batches, respectively. This refers to the high amount of CaO inside WN0 and WPN3 batches comparing to the amount of CaO inside WN0-0 and WPN3-0 batches. CaO is mainly provided to the batches from calcite, as CaO the main chemical component of the calcite. Thus, CaO had a positive effect on enhancing the wave absorption amount. However, as none of the batches mentioned above could absorb -20 dB at 5000 MHz frequency, those batches are going to fail in blocking the wave produced by Wi-Fi frequencies.

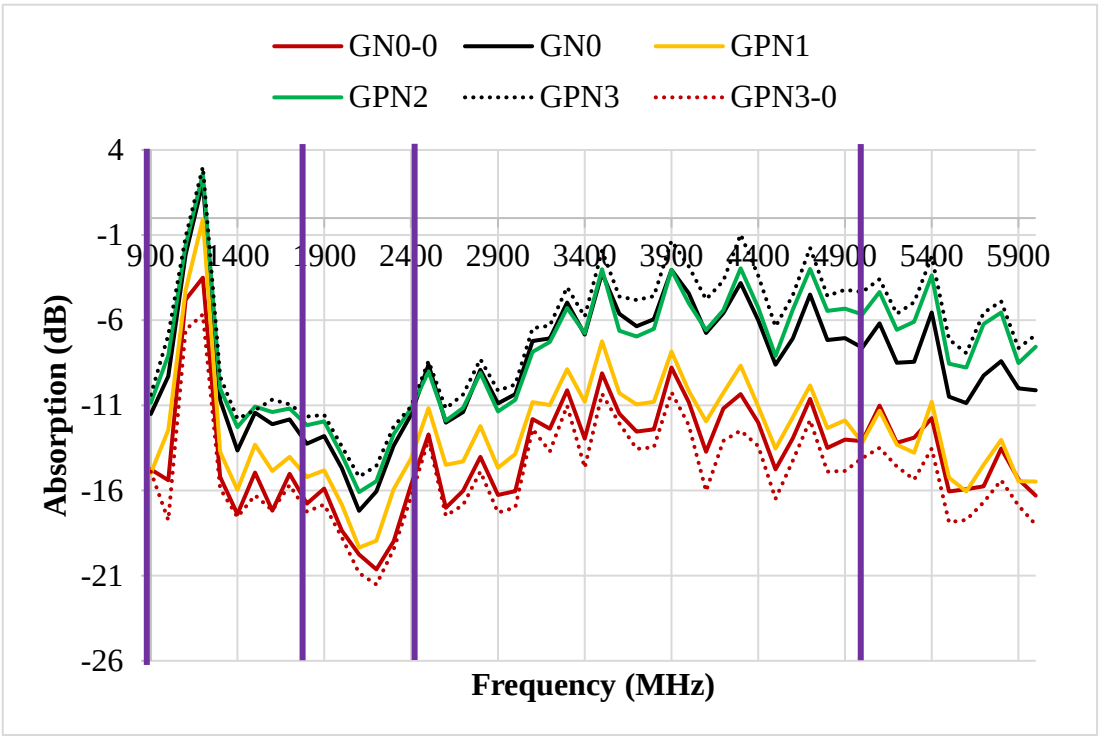

Figure 4.29. Absorption behavior of the N series batches made with GT and reinforced with PP fiber.

Figure 4.21. a) GPN1 tile. b) GPN2 tile at the 50th day of production. c) GPN3 tile at the 50th day of production.

Figure 4-29 illustrates the absorption behavior of the N series batches made with GT and reinforced with PP fiber. Figure 4-30 shows GPN1, GPN2, and GPN3 tiles. Figure 4-29 results are discussed below:

- The wave absorption amount of GN0-0, GN0, GPN1, GPN2, GPN3, and GPN3-0 batches at 900 MHz frequency were -14.76 dB, -11.51 dB, -14.98 dB, -10.84 dB, -10.38 dB, and -14.89 dB, respectively. GPN1 absorbed the highest amount of waves and increased the wave absorption by -3.47 dB comparing to the batch without PP fiber reinforcement (GN0). This refers to the assessment of this fiber to reduce the shrinkage of the samples leading to reduce cracks and permeability. However, increasing the PP fiber content did not show a notable effect on the wave absorption, as this fiber could transmit the waves because PP fiber has no electric-conductive behavior. Thus, the matrix of the samples was the main definer of the waves' absorption behavior. For the batches with and without calcite, GN0 and GPN3 batches absorbed -3.25 dB and -4.51 dB less than the GN0-0 and GPN3-0 batches, respectively. This refers to the high amount of oxides as SiO_2, Al_2O_3, and Fe_2O_3 inside GN0-0 and GPN3-0 batches comparing to the amount of the same materials inside GN0 and GPN3 batches. Oxides are mainly provided to the batches from GT, as SiO_2, Al_2O_3, and Fe_2O_3 are the main chemical component of the GT. Thus, high amount of Oxides had a positive effect on enhancing the wave absorption amount. However, as none of the batches mentioned above could absorb -20 dB at 900 MHz frequency, those batches are going to fail in blocking the wave produced by mobiles frequencies.
- The wave absorption amount of GN0-0, GN0, GPN1, GPN2, GPN3, and GPN3-0 batches at 1800 MHz frequency were -16.77 dB, -13.25 dB, -15.21 dB, -12.16 dB, -11.65 dB, and -17.24 dB, respectively. GPN1 absorbed the highest amount of waves and increased the wave absorption by -1.96 dB comparing to the batch without PP fiber reinforcement (GN0). This refers to the assessment of this fiber to reduce the shrinkage of the samples leading to reduce cracks and permeability. However, increasing the PP fiber content did not show a notable effect on the wave absorption, as this fiber could transmit the waves because PP fiber has no electric-conductive behavior. Thus, the matrix of the samples was the main definer of the waves' absorption behavior. For the batches with and without calcite, GN0 and GPN3 batches absorbed -3.45 dB and -5.59 dB less than the GN0-0 and GPN3-0 batches, respectively. This refers to the high amount of oxides as SiO_2, Al_2O_3, and Fe_2O_3 inside GN0-

0 and GPN3-0 batches comparing to the amount of the same materials inside GN0 and GPN3 batches. Oxides are mainly provided to the batches from GT, as SiO_2, Al_2O_3, and Fe_2O_3 are the main chemical component of the GT. Thus, high amount of Oxides had a positive effect on enhancing the wave absorption amount. However, as none of the batches mentioned above could absorb -20 dB at 1800 MHz frequency, those batches are going to fail in blocking the wave produced by mobiles frequencies.

- The wave absorption amount of GN0-0, GN0, GPN1, GPN2, GPN3, and GPN3-0 batches at 1800 MHz frequency were -15.69 dB, -11.56 dB, -14.14 dB, -11.18 dB, -11.07 dB, and -16.39 dB, respectively. GPN1 absorbed the highest amount of waves and increased the wave absorption by -2.58 dB comparing to the batch without PP fiber reinforcement (GN0). This refers to the assessment of this fiber to reduce the shrinkage of the samples leading to reduce cracks and permeability. However, increasing the PP fiber content did not show a notable effect on the wave absorption, as this fiber could transmit the waves because PP fiber has no electric-conductive behavior. Thus, the matrix of the samples was the main definer of the waves' absorption behavior. For the batches with and without calcite, GN0 batch absorbed -4.13 dB less than GN0-0 batch and the wave absorption amount for GPN3 and GPN3-0 batches were approximately the same. This refers to the high amount of oxides as SiO2, Al2O3, and Fe2O3 inside GN0-0 and GPN3-0 batches comparing to the amount of the same materials inside GN0 and GPN3 batches. Oxides are mainly provided to the batches from GT, as SiO_2, Al_2O_3, and Fe_2O_3 are the main chemical component of the GT. Thus, high amount of Oxides had a positive effect on enhancing the wave absorption amount. However, as none of the batches mentioned above could absorb -20 dB at 2400 MHz frequency, those batches are going to fail in blocking the wave produced by Bluetooth and Wi-Fi frequencies.
- The wave absorption amount of GN0-0, GN0, GPN1, GPN2, GPN3, and GPN3-0 batches at 5000 MHz frequency were -13.1 dB, -7.62 dB, -13.17 dB, -5.66 dB, -4.35 dB, and -14.09 dB, respectively. GPN1 absorbed the highest amount of waves and increased the wave absorption by -5.55 dB comparing to the batch without PP fiber reinforcement (GN0). This refers to the assessment

of this fiber to reduce the shrinkage of the samples leading to reduce cracks and permeability. However, increasing the PP fiber content did not show a notable effect on the wave absorption, as this fiber could transmit the waves because PP fiber has no electric-conductive behavior. Thus, the matrix of the samples was the main definer of the waves' absorption behavior. For the batches with and without calcite, GN0 and GPN3 batches absorbed -5.48 dB and -9.74 dB less than the GN0-0 and GPN3-0 batches, respectively. This refers to the high amount of oxides as SiO_2, Al_2O_3, and Fe_2O_3 inside GN0-0 and GPN3-0 batches comparing to the amount of the same materials inside GN0 and GPN3 batches. Oxides are mainly provided to the batches from GT, as SiO_2, Al_2O_3, and Fe_2O_3 are the main chemical component of the GT. Thus, high amount of Oxides had a positive effect on enhancing the wave absorption amount. However, as none of the batches mentioned above could absorb -20 dB at 5000 MHz frequency, those batches are going to fail in blocking the wave produced by Wi-Fi frequencies.

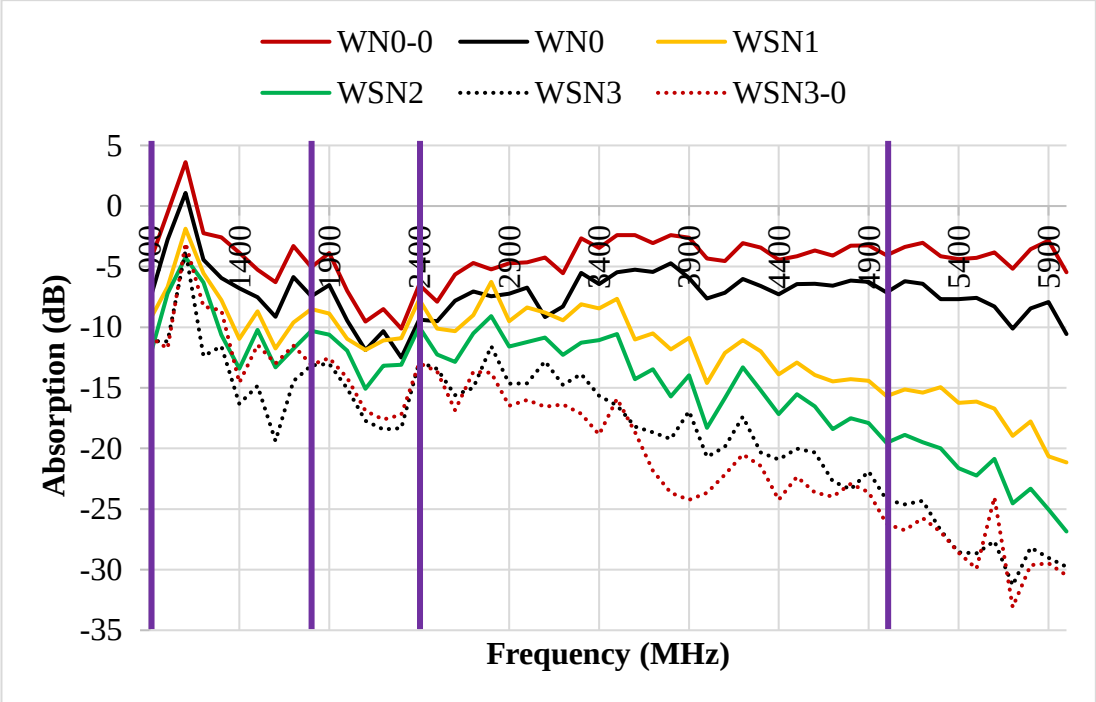

Figure 4.22. Absorption behavior of the N series batches made with WT and reinforced with steel fiber.

Figure 4.23. a) WSN1 tile at the 50th day of production. b) WSN2 tile. c) WSN3 tile at the 50th day of production.

Figure 4-31 illustrates the absorption behavior of the N series batches made with WT and reinforced with steel fiber. Figure 4-32 shows WSN1, WSN2, and WSN3 tiles. Figure 4-31 results are discussed below:

- The wave absorption amount of WN0-0, WN0, WSN1, WSN2, WSN3, and WSN3-0 batches at 900 MHz frequency were -4.72 dB, -7.84 dB, -9.44 dB, -12.55 dB, -11.14 dB, and -10.80 dB, respectively. WSN2 absorbed the highest amount of waves and increased the wave absorption by -4.71 dB comparing to the batch without steel fiber reinforcement (WN0). Reinforcement of the samples with the steel fiber did a notable effect on enhancing the absorption behavior of the samples. This refers to the electric-conductivity behavior of this fiber. Steel fiber is a metallic material that has good electric-conductivity behavior. Besides, increasing the steel fiber percentage led to increase the wave absorption amount. For the batches with and without calcite, WN0 and WSN3 batches absorbed -3.12 dB and -0.34 dB more than the WN0-0 and WSN3-0 batches, respectively. This refers to the high amount of CaO inside WN0 and WSN3 batches comparing to the amount of CaO inside WN0-0 and WSN3-0 batches. CaO is mainly provided to the batches from calcite, as CaO the main chemical component of the calcite. Thus, CaO had a positive effect on enhancing the wave absorption amount. However, as none of the batches mentioned above could absorb -20 dB at 900 MHz frequency, those batches are going to fail in blocking the wave produced by mobiles frequencies.

- The wave absorption amount of WN0-0, WN0, WSN1, WSN2, WSN3, and WSN3-0 batches at 1800 MHz frequency were -5.03 dB, -7.45 dB, -8.49 dB, -10.29 dB, -13.15 dB, and -13.10 dB, respectively. WSN3 absorbed the highest amount of waves and increased the wave absorption by -5.7 dB comparing to the batch without steel fiber reinforcement (WN0). Reinforcement of the samples with the steel fiber did a notable effect on enhancing the absorption behavior of the samples. This refers to the electric-conductivity behavior of this fiber. Steel fiber is a metallic material that has good electric-conductivity behavior. Besides, increasing the steel fiber percentage led to increase the wave absorption amount. For the batches with and without calcite, WN0 and WSN3 batches absorbed -2.42 dB and -0.5 dB more than the WN0-0 and WSN3-0 batches, respectively. This refers to the high amount of CaO inside WN0 and WSN3 batches comparing to the amount of CaO inside WN0-0 and WSN3-0 batches. CaO is mainly provided to the batches from calcite, as CaO the main chemical component of the calcite. Thus, CaO had a positive effect on enhancing the wave absorption amount. However, as none of the batches mentioned above could absorb -20 dB at 1800 MHz frequency, those batches are going to fail in blocking the wave produced by mobiles frequencies.
- The wave absorption amount of WN0-0, WN0, WSN1, WSN2, WSN3, and WSN3-0 batches at 2400 MHz frequency were -6.49 dB, -9.37 dB, -7.70 dB, -9.98 dB, -12.85 dB, and -12.96 dB, respectively. WSN3 absorbed the highest amount of waves and increased the wave absorption by -3.48 dB comparing to the batch without steel fiber reinforcement (WN0). Reinforcement of the samples with the steel fiber did a notable effect on enhancing the absorption behavior of the samples. This refers to the electric-conductivity behavior of this fiber. Steel fiber is a metallic material that has good electric-conductivity behavior. Besides, increasing the steel fiber percentage led to increase the wave absorption amount. For the batches with and without calcite, WN0 batch absorbed -2.88 dB more than WN0-0 batch and the wave absorption amount for WSN3 and WSN3-0 batches were approximately the same. This refers to the high amount of CaO inside WN0 and WSN3 batches comparing to the amount of CaO inside WN0-0 and WSN3-0 batches. CaO is mainly provided to the batches from calcite, as CaO the main chemical component of the calcite.

Thus, CaO had a positive effect on enhancing the wave absorption amount. However, as none of the batches mentioned above could absorb -20 dB at 2400 MHz frequency, those batches are going to fail in blocking the wave produced by Bluetooth and Wi-Fi frequencies.

- The wave absorption amount of WN0-0, WN0, WSN1, WSN2, WSN3, and WSN3-0 batches at 5000 MHz frequency were -4.07 dB, -7.12 dB, -15.68 dB, -19.53 dB, -24.23 dB, and -26.21 dB, respectively. WSN3 absorbed the highest amount of waves and increased the wave absorption by -17.11 dB comparing to the batch without steel fiber reinforcement (WN0). Reinforcement of the samples with the steel fiber did a notable effect on enhancing the absorption behavior of the samples. This refers to the electric-conductivity behavior of this fiber. Steel fiber is a metallic material that has good electric-conductivity behavior. Besides, increasing the steel fiber percentage led to increase the wave absorption amount. For the batches with and without calcite, WN0 batch absorbed -3.07 dB more than WN0-0 batch. This refers to the high amount of CaO inside WN0 and WSN3 batches comparing to the amount of CaO inside WN0-0 and WSN3-0 batches. CaO is mainly provided to the batches from calcite, as CaO the main chemical component of the calcite. Thus, CaO had a positive effect on enhancing the wave absorption amount. WSN3 batch absorbed -1.98 dB less than WSN3-0 batch. This refers to the random distribution of the steel fiber. WSN3 and WSN3-0 batches can absorbs more than -20 dB at 5000 MHz frequency. Thus, those batches are going to succeed in blocking the wave produced by Wi-Fi frequencies.

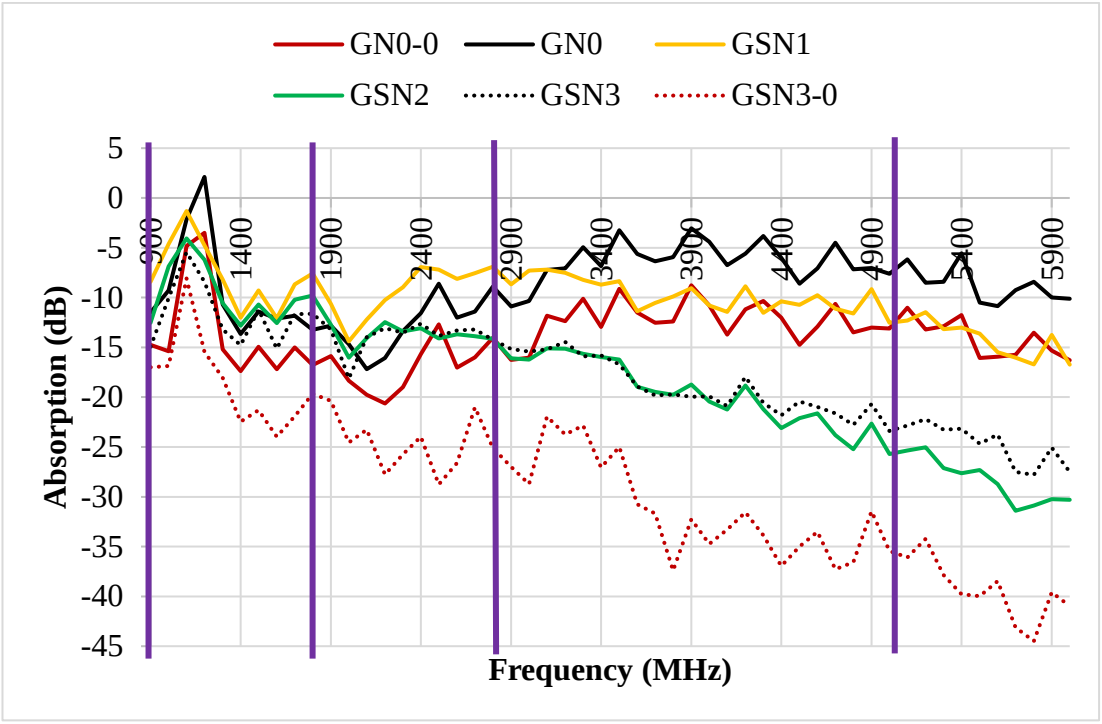

Figure 4.24. Absorption behavior of the N series batches made with GT and reinforced with steel fiber.

Figure 4.25. a) GSN1 tile. b) GSN2 tile at the 50th day of production. c) GSN3 tile at the 50th day of production.

Figure 4-33 illustrates the absorption behavior of the N series batches made with GT and reinforced with steel fiber. Figure 4-34 shows GSN1, GSN2, and GSN3 tiles. Figure 4-33 results are discussed below:

- The wave absorption amount of GN0-0, GN0, GSN1, GSN2, GSN3, and GSN3-0 batches at 900 MHz frequency were -14.76 dB, -11.51 dB, -8.40 dB,

-12.53 dB, -14.93 dB, and -16.99 dB, respectively. GSN3 absorbed the highest amount of waves and increased the wave absorption by -3.42 dB comparing to the batch without steel fiber reinforcement (GN0). Reinforcement of the samples with the steel fiber did a notable effect on enhancing the absorption behavior of the samples. This refers to the electric-conductivity behavior of this fiber. Steel fiber is a metallic material that has good electric-conductivity behavior. Besides, increasing the steel fiber percentage led to increase the wave absorption amount. For the batches with and without calcite, GN0 and GSN3 batches absorbed -3.25 dB and -2.06 dB less than the GN0-0 and GSN3-0 batches, respectively. This refers to the high amount of oxides as SiO_2, Al_2O_3, and Fe_2O_3 inside GN0-0 and GSN3-0 batches comparing to the amount of the same materials inside GN0 and GSN3 batches. Oxides are mainly provided to the batches from GT, as SiO_2, Al_2O_3, and Fe_2O_3 are the main chemical component of the GT. Thus, high amount of Oxides had a positive effect on enhancing the wave absorption amount. However, as none of the batches mentioned above could absorb -20 dB at 900 MHz frequency, those batches are going to fail in blocking the wave produced by mobiles frequencies.

- The wave absorption amount of GN0-0, GN0, GSN1, GSN2, GSN3, and GSN3-0 batches at 1800 MHz frequency were -16.77 dB, -13.25 dB, -7.57 dB, -9.80 dB, -11.63 dB, and -19.67 dB, respectively. GSN0 absorbed the highest amount of waves comparing to the batches with steel fiber reinforcement at 1800 MHz frequency. Nevertheless, in general reinforcement of the samples with the steel fiber makes a notable effect on enhancing the absorption behavior of the samples. This refers to the electric-conductivity behavior of this fiber. Steel fiber is a metallic material that has good electric-conductivity behavior. For the batches with and without calcite, GN0 and GSN3 batches absorbed -3.52 dB and -8.04 dB less than the GN0-0 and GSN3-0 batches, respectively. This refers to the high amount of oxides as SiO_2, Al_2O_3, and Fe_2O_3 inside GN0-0 and GSN3-0 batches comparing to the amount of the same materials inside GN0 and GSN3 batches. Oxides are mainly provided to the batches from GT, as SiO_2, Al_2O_3, and Fe_2O_3 are the main chemical component of the GT. Thus, high amount of Oxides had a positive effect on enhancing the wave absorption amount. However, as none of the batches mentioned above could absorb -20

dB at 1800 MHz frequency, those batches are going to fail in blocking the wave produced by mobiles frequencies.

- The wave absorption amount of GN0-0, GN0, GSN1, GSN2, GSN3, and GSN3-0 batches at 2400 MHz frequency were -15.69 dB, -11.56 dB, -6.93 dB, -13.07 dB, -12.62 dB, and -23.97 dB, respectively. GSN2 absorbed the highest amount of waves and increased the wave absorption by -1.51 dB comparing to the batch without steel fiber reinforcement (GN0). Reinforcement of the samples with the steel fiber did a notable effect on enhancing the absorption behavior of the samples. This refers to the electric-conductivity behavior of this fiber. Steel fiber is a metallic material that has good electric-conductivity behavior. Besides, increasing the steel fiber percentage led to increase the wave absorption amount. For the batches with and without calcite, GN0 and GSN3 batches absorbed -4.13 dB and -11.35 dB less than the GN0-0 and GSN3-0 batches, respectively. This refers to the high amount of oxides as SiO_2, Al_2O_3, and Fe_2O_3 inside GN0-0 and GSN3-0 batches comparing to the amount of the same materials inside GN0 and GSN3 batches. Oxides are mainly provided to the batches from GT, as SiO_2, Al_2O_3, and Fe_2O_3 are the main chemical component of the GT. Thus, high amount of Oxides had a positive effect on enhancing the wave absorption amount. GSN3-0 batch can absorbs more than -20 dB at 2400 MHz frequency. Thus, GSN3-0 batch is going to succeed in blocking the wave produced by Bluetooth and Wi-Fi frequencies.
- The wave absorption amount of GN0-0, GN0, GSN1, GSN2, GSN3, and GSN3-0 batches at 5000 MHz frequency were -13.1 dB, -7.62 dB, -12.54 dB, -25.71 dB, -23.38 dB, and -35.45 dB, respectively. GSN2 absorbed the highest amount of waves and increased the wave absorption by -18.09 dB comparing to the batch without steel fiber reinforcement (GN0). Reinforcement of the samples with the steel fiber did a notable effect on enhancing the absorption behavior of the samples. This refers to the electric-conductivity behavior of this fiber. Steel fiber is a metallic material that has good electric-conductivity behavior. Besides, increasing the steel fiber percentage led to increase the wave absorption amount. For the batches with and without calcite, GN0 and GSN3 batches absorbed -5.48 dB and -12.12 dB less than GN0-0 and GSN3-0 batches, respectively. This refers to the high amount of oxides as SiO_2, Al_2O_3,

and Fe_2O_3 inside GN0-0 and GSN3-0 batches comparing to the amount of the same materials inside GN0 and GSN3 batches. Oxides are mainly provided to the batches from GT, as SiO_2, Al_2O_3, and Fe_2O_3 are the main chemical component of the GT. Thus, high amount of Oxides had a positive effect on enhancing the wave absorption amount. GSN2, GSN3, and GSN3-0 batches can absorb more than -20 dB at 2400 MHz frequency. Thus, those batches are going to succeed in blocking the wave produced by Wi-Fi frequencies.

The following could be observed from the wave absorption behavior of all the batches in the N series:

- Generally, the batches reinforced with steel fiber had a better performance regarding the wave absorption comparing to the batches reinforced with PP fiber. This refers to the electric-conductivity behavior of this fiber. Steel fiber is a metallic material that has good electric-conductivity behavior. However, the PP fiber content did not show a notable effect on increasing the wave absorption, as this fiber could transmit the waves because PP fiber has no electric-conductive behavior. And the matrix of the samples reinforced with PP fiber was the main definer of the waves' absorption behavior.
- Generally, the batches made with GT had a better performance regarding the wave absorption comparing to the batches made with WT. This refers to the chemical components of GT and WT. GT have a higher amount of CaO comparing to the WT, which could give a positive contribution in wave absorption.
- Generally, for the batches made with WT, the batches made with calcite had a better performance regarding the wave absorption comparing to the batches made without calcite. This refers to the high amount of CaO inside batches with calcite comparing to the amount of CaO inside the batches without calcite. CaO is mainly provided to the batches from calcite, as CaO the main chemical component of the calcite.
- Generally, for the batches made with GT, the batches made with calcite had a worse performance regarding the wave absorption comparing to the batches made without calcite. This refers to the high amount of oxides as SiO2, Al2O3,

and Fe2O3 inside the batches without calcite comparing to the amount of the same materials inside the batches with calcite. Oxides are mainly provided to the batches from GT, as SiO_2, Al_2O_3, and Fe_2O_3 are the main chemical component of the GT. Thus, high amount of Oxides had a positive effect on enhancing the wave absorption amount.

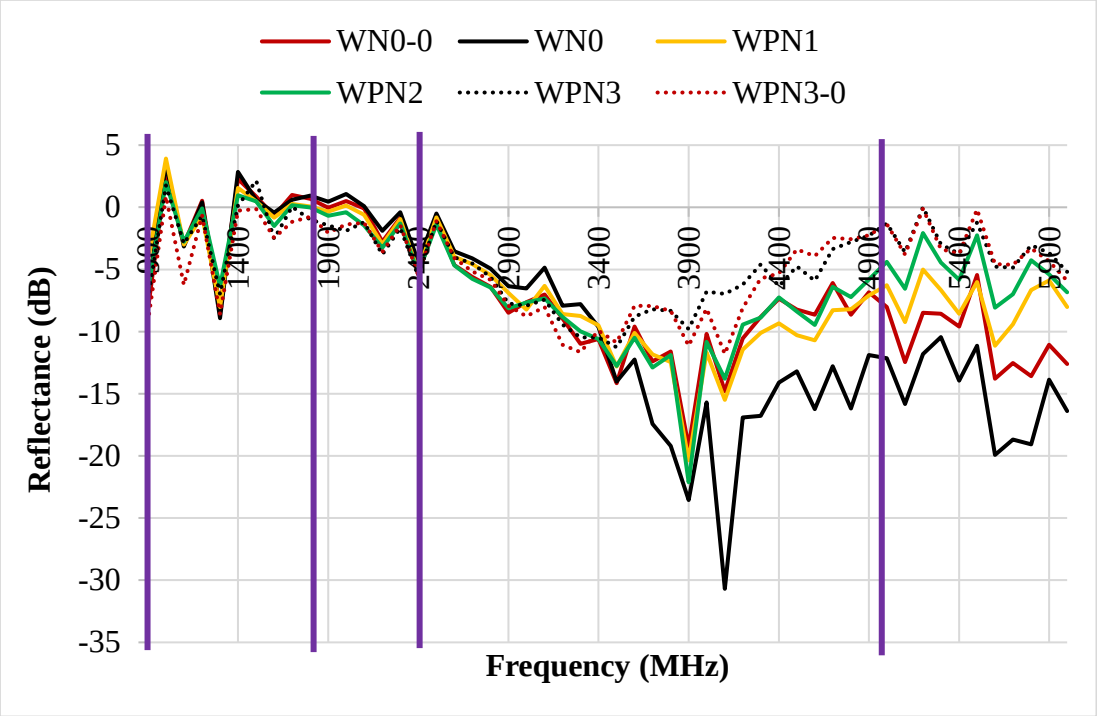

Figure 4.26. Reflection behavior of the N series batches made with WT and reinforced with PP fiber.

Figure 4-35 illustrates the reflection behavior of the N series batches made with WT and reinforced with PP fiber. Figure 4-35 results are discussed below:

- The wave reflection amount of WN0-0, WN0, WPN1, WPN2, WPN3, and WPN3-0 batches at 900 MHz frequency were -8.24 dB, -7.00 dB, -4.36 dB, -6.7 dB, -7.43 dB, and -9.23 dB, respectively. WPN3 reflected the highest amount of waves and increased the wave reflection by -0.43 dB comparing to the batch without PP fiber reinforcement (WN0). This refers to the assessment of this fiber to reduce the shrinkage of the samples leading to reduce cracks and permeability. However, this fiber had no major effect on the reflection amount, as this fiber could transmit the waves because PP fiber has no electric-

conductive behavior. Thus, the matrix of the samples was the main definer of the waves' reflection behavior. For the batches with and without calcite, WN0, WN0-0, WPN3, and WPN3-0 had approximately the same amount of wave reflection, and the wave reflection range was between ((-7.00 dB) - (-9.23 dB)). This difference in reflection was not significant, thus the calcite did not have a major effect on the reflection behavior. However, as none of the batches mentioned above could absorb -20 dB at 900 MHz frequency, those batches are going to fail in blocking the wave produced by mobiles frequencies.

- The wave reflection amount of WN0-0, WN0, WPN1, WPN2, WPN3, and WPN3-0 batches at 900 MHz frequency were 0.69 dB, 0.94 dB, 0.07 dB, -0.01 dB, -1 dB, and -0.77 dB, respectively. WPN3 reflected the highest amount of waves and increased the wave reflection by -1.94 dB comparing to the batch without PP fiber reinforcement (WN0). This refers to the assessment of this fiber to reduce the shrinkage of the samples leading to reduce cracks and permeability. However, this fiber had no major effect on the reflection amount, as this fiber could transmit the waves because PP fiber has no electric-conductive behavior. Thus, the matrix of the samples was the main definer of the waves' reflection behavior. For the batches with and without calcite, WN0, WN0-0, WPN3, and WPN3-0 had approximately the same amount of wave reflection, and the wave reflection range was between ((-1 dB) - (0.94 dB)).. This difference in reflection was not significant, thus the calcite did not have a major effect on the reflection behavior. However, as none of the batches mentioned above could absorb -20 dB at 1800 MHz frequency, those batches are going to fail in blocking the wave produced by mobiles frequencies.
- The wave reflection amount of WN0-0, WN0, WPN1, WPN2, WPN3, and WPN3-0 batches at 2400 MHz frequency were -5.41 dB, -4.34 dB, -5.17 dB, -5.3 dB, -5.52 dB, and -5.43 dB, respectively. WPN3 reflected the highest amount of waves and increased the wave reflection by -1.18 dB comparing to the batch without PP fiber reinforcement (WN0). This refers to the assessment of this fiber to reduce the shrinkage of the samples leading to reduce cracks and permeability. However, this fiber had no major effect on the reflection amount, as this fiber could transmit the waves because PP fiber has no electric-conductive behavior. Thus, the matrix of the samples was the main definer of

the waves' reflection behavior. For the batches with and without calcite, WN0, WN0-0, WPN3, and WPN3-0 had approximately the same amount of wave reflection, and the wave reflection range was between ((-4.34 dB) - (-5.52 dB)). This difference in reflection was not significant, thus the calcite did not have a major effect on the reflection behavior. However, as none of the batches mentioned above could absorb -20 dB at 2400 MHz frequency, those batches are going to fail in blocking the wave produced by Bluetooth and Wi-Fi frequencies.

- The wave reflection amount of WN0-0, WN0, WPN1, WPN2, WPN3, and WPN3-0 batches at 5000 MHz frequency were -8.02 dB, -12.15 dB, -6.27 dB, -4.38 dB, -1.3 dB, and -1.35 dB, respectively. WPN0 reflected the highest amount of waves comparing to the batch with PP fiber reinforcement. PP fiber decreased the reflection amount, as this fiber could transmit the waves because PP fiber has no electric-conductive behavior. Thus, the matrix of the samples was the main definer of the waves' reflection behavior. For the batches with and without calcite, WN0 batch reflected -4.13 dB more than WN0-0 and WPN3, and WPN3-0 batches had approximately the same reflection amount. This difference in reflection was not significant, thus the calcite did not have a major effect on the reflection behavior. However, as none of the batches mentioned above could absorb -20 dB at 5000 MHz frequency, those batches are going to fail in blocking the wave produced by Wi-Fi frequencies.

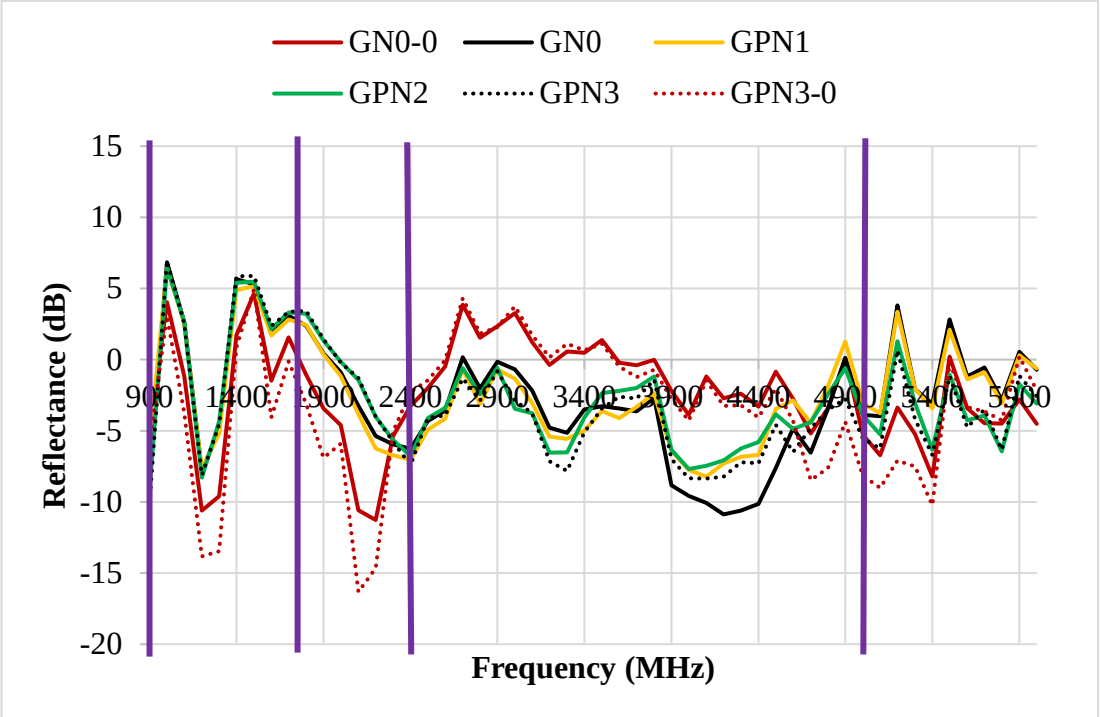

Figure 4.27. Reflection behavior of the N series batches made with GT and reinforced with PP fiber.

Figure 4-36 illustrates the reflection behavior of the N series batches made with GT and reinforced with PP fiber. Figure 4-36 results are discussed below:

- The wave reflection amount of GN0-0, GN0, GPN1, GPN2, GPN3, and GPN3-0 batches at 900 MHz frequency were -5.18 dB, -8.22 dB, -5.89 dB, -9.23 dB, -10.15 dB, and -5.89 dB, respectively. GPN3 reflected the highest amount of waves and increased the wave reflection by -1.93 dB comparing to the batch without PP fiber reinforcement (GN0). This refers to the assessment of this fiber to reduce the shrinkage of the samples leading to reduce cracks and permeability. However, this fiber had no major effect on the reflection amount, as this fiber could transmit the waves because PP fiber has no electric-conductive behavior. Thus, the matrix of the samples was the main definer of the waves' reflection behavior. For the batches with and without calcite, GN0 and GPN3 batches absorbed -3.04 dB and -4.26 dB more than the GN0-0 and GPN3-0 batches, respectively. This refers to the high amount of CaO inside GN0 and GPN3 batches comparing to the amount of CaO inside GN0-0 and GPN3-0 batches. CaO is mainly provided to the batches from calcite, as CaO

the main chemical component of the calcite. Thus, CaO had a positive effect on enhancing the wave absorption amount. However, as none of the batches mentioned above could absorb -20 dB at 900 MHz frequency, those batches are going to fail in blocking the wave produced by mobiles frequencies.

- The wave reflection amount of GN0-0, GN0, GPN1, GPN2, GPN3, and GPN3-0 batches at 1800 MHz frequency were -1.07 dB, 2.36 dB, 2.43 dB, 3.23 dB, 3.42 dB, and -3.12 dB, respectively. GPN0 reflected the highest amount of waves comparing to the batch with PP fiber reinforcement. PP fiber decreased the reflection amount, as this fiber could transmit the waves because PP fiber has no electric-conductive behavior. Thus, the matrix of the samples was the main definer of the waves' reflection behavior. For the batches with and without calcite, GN0, GN0-0, GPN3, and GPN3-0 had approximately the same amount of wave reflection. And as the difference in reflection was not significant, the calcite did not have a major effect on the reflection behavior. However, as none of the batches mentioned above could absorb -20 dB at 1800 MHz frequency, those batches are going to fail in blocking the wave produced by mobiles frequencies.
- The wave reflection amount of GN0-0, GN0, GPN1, GPN2, GPN3, and GPN3-0 batches at 2400 MHz frequency were -3.25 dB, -6.27 dB, -7.04 dB, -6.78 dB, -7.42 dB, and -2.27 dB, respectively. GPN3 reflected the highest amount of waves and increased the wave reflection by -1.15 dB comparing to the batch without PP fiber reinforcement (GN0). This refers to the assessment of this fiber to reduce the shrinkage of the samples leading to reduce cracks and permeability. However, this fiber had no major effect on the reflection amount, as this fiber could transmit the waves because PP fiber has no electric-conductive behavior. Thus, the matrix of the samples was the main definer of the waves' reflection behavior. For the batches with and without calcite, GN0 and GPN3 batches absorbed -3.02 dB and -5.15 dB more than the GN0-0 and GPN3-0 batches, respectively. This refers to the high amount of CaO inside GN0 and GPN3 batches comparing to the amount of CaO inside GN0-0 and GPN3-0 batches. CaO is mainly provided to the batches from calcite, as CaO the main chemical component of the calcite. Thus, CaO had a positive effect on enhancing the wave absorption amount. However, as none of the batches

mentioned above could absorb -20 dB at 900 MHz frequency, those batches are going to fail in blocking the wave produced by Bluetooth and Wi-Fi frequencies.

- The wave reflection amount of GN0-0, GN0, GPN1, GPN2, GPN3, and GPN3-0 batches at 5000 MHz frequency were -5.28 dB, -3.89 dB, -3.07 dB, -3.91 dB, -5.55 dB, and -8.15 dB, respectively. GPN3 reflected the highest amount of waves and increased the wave reflection by -1.66 dB comparing to the batch without PP fiber reinforcement (GN0). This refers to the assessment of this fiber to reduce the shrinkage of the samples leading to reduce cracks and permeability. However, this fiber had no major effect on the reflection amount, as this fiber could transmit the waves because PP fiber has no electric-conductive behavior. Thus, the matrix of the samples was the main definer of the waves' reflection behavior. For the batches with and without calcite, GN0, GN0-0, GPN3, and GPN3-0 had approximately the same amount of wave reflection. And as the difference in reflection was not significant, the calcite did not have a major effect on the reflection behavior. However, as none of the batches mentioned above could absorb -20 dB at 5000 MHz frequency, those batches are going to fail in blocking the wave produced by Wi-Fi frequencies.

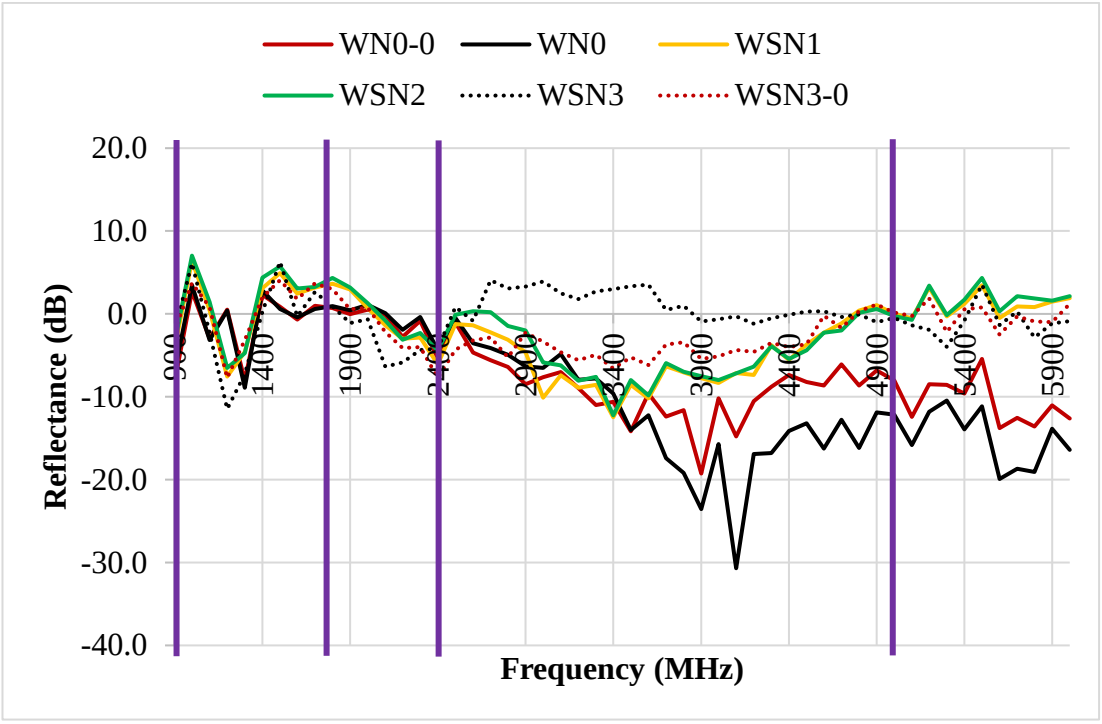

Figure 4.28. Reflection behavior of the N series batches made with WT and reinforced with steel fiber.

Figure 4-37 illustrates the reflection behavior of the N series batches made with WT and reinforced with steel fiber. Figure 4-37 results are discussed below:

- The wave reflection amount of WN0-0, WN0, WSN1, WSN2, WSN3, and WSN3-0 batches at 900 MHz frequency were -8.24 dB, -7.00 dB, -4.24 dB, -3.54 dB, -2.09 dB, and -2.07 dB, respectively. WN0 reflected the highest amount of waves comparing to the batch without steel fiber reinforcement. Steel fiber worked well as an electromagnetic wave absorber and absorbed the electric part due to its good electric-conductivity behavior. However, steel fiber did not work well with the magnetics parts leading to a decrease in the wave reflection. Thus, the matrix of the samples was the main definer of the waves' reflection behavior. For the batches with and without calcite, WN0, WN0-0, WSN3, and WSN3-0 had approximately the same amount of wave reflection. And as the difference in reflection was not significant, the calcite did not have a major effect on the reflection behavior. However, as none of the batches mentioned above could absorb -20 dB at 900 MHz frequency, those batches are going to fail in blocking the wave produced by mobiles frequencies.

- The wave reflection amount of WN0-0, WN0, WSN1, WSN2, WSN3, and WSN3-0 batches at 1800 MHz frequency were 0.69 dB, 0.94 dB, 3.64 dB, 4.33 dB, 0.92 dB, and 2.99 dB, respectively. All the batches in this group had approximately the same amount of wave reflection. Steel fiber worked well as an electromagnetic wave absorber and absorbed the electric part due to its good electric-conductivity behavior. However, steel fiber did not work well with the magnetics parts leading to a decrease in the wave reflection. Thus, the matrix of the samples was the main definer of the waves' reflection behavior. For the batches with and without calcite, WN0, WN0-0, WSN3, and WSN3-0 had approximately the same amount of wave reflection. And as the difference in reflection was not significant, the calcite did not have a major effect on the reflection behavior. However, as none of the batches mentioned above could absorb -20 dB at 1800 MHz frequency, those batches are going to fail in blocking the wave produced by mobiles frequencies.
- The wave reflection amount of WN0-0, WN0, WSN1, WSN2, WSN3, and WSN3-0 batches at 2400 MHz frequency were -5.41 dB, -4.34 dB, -6.08 dB, -4.42 dB, -4.20 dB, and -7.70 dB, respectively. WSN1 reflected the highest amount of waves and increased the wave reflection by -1.74 dB comparing to the batch without steel fiber reinforcement (WN0). Steel fiber worked well as an electromagnetic wave absorber and absorbed the electric part due to its good electric-conductivity behavior. However, steel fiber did not work well with the magnetics parts leading to a decrease in the wave reflection. Thus, the matrix of the samples was the main definer of the waves' reflection behavior. For the batches with and without calcite, WN0, WN0-0, WSN3, and WSN3-0 had approximately the same amount of wave reflection. And as the difference in reflection was not significant, the calcite did not have a major effect on the reflection behavior. However, as none of the batches mentioned above could absorb -20 dB at 2400 MHz frequency, those batches are going to fail in blocking the wave produced by Bluetooth and Wi-Fi frequencies.
- The wave reflection amount of WN0-0, WN0, WSN1, WSN2, WSN3, and WSN3-0 batches at 5000 MHz frequency were -8.02 dB, -12.15 dB, 0.02 dB, -0.25 dB, -0.49 dB, and 0.17 dB, respectively. All the batches in this group had approximately the same amount of wave reflection. Steel fiber worked well as

an electromagnetic wave absorber and absorbed the electric part due to its good electric-conductivity behavior. However, steel fiber did not work well with the magnetics parts leading to a decrease in the wave reflection. Thus, the matrix of the samples was the main definer of the waves' reflection behavior. For the batches with and without calcite, WN0, WN0-0, WSN3, and WSN3-0 had approximately the same amount of wave reflection. And as the difference in reflection was not significant, the calcite did not have a major effect on the reflection behavior. However, as none of the batches mentioned above could absorb -20 dB at 1800 MHz frequency, those batches are going to fail in blocking the wave produced by Wi-Fi frequencies.

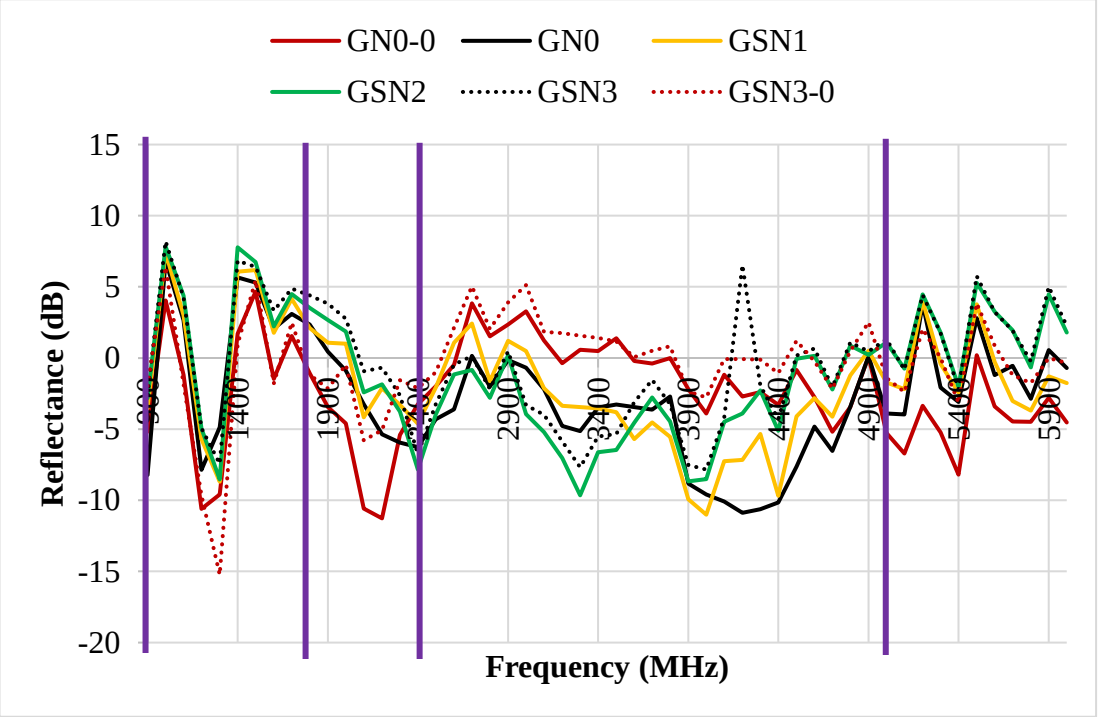

Figure 4.38. Reflection behavior of the N series batches made with GT and reinforced with steel fiber.

Figure 4-38 illustrates the reflection behavior of the N series batches made with GT and reinforced with steel fiber. Figure 4-38 results are discussed below:

- The wave reflection amount of GN0-0, GN0, GSN1, GSN2, GSN3, and GSN3-0 batches at 900 MHz frequency were -5.18 dB, -8.22 dB, -3.52 dB, -2.83 dB, -2.58 dB, and -1.96 dB, respectively. GN0 reflected the highest amount of

waves comparing to the batch without steel fiber reinforcement. Steel fiber worked well as an electromagnetic wave absorber and absorbed the electric part due to its good electric-conductivity behavior. However, steel fiber did not work well with the magnetics parts leading to a decrease in the wave reflection. Thus, the matrix of the samples was the main definer of the waves' reflection behavior. For the batches with and without calcite, GN0, GN0-0, GSN3, and GSN3-0 had approximately the same amount of wave reflection. And as the difference in reflection was not significant, the calcite did not have a major effect on the reflection behavior. However, as none of the batches mentioned above could absorb -20 dB at 900 MHz frequency, those batches are going to fail in blocking the wave produced by mobiles frequencies.

- The wave reflection amount of GN0-0, GN0, GSN1, GSN2, GSN3, and GSN3-0 batches at 1800 MHz frequency were -1.07 dB, 2.36 dB, 2.11 dB, 3.52 dB, 4.40 dB, and -1.18 dB, respectively. All the batches in this group had approximately the same amount of wave reflection. Steel fiber worked well as an electromagnetic wave absorber and absorbed the electric part due to its good electric-conductivity behavior. However, steel fiber did not work well with the magnetics parts leading to a decrease in the wave reflection. Thus, the matrix of the samples was the main definer of the waves' reflection behavior. For the batches with and without calcite, GN0, GN0-0, GSN3, and GSN3-0 had approximately the same amount of wave reflection. And as the difference in reflection was not significant, the calcite did not have a major effect on the reflection behavior. However, as none of the batches mentioned above could absorb -20 dB at 1800 MHz frequency, those batches are going to fail in blocking the wave produced by mobiles frequencies.
- The wave reflection amount of GN0-0, GN0, GSN1, GSN2, GSN3, and GSN3-0 batches at 2400 MHz frequency were -3.25 dB, -6.27 dB, -4.63 dB, -7.84 dB, -6.76 dB, and -2.13 dB, respectively. All the batches in this group had approximately the same amount of wave reflection. Steel fiber worked well as an electromagnetic wave absorber and absorbed the electric part due to its good electric-conductivity behavior. However, steel fiber did not work well with the magnetics parts leading to a decrease in the wave reflection. Thus, the matrix of the samples was the main definer of the waves' reflection behavior. For the

batches with and without calcite, GN0, GN0-0, GSN3, and GSN3-0 had approximately the same amount of wave reflection. And as the difference in the wave reflection behavior was not significant for the batches mentioned above, the calcite did not have a major effect on the reflection behavior. However, as none of the batches mentioned above could absorb -20 dB at 2400 MHz frequency, those batches are going to fail in blocking the wave produced by Bluetooth and Wi-Fi frequencies.

- The wave reflection amount of GN0-0, GN0, GSN1, GSN2, GSN3, and GSN3-0 batches at 900 MHz frequency were -5.28 dB, -3.89 dB, -1.71 dB, 1.10 dB, 1.33 dB, and -1.4 dB, respectively. All the batches in this group had approximately the same amount of wave reflection. Steel fiber worked well as an electromagnetic wave absorber and absorbed the electric part due to its good electric-conductivity behavior. However, steel fiber did not work well with the magnetics parts leading to a decrease in the wave reflection. Thus, the matrix of the samples was the main definer of the waves' reflection behavior. For the batches with and without calcite, GN0, GN0-0, GSN3, and GSN3-0 had approximately the same amount of wave reflection. And as the difference in reflection was not significant, the calcite did not have a major effect on the reflection behavior. However, as none of the batches mentioned above could absorb -20 dB at 900 MHz frequency, those batches are going to fail in blocking the wave produced by Wi-Fi frequencies.

The following could be observed from the wave reflection behavior of all the batches in the N series:

- Generally, PP fiber did not show a notable effect on increasing the wave reflection, as this fiber could transmit the waves because PP fiber has no electric-conductive behavior. And steel fiber did not work well with the magnetics parts leading to a decrease in the wave reflection. Thus, the matrix of the samples reinforced with PP and steel fibers was the main definer of the waves' absorption behavior.
- Generally, the batches made with WT had the same performance regarding the wave reflection amount comparing to the batches made with GT. This refers to

the chemical components of WT and GT. Both tuffs have the same types of oxides in their structures with a small variation leading to give the same wave reflection amount.

- Generally, the batches made with calcite had the same performance regarding the wave absorption comparing to the batches made without calcite. The chemical components of calcite, which is mainly CaO, enhanced the wave absorption amount and did not enhance the reflection amount.

PART 5

CONCLUSION

In this study, white and green volcanic tuff collected from the Bayburt region in Turkey were used as silica and alumina sources. Calcite was used as a calcium source. Sodium Hydroxide (NaOH) and Sodium Silicate (Na_2SiO_3) in combination were used as an alkali activators. Polypropylene and steel fibers used in this study to improve the AAPs' electromagnet properties, mechanical strength, and physical properties that will be produced. The new composite materials' electromagnet absorption and reflection features are determined in the range of 100 MHz - 6000 MHz between the 28^{th} and 56^{th} days of production. In addition, the mechanical and physical properties of the pastes were examined at 2, 28, and 90 days of production. Based on the results of this study, the following conclusions could be drawn:

- The maximum 90 days flexural strength from the AAP batches made with WT and activated with a combination of Sodium Hydroxide and Sodium Silicate was 10.99 MPa and found with the batch that is reinforced with 3% PP fiber (WPN3 batch). And the maximum 90 days compressive strength was 30.72 MPa and found with the batch that is reinforced with 2% PP fiber (WPN2 batch).
- The maximum 90 days flexural strength from the AAP batches made with GT and activated with a combination of Sodium Hydroxide and Sodium Silicate was 11.70 MPa and found with the batch that is reinforced with 3% PP fiber (GPN3 batch). And the maximum 90 days compressive strength was 15.32 MPa and found with the batch that is reinforced with 2% PP fiber (GPN2 batch).
- The water absorption of all the AAP batches made with WT was between 16.54% and 46.81%. The lowest water absorption was by WN0-0 batch and the highest water absorption was by WN 3-0 batch.

- The water absorption of all the AAP batches made with GT was between 22.08% and 34.14%. The lowest water absorption was by GPN2 batch, and the highest water absorption was by GPN1 batch.
- The lowest maximum shrinkage percentage for the AAP batches made with WT was 0.37% and found with WN0-0 batch.
- The lowest maximum shrinkage percentage for the AAP batches made with GT was 0.48% and found with GPN2 batch.
- The maximum electromagnetic wave's absorption peak for the AAP batches made with WT from the frequencies of 900 MHz, 1800 MHz, 2400 MHz, and 5000 MHz was found with WSN3-0 batch at 5000 MHz, and it was -26.21 dB.
- The maximum electromagnetic wave's reflection peak for the AAP batches made with WT from the frequencies of 900 MHz, 1800 MHz, 2400 MHz, and 5000 MHz was found with WN0 batch at 5000 MHz, and it was -12.15 dB.
- The maximum electromagnetic wave's absorption peak for the AAP batches made with GT from the frequencies of 900 MHz, 1800 MHz, 2400 MHz, and 5000 MHz was found with GSN3-0 batch at 5000 MHz, and it was -35.45 dB.
- The maximum electromagnetic wave's reflection peak for the AAP batches made with GT from the frequencies of 900 MHz, 1800 MHz, 2400 MHz, and 5000 MHz was found with GPN3 batch at 900 MHz, and it was -10.15 dB.

REFERENCES

1. Fernández-Jiménez, A. and Palomo, A., "Properties and uses of alkali cements", ***Revista Ingenieria De Construccion***, 24 (3): 213–232 (2009).

2. McLellan, B. C., Williams, R. P., Lay, J., Van Riessen, A., and Corder, G. D., "Costs and carbon emissions for geopolymer pastes in comparison to ordinary portland cement", ***Journal Of Cleaner Production***, 19 (9–10): 1080–1090 (2011).

3. Intergovernmental Panel on Climate Change, "Climate Change 2007 - Mitigation of Climate Change: Working Group III Contribution to the Fourth Assessment Report of the IPCC", ***Cambridge University Press***, Cambridge, (2007).

4. Vermeulen, J. W., "Biodiversity and cultural property in the management of limestone resources - lessons from East Asia", (1999).

5. Juenger, M. C. G., Winnefeld, F., Provis, J. L., and Ideker, J. H., "Advances in alternative cementitious binders", ***Cement And Concrete Research***, 41 (12): 1232–1243 (2011).

6. Unless, R., Act, P., Rose, W., If, T., and Rose, W., "Advances in understanding alkali activated materials", (2015).

7. Puertas, F., Martínez-Ramírez, S., Alonso, S., and Vázquez, T., "Alkali-activated fly ash/slag cements: Strength behaviour and hydration products", ***Cement And Concrete Research***, 30 (10): 1625–1632 (2000).

8. Singh, B., Ishwarya, G., Gupta, M., and Bhattacharyya, S. K., "Geopolymer concrete: A review of some recent developments", ***Construction And Building Materials***, 85: 78–90 (2015).

9. San Nicolas, R., Bernal, S. A., Mejía de Gutiérrez, R., van Deventer, J. S. J., and Provis, J. L., "Distinctive microstructural features of aged sodium silicate-activated slag concretes", ***Cement And Concrete Research***, 65: 41–51 (2014).

10. Purdon, A. O., "The action of alkalis on blast-furnace slag", ***Journal Of The Society Of Chemical Industry***, 59 (9): 191–202 (1940).

11. Glukhovsky, V. D., "Ancient, modern and future concretes", ***Proceedings Of The First International Conference On Alkaline Cements And Concretes***, 1–9 (1994).

12. Zhang, J., Shi, C., and Zhang, Z., "Chloride binding of alkali-activated slag/fly ash cements", ***Construction And Building Materials***, 226: 21–31 (2019).

13. Fernández-Jiménez, A. and Palomo, A., "Characterisation of fly ashes. Potential reactivity as alkaline cements☆", ***Fuel***, 82 (18): 2259–2265 (2003).

14. Gevaudan, J. P., Campbell, K. M., Kane, T. J., Shoemaker, R. K., and Srubar, W. V, "Mineralization dynamics of metakaolin-based alkali-activated cements", ***Cement And Concrete Research***, 94: 1–12 (2017).

15. Tekin, I., "Properties of NaOH activated geopolymer with marble, travertine and volcanic tuff wastes", ***Construction And Building Materials***, 127: 607–617 (2016).

16. Tekin, I., Gencel, O., Gholampour, A., Oren, O. H., Koksal, F., and Ozbakkaloglu, T., "Recycling zeolitic tuff and marble waste in the production of eco-friendly geopolymer concretes", ***Journal Of Cleaner Production***, 268: 122298 (2020).

17. Ye, H., Huang, L., and Chen, Z., "Influence of activator composition on the chloride binding capacity of alkali-activated slag", ***Cement And Concrete Composites***, 104: 103368 (2019).

18. Ortega, E. A., Cheeseman, C., Knight, J., and Loizidou, M., "Properties of alkali-activated clinoptilolite", ***Cement And Concrete Research***, 30 (10): 1641–1646 (2000).

19. Myers, R. J., Bernal, S. A., and Provis, J. L., "Phase diagrams for alkali-activated slag binders", ***Cement And Concrete Research***, 95: 30–38 (2017).

20. Ye, H. and Radlińska, A., "Quantitative Analysis of Phase Assemblage and Chemical Shrinkage of Alkali-Activated Slag", ***Journal Of Advanced Concrete Technology***, 14: 245–260 (2016).

21. Ye, H., "Nanoscale attraction between calcium-aluminosilicate-hydrate and Mg-Al layered double hydroxides in alkali-activated slag", ***Materials Characterization***, 140: 95–102 (2018).

22. Pacheco-Torgal, F., Castro-Gomes, J., and Jalali, S., "Alkali activated binders: A review. Part 2 - About mater and binder manufacture", ***Constr. Build. Mater.***, 22: 1305–1314 (2007).

23. Wang, S.-D., Pu, X.-C., Scrivener, K. L., and Pratt, P. L., "Alkali-activated slag cement and concrete: a review of properties and problems", ***Advances In Cement Research***, 7 (27): 93–102 (1995).

24. Dias, D. P. and Thaumaturgo, C., "Fracture toughness of geopolymeric concretes reinforced with basalt fibers", ***Cement And Concrete Composites***, 27 (1): 49–54 (2005).

25. Savastano, H., Warden, P. G., and Coutts, R. S. P., "Potential of alternative fibre cements as building materials for developing areas", ***Cement And Concrete Composites***, 25 (6): 585–592 (2003).

26. Puertas, F., Gil-Maroto, A., Palacios, M., and Amat, T., "Alkali-activated slag mortars reinforced with ar glassfibre. Performance and properties", ***Materiales De Construccion***, 56: (2006).

27. Vilaplana, J. L., Baeza, F. J., Galao, O., Alcocel, E. G., Zornoza, E., and Garcés, P., "Mechanical properties of alkali activated blast furnace slag pastes reinforced with carbon fibers", ***Construction And Building Materials***, 116: 63–71 (2016).

28. Blackman, C., "Cell phone radiation: Evidence from ELF and RF studies supporting more inclusive risk identification and assessment", ***Pathophysiology***, 16 (2): 205–216 (2009).

29. Volkow, N. D., Tomasi, D., Wang, G.-J., Vaska, P., Fowler, J. S., Telang, F., Alexoff, D., Logan, J., and Wong, C., "Effects of Cell Phone Radiofrequency Signal Exposure on Brain Glucose Metabolism", ***JAMA***, 305 (8): 808–813 (2011).

30. Sivani, S. and Sudarsanam, D., "Impacts of radio-frequency electromagnetic field (RF-EMF) from cell phone towers andwireless devices on biosystem and ecosystem-a review", ***Biology And Medicine***, 4 (4): 202–216 (2012).

31. Adang, D., Campo, B., and Vorst, A. V, "Has a 970 MHz Pulsed Exposure an Effect on the Memory Related Behaviour of Rats?", ***2006 European Conference On Wireless Technology***, 135–138 (2006).

32. Aniołczyk, H. and Koprowska, J., "Occupational and public EMF exposure-textiles shields as a modern approach for protection", ***11th International Congress Of The International Radiation Protection Association, Madrid, Spain***, 23–28 (2004).

33. Radicati, S., "Mobile Statistics Report, 2014-2018", ***Mobile Statistics Report, 2014-2018***, 44 (0): 1–4 (2014).

34. Wen, S. and Chung, D. D. L., "Electromagnetic interference shielding reaching 70 dB in steel fiber cement", ***Cement And Concrete Research***, 34 (2): 329–332 (2004).

35. Zhang, X. and Sun, W., "Microwave absorbing properties of double-layer cementitious composites containing Mn–Zn ferrite", ***Cement And Concrete Composites***, 32 (9): 726–730 (2010).

36. Dai, Y., Sun, M., Liu, C., and Li, Z., "Electromagnetic wave absorbing characteristics of carbon black cement-based composites", ***Cement And Concrete Composites***, 32 (7): 508–513 (2010).

37. Singhal, S., Bhukal, S., Singh, J., Chandra, K., and Bansal, S., "Optical, X-ray diffraction, and magnetic properties of the cobalt-substituted nickel chromium ferrites (CrCo x Ni 1-x FeO 4, x = 0, 0.2, 0.4, 0.6, 0.8, 1.0) synthesized using sol-gel autocombustion method", ***Journal Of Nanotechnology***, 2011: (2011).

38. Wang, B., Guo, Z., Han, Y., and Zhang, T., "Electromagnetic wave absorbing properties of multi-walled carbon nanotube/cement composites", ***Construction And Building Materials***, 46: 98–103 (2013).

39. Singh, A. P., Gupta, B. K., Mishra, M., Govind, Chandra, A., Mathur, R. B., and Dhawan, S. K., "Multiwalled carbon nanotube/cement composites with exceptional electromagnetic interference shielding properties", ***Carbon***, 56: 86–96 (2013).

40. Chung, D. D. L., "Carbon materials for structural self-sensing, electromagnetic shielding and thermal interfacing", ***Carbon***, 50 (9): 3342–3353 (2012).

41. Wang, Z., Li, K., and Wang, C., "Freezing–thawing effects on electromagnetic wave reflectivity of carbon fiber cement based composites", ***Construction And Building Materials***, 64: 288–292 (2014).

42. Yoo, D.-Y., Kang, M.-C., Choi, H.-J., Shin, W., and Kim, S., "Electromagnetic interference shielding of multi-cracked high-performance fiber-reinforced cement composites – Effects of matrix strength and carbon fiber", ***Construction And Building Materials***, 261: 119949 (2020).

43. Folgueras, L. de C., Alves, M. A., and Rezende, M. C., "Microwave absorbing paints and sheets based on carbonyl iron and polyaniline: measurement and simulation of their properties", ***Journal Of Aerospace Technology And Management***, 2 (1): 63–70 (2010).

44. Huang, Y. Bin, Qian, J. S., and Zhang, J. Y., "Electromagnetic properties of high ferric oxide fly ash", ***Jianzhu Cailiao Xuebao/Journal Of Building Materials***, 13 (3): 291–294 (2010).

45. Kaushal, A. and Singh, V., "Effect of filler loading on the shielding of electromagnetic interference of reduced graphene oxide reinforced polypropylene nanocomposites prepared via a twin-screw extruder", ***Journal Of Materials Science: Materials In Electronics***, 31 (24): 22162–22170 (2020).

46. MCCAFFREY, R., "Climate Change and Cement Industry", ***Global Cement And Lime Magazine***, 15–19 (2002).

47. Roy, D. M., "Alkali-activated cements Opportunities and challenges", ***Cement And Concrete Research***, 29 (2): 249–254 (1999).

48. Malhotra, V. M., "Introduction: Sustainable Development and Concrete Technology", ***Concrete International***, 24 (7): .

49. Mehta, P. K., "Greening of the Concrete Industry for Sustainable Development", ***Concrete International***, 24 (7): 23–28 (2002).

50. Kuhl, H., "Slag cement and process of making the same. - US900939 A", (1908).

51. Glukhovsky, V. D., "Soil silicates", ***Gosstroyizdat, Kiev***, 154: (1959).

52. Panagiotopoulou, C., Tsivilis, S., and Kakali, G., "Application of the Taguchi approach for the composition optimization of alkali activated fly ash binders", ***Construction And Building Materials***, 91: 17–22 (2015).

53. Davidovits, J., "SYNTHESIS OF NEW HIGH-TEMPERATURE GEO-POLYMERS FOR REINFORCED PLASTICS/COMPOSITES.", (1979).

54. PAS 8820:2016, "Construction Materials – Alkali-Activated Cementitious Material and Concrete – Specification", ***BSI Standards Limited***, (2016).

55. Li, C., Sun, H., and Li, L., "A review: The comparison between alkali-activated slag (Si + Ca) and metakaolin (Si + Al) cements", ***Cement And Concrete Research***, 40 (9): 1341–1349 (2010).

56. Provis, J. L. and Deventer, V., "Alkali-Activated Materials State-of-the-Art Report", Alkali Activated Materials: State of The Art Report, (2014).

57. Junaid, M. T., Kayali, O., and Khennane, A., "A Mix Design Procedure for Alkali Activated Fly Ash-Based Geopolymer Concretes", (2012).

58. Davidovits, J., "Geopolymer chemistry and properties", ***Geopolymer***, 88 (1): 25–48 (1988).

59. Davidovits, J., "Geopolymers Inorganic polymeric new materials", ***Journal Of Thermal Analysis And Calorimetry***, 37 (8): 1633–1656 .

60. Palomo, A., Blanco-Varela, M. T., Granizo, M. L., Puertas, F., Vazquez, T., and Grutzeck, M. W., "Chemical stability of cementitious materials based on metakaolin - Isothermal conduction calorimetry study", ***Cement And Concrete Research***, 29: 997–1004 (1999).

61. Brough, A. R. and Atkinson, A., "Sodium silicate-based, alkali-activated slag mortars: Part I. Strength, hydration and microstructure", ***Cement And Concrete Research***, 32 (6): 865–879 (2002).

62. Granizo, M. L., Alonso, S., Blanco-Varela, M. T., and Palomo, A., "Alkaline Activation of Metakaolin: Effect of Calcium Hydroxide in the Products of Reaction", ***Journal Of The American Ceramic Society***, 85 (1): 225–231 (2002).

63. Duxson, P. and Provis, J. L., "Designing Precursors for Geopolymer Cements", ***Journal Of The American Ceramic Society***, 91 (12): 3864–3869 (2008).

64. Fernández-Jiménez, A. and Puertas, F., "Alkali-activated slag cements: Kinetic studies", ***Cement And Concrete Research***, 27 (3): 359–368 (1997).

65. Wang, S.-D. and Scrivener, K. L., "Hydration products of alkali activated slag cement", ***Cement And Concrete Research***, 25 (3): 561–571 (1995).

66. Shi, C., Jiménez, A. F., and Palomo, A., "New cements for the 21st century: The pursuit of an alternative to Portland cement", ***Cement And Concrete Research***, 41 (7): 750–763 (2011).

67. Tekin, I., "Properties of NaOH activated geopolymer with marble, travertine and volcanic tuff wastes", ***Construction And Building Materials***, 127: 607–617 (2016).

68. TABAN, S. and ŞİMŞEK, O., "The Effect of Zeolitic Tuff Addition Ratio and Sea Water on Physical and Mechanical Properties on Cement", 24 (1): 145–153 (2008).

69. "ASTM C618 - 03 Standard Specification for Coal Fly Ash and Raw or Calcined Natural Pozzolan for Use in Concrete", **https://www.astm.org/DATABASE.CART/HISTORICAL/C618-03.htm** (2021).

70. Adam, A., "Strength and durability properties of alkali activated slag and fly ash-based geopolymer concrete", (August): (2009).

71. DİRİKOLU, İ., "Physical and Mechanical Properties of Volcanic Tuff Based Alkali-Activated Binders", (2019).

72. Nedeljković, M., "Carbonation Mechanism of Alkali-Activated Fly Ash and Slag Materials In View of Long-Term Performance Predictions", TU Delft University, 289 (2019).

73. Nurullah ÖKSÜZER, "Utilization of different fineness marble and Bayburt stone wastes in fiber-reinforced geopolymer binder system", 42 (1): 1–10 (2016).

74. Shi, C., "Alkali-Activated Cements and Concretes", (2003).

75. Xu, H. and Van Deventer, J., "The geopolymerisation of alumino-silicate minerals", ***International Journal Of Mineral Processing***, 59: 247–266 (2000).

76. Xu, Y., Chen, H., and Wang, P., "Effect of Polypropylene Fiber on Properties of Alkali-Activated Slag Mortar", ***Advances In Civil Engineering***, 2020: (2020).

77. Kumar, V. S. and Ariyannan, P. P., "Retrofitting of Rc Beam Using Simcon Laminate", ***JETCSE***, 20 (3): 219–225 (2016).

78. PURCELL, E. M. and MORIN, D. J., "ELECTRICITY ANDMAGNETISM", (2013).

79. Browne, M., "Schaum's Outline of Physics for Engineering and Science, Third Edition", 3rd ed. Ed., ***McGraw-Hill Education***, New York, (2013).

80. Serway, R. A., "Physics for Scientists & Engineers with Modern Physics", ***Second Edition. Philadelphia : Saunders College Pub., 1986, C1983.***, .

81. Gurer, G., "Design and Characterization of Electromagnetic Wave", (September): (2010).

82. Gupta, M., Leong, W. W., and Eugene, .

83. R, R. M., Mridula, S., and Mohanan, P., "Study and Analysis of Dielectric Behavior of Fertilized Soil at Microwave Frequency", ***European Journal Of Advances In Engineering And Technology***, 2 (2): 73–79 (2015).

84. Nelson, S. O., "Measurement of microwave dielectric properties of particulate materials", ***Journal Of Food Engineering***, 21 (3): 365–384 (1994).

85. Rocha, L. S., Junqueira, C. C., Gambin, E., Vicente, A. N., Culhaoglu, A. E., and Kemptner, E., "A free space measurement approach for dielectric material characterization", ***2013 SBMO/IEEE MTT-S International Microwave & Optoelectronics Conference (IMOC)***, 1–5 (2013).

86. Tereshchenko, O. V., Buesink, F. J. K., and Leferink, F. B. J., "An overview of the techniques for measuring the dielectric properties of materials", ***2011 30th URSI General Assembly And Scientific Symposium, URSIGASS 2011***, 1–4 (2011).

87. Ghodgaonkar, D. K., Varadan, V. V, and Varadan, V. K., "Free-space measurement of complex permittivity and complex permeability of magnetic materials at microwave frequencies", ***IEEE Transactions On Instrumentation And Measurement***, 39 (2): 387–394 (1990).

88. Tang, S. C., Hui, S. Y. R., and Chung, H. S. H., "Evaluation of the shielding effects on printed-circuit-board transformers using ferrite plates and copper sheets", ***IEEE Transactions On Power Electronics***, 17 (6): 1080–1088 (2002).

89. He, Y., Ao, J., Yang, J., and Tang, X., "The Shielding-Effectiveness Based Magnetic Field Shielding Theory and Its Application in Mobile Payment Systems", ***2014 IEEE 80th Vehicular Technology Conference (VTC2014-Fall)***, 1–5 (2014).

90. Al-khlaiwi, T. and Sultan, A., "Association of mobile phone radiation with fatigue, headache, dizziness, tension and sleep disturbance in Saudi population", ***Saudi Medical Journal***, 25: 732–736 (2004).

91. Zhang, X.-Y. and Zhang, P.-Y., "Mobile technology in health information systems - a review.", ***European Review For Medical And Pharmacological Sciences***, 20 (10): 2140–2143 (2016).

92. Subhan, F., Khan, A., Ahmed, S., Malik, M., Bakshah, S., and Tahir, S., "Mobile Antenna's and Its Impact on Human Health", ***Journal Of Medical Imaging And Health Informatics***, 8: 1266–1273 (2018).

93. Taye, R. R., Deka, M. K., Borkataki, S., Panda, S., and Gogoi, J., "Effect of Electromagnetic Radiation of Cell Phone Tower on Development of Asiatic Honey Bee, Apis cerana F. (Hymenoptera: Apidae)", ***International Journal Of Current Microbiology And Applied Sciences***, 7 (08): 4334–4339 (2018).

94. Hocking, B., Gordon, I. R., Grain, H. L., and Hatfield, G. E., "Cancer incidence and mortality and proximity to TV towers.", ***The Medical Journal Of Australia***, 165 (11–12): 601–605 (1996).

95. Batool, S., Bibi, A., Frezza, F., and Mangini, F., "Benefits and hazards of electromagnetic waves, telecommunication, physical and biomedical: A review", ***European Review For Medical And Pharmacological Sciences***, 23 (7): 3121–3128 (2019).

96. Vlasceanu, I. N., Gharzouni, A., Tantot, O., Lalande, M., Elissalde, C., and Rossignol, S., "Geopolymer as dielectric materials for ultra-wideband antenna applications: Impact of magnetite addition and humidity", ***Open Ceramics***, 2 (May): 100013 (2020).

97. Lee, H. S., Park, J. ho, Singh, J. K., Choi, H. J., Mandal, S., Jang, J. M., and Yang, H. M., "Electromagnetic shielding performance of carbon black mixed concrete with zn-Al metal thermal spray coating", ***Materials***, 13 (4): (2020).

98. Rajak, M. and Rai, B., "Effect of Micro Polypropylene Fibre on the Performance of Fly Ash-Based Geopolymer Concrete", ***Journal Of Applied Engineering Sciences***, 9 (1): 97–108 (2019).

99. Ding, Y. and Bai, Y. L., "Fracture properties and softening curves of steel fiber-reinforced slag-based geopolymer mortar and concrete", ***Materials***, 11 (8): (2018).

100. Ekinci, E., "The Investigation of Some Mechanical and Physical Properties of Geopolimer Concrete Produced By Using Volcanic Tuff", (2017).

101. Koppel, T., Shishkin, A., Haldre, H., Toropovs, N., Vilcane, I., and Tint, P., "Reflection and Transmission Properties of Common Construction Materials at 2.4 GHz Frequency", ***Energy Procedia***, 113: 158–165 (2017).

102. Guan, B., Ding, D., Wang, L., Wu, J., and Xiong, R., "The electromagnetic wave absorbing properties of cement-based composites using natural magnetite powders as absorber", ***Materials Research Express***, 4 (5): (2017).

103. Chi, M. C., Chang, J. J., Huang, R., and Weng, Z. L., "Effect of Alkali-Activators on the Strength Development and Drying Shrinkage of Alkali-Activated Binder", ***Advanced Materials Research***, 482–484: 1012–1016 (2012).

104. Ranjbar, N., Mehrali, M., Behnia, A., Javadi Pordsari, A., Mehrali, M., Alengaram, U. J., and Jumaat, M. Z., "A Comprehensive Study of the Polypropylene Fiber Reinforced Fly Ash Based Geopolymer", ***PLOS ONE***, 11 (1): e0147546 (2016).

105. Lee, P. C., Kim, B. R., Jeoung, S. K., and Kim, Y. K., "Electromagnetic interference shielding effectiveness of polypropylene/conducting fiber composites", ***AIP Conference Proceedings***, 1713 (March): (2016).

106. Jenifer, M. A., Kumar, S. S., and Devadass, D. C. S. C., "Fracture behaviour of fibre reinforced geopolymer concrete", ***Current Science***, 113 (1): 116–122 (2017).

107. prakash, A. S. and kumar, G. S., "Experimental Study on Geopolymer Concrete using Steel Fibres", ***International Journal Of Engineering Trends And Technology***, 21 (8): 396–399 (2015).

108. Iqbal, S., Ali, A., Holschemacher, K., and Bier, T. A., "Effect of Change in Micro Steel Fiber Content on Properties of High Strength Steel Fiber Reinforced Lightweight Self-Compacting Concrete (HSLSCC)", ***Procedia Engineering***, 122: 88–94 (2015).

109. Xingjun, L., Mingli, C., Yan, L., Xin, L., Qian, L., Rong, T., Qi, W., and Yuping, D., "A new absorbing foam concrete: preparation and microwave absorbing properties", ***Advances In Concrete Construction***, 3 (2): 103–111 (2015).

110. Memon, F. A., Nuruddin, M. F., Demie, S., and Shafiq, N., "Effect of curing conditions on strength and durability of high-performance concrete", ***Scientia Iranica***, 24 (2): 576–583 (2017).

111. Aire, C., Mendoza, C., and Davila, P., "Polypropylene Fibers Reinforced Concrete : Optimization on Plastic Shrinkage Cracking", (December 2011): 1–12 (2011).

112. Dai, Y., Lu, C., Ni, Y., and Xu, Z., "Radar-wave absorbing property of cement-based composite doped with steel slag", ***Kuei Suan Jen Hsueh Pao/Journal Of The Chinese Ceramic Society***, 37: 2097–2101 (2009).

113. Cao, J. and Chung, D. D. L., "Use of fly ash as an admixture for electromagnetic interference shielding", ***Cement And Concrete Research***, 34 (10): 1889–1892 (2004).

114. Puertas, F., Amat, T., Fernández-Jiménez, A., and Vázquez, T., "Mechanical and durable behaviour of alkaline cement mortars reinforced with polypropylene fibres", ***Cement And Concrete Research***, 33 (12): 2031–2036 (2003).

115. ARSLAN, M., ASLAN, Z., and DOKUZ, A., "Petrographical, Geochemical and Petrological Characteristics of the Bayburt Tuffs: Eocene Calk-Alkaline Felsic Volcanism in the Southern Zone of Eastern Pontide", ***Selcuk University Journal Of Engineering, Science And Technology***, 20 (1): 49–68 (2005).

116. Yılmaz, F., "Investigation usage of tuffite stone with lime in soil stabilization by standard tests and computed tomography method", (2015).

117. Toy, S., "TRA1 NUTS II Regional Development Plan (2014–2023); Planning Process and Content", (2014).

118. Internet: ASTM C1437-20, "ASTM C1437 - 20 Standard Test Method for Flow of Hydraulic Cement Mortar", **https://www.astm.org/Standards/C1437** (2021).

119. ASTM C348, A., "Flexural strength of hydraulic-cement mortars", ***American Society For Testing And Material***, (2018).

120. ASTM C109/C109M-02., "Standard Test Method for Compressive Strength of Hydraulic Cement Mortars", ***Annual Book Of ASTM Standards***, (2016).

121. C20, A., "ASTM C20 - Standard Test Methods for Apparent Porosity, Water Absorption, Apparent Specific Gravity, and Bulk Density of Burned Refractory Brick and Shapes by Boiling Water 1", (2019).

122. Internet: 18, A. C.-, "ASTM C596 - 18 Standard Test Method for Drying Shrinkage of Mortar Containing Hydraulic Cement", **https://www.astm.org/Standards/C596** (2021).

APPENDIX A.

ELECTROMAGNETIC ABSORPTION AND REFLECTION DATA

Table Appendix A. 1. Electromagnetic wave's absorption and reflection data of the batches made with WT and reinforced with PP fiber from the N series.

Frequency	Reference		WN0-0		WN0		WPN1	
MHz	**Absorption**	**Reflection**	**Absorption**	**Reflection**	**Absorption**	**Reflection**	**Absorption**	**Reflection**
900.0	-15.43	-17.07	-4.72	-8.24	-7.84	-7	-13.3	-4.36
1000.0	-26.35	-33.63	-0.56	2.72	-2.78	3.48	-6.16	3.92
1100.0	-24.39	-21.5	3.62	-2.97	1.08	-3.15	-0.08	-3
1200.0	-21.85	-18.14	-2.25	0.53	-4.42	0.4	-6.45	-0.71
1300.0	-16.74	-19.17	-2.58	-8.06	-5.93	-8.92	-7.74	-8.01
1400.0	-14.71	-26.15	-3.85	2.29	-6.79	2.85	-8.86	1.56
1500.0	-15.65	-24.66	-5.26	0.85	-7.53	0.58	-8.34	0.47
1600.0	-15.99	-20.19	-6.28	-0.69	-9.14	-0.43	-11.16	-0.83
1700.0	-14.81	-23.39	-3.29	0.98	-5.87	0.6	-7.16	0.28
1800.0	-14.92	-24.91	-5.03	0.69	-7.45	0.94	-8.92	0.07
1900.0	-15.05	-21.48	-3.88	-0.03	-6.51	0.44	-7.71	-0.35
2000.0	-13.84	-20.39	-6.99	0.5	-9.46	1.08	-10.68	0.13
2100.0	-14.66	-22.94	-9.53	-0.1	-11.89	0.1	-13.21	-0.61
2200.0	-15.43	-22.78	-8.49	-2.76	-10.33	-1.9	-11.47	-2.97
2300.0	-14.88	-21.53	-10.11	-0.84	-12.5	-0.39	-13.68	-0.94
2400.0	-14.98	-22.06	-6.49	-5.41	-9.37	-4.34	-10.25	-5.17
2500.0	-13.78	-19.74	-7.89	-1.02	-9.51	-0.49	-10.95	-0.82
2600.0	-18.73	-26.38	-5.65	-4.66	-7.82	-3.54	-8.76	-3.97
2700.0	-17.15	-27.01	-4.7	-5.59	-7.05	-4.12	-7.39	-4.57
2800.0	-20.81	-27.02	-5.22	-6.4	-7.45	-4.93	-7.92	-5.44
2900.0	-18.89	-25.71	-4.71	-8.48	-7.23	-6.34	-7.95	-6.88
3000.0	-19.74	-27.44	-4.65	-7.64	-6.72	-6.53	-7.22	-8.23
3100.0	-19.74	-24.16	-4.26	-7.03	-9.17	-4.85	-7.46	-6.33
3200.0	-20.9	-23.98	-5.53	-8.96	-8.3	-7.93	-8.7	-8.59
3300.0	-20.69	-23.68	-2.66	-10.98	-5.51	-7.8	-5.78	-8.75
3400.0	-20.31	-23.89	-3.45	-10.61	-6.45	-9.62	-6.52	-9.49
3500.0	-24.79	-26.48	-2.4	-14.15	-5.45	-14.01	-5.57	-12.8
3600.0	-32.36	-34.51	-2.39	-9.59	-5.25	-12.24	-5.9	-10.1
3700.0	-21.54	-24.55	-3.05	-12.4	-5.44	-17.42	-5.94	-11.84
3800.0	-23.8	-25.22	-2.39	-11.61	-4.73	-19.2	-5.5	-12.44
3900.0	-25.66	-25.38	-2.62	-19.26	-5.94	-23.56	-6.71	-20.35
4000.0	-24.07	-23.72	-4.32	-10.18	-7.64	-15.69	-8.44	-11.68
4100.0	-21.27	-26.08	-4.53	-14.8	-7.15	-30.69	-8.27	-15.49
4200.0	-24.32	-27.26	-3.05	-10.55	-6.03	-16.91	-6.43	-11.44
4300.0	-24.72	-26.72	-3.42	-8.81	-6.6	-16.78	-7.62	-10.12
4400.0	-22.77	-26.54	-4.44	-7.35	-7.28	-14.11	-7.72	-9.33
4500.0	-21.69	-28.74	-4.15	-8.23	-6.44	-13.19	-7.3	-10.28
4600.0	-22.64	-29.87	-3.67	-8.65	-6.42	-16.24	-7.27	-10.7
4700.0	-26.14	-29.46	-4.09	-6.08	-6.57	-12.79	-7.64	-8.29
4800.0	-23	-29.57	-3.26	-8.65	-6.15	-16.19	-7.36	-8.19
4900.0	-24.41	-32.18	-3.24	-6.84	-6.25	-11.89	-7.48	-7.1
5000.0	-24.13	-31.22	-4.07	-8.02	-7.12	-12.15	-7.87	-6.27
5100.0	-23.05	-29.79	-3.37	-12.44	-6.21	-15.83	-7.51	-9.22
5200.0	-23.6	-32.76	-3.03	-8.48	-6.42	-11.8	-7.59	-5.01
5300.0	-27.05	-33.38	-4.13	-8.57	-7.68	-10.44	-8.62	-6.67
5400.0	-24.2	-29.36	-4.37	-9.6	-7.69	-13.94	-8.94	-8.57
5500.0	-23.44	-34.37	-4.27	-5.45	-7.57	-11.15	-8.37	-6.02
5600.0	-22.81	-32.08	-3.82	-13.78	-8.29	-19.91	-8.02	-11.14
5700.0	-24.96	-32.28	-5.16	-12.54	-10.11	-18.69	-9.83	-9.42
5800.0	-24.4	-30.91	-3.55	-13.59	-8.44	-19.06	-7.85	-6.67
5900.0	-25.23	-33.35	-2.86	-11.05	-7.93	-13.86	-7.32	-5.88
6000.0	-26.54	-33.1	-5.45	-12.6	-10.57	-16.4	-10.08	-8.01
Frequency	Reference		WPN2		WPN3		WPN3-0	
MHz	**Absorption**	**Reflection**	**Absorption**	**Reflection**	**Absorption**	**Reflection**	**Absorption**	**Reflection**
900.0	-15.43	-17.07	-6.96	-6.7	-5.59	-7.43	-4.33	-9.23
1000.0	-26.35	-33.63	-4.87	2.02	-3.19	1.76	-1.36	0.88
1100.0	-24.39	-21.5	0.9	-2.76	1.67	-2.92	2.87	-6.25
1200.0	-21.85	-18.14	-4.9	-0.09	-4.45	-0.69	-2.05	-0.66
1300.0	-16.74	-19.17	-7.01	-6.34	-7.22	-6.98	-2.77	-8.59
1400.0	-14.71	-26.15	-7.1	0.96	-6.87	0.14	-3.94	-0.27
1500.0	-15.65	-24.66	-7.67	0.47	-6.92	2.14	-4.97	-0.15
1600.0	-15.99	-20.19	-12.43	-1.51	-12.09	-2.54	-7.04	-2.46
1700.0	-14.81	-23.39	-6.93	0.16	-6.96	0.04	-3.88	-1.16

Frequency	Reference		WPN2		WPN3		WPN3-0	
MHz	**Absorption**	**Reflection**	**Absorption**	**Reflection**	**MHz**	**Absorption**	**Reflection**	**Absorption**
1800.0	-14.92	-24.91	-9.63	-0.01	-8.62	-1	-5.9	-0.77
1900.0	-15.05	-21.48	-7.95	-0.69	-7.81	-1.46	-4.18	-2.04
2000.0	-13.84	-20.39	-11.19	-0.4	-10.02	-1.89	-7.23	-1.39
2100.0	-14.66	-22.94	-12.64	-1.46	-11.86	-1.19	-9.54	-1.25
2200.0	-15.43	-22.78	-11.78	-3.27	-10.53	-3.81	-8.7	-3.59
2300.0	-14.88	-21.53	-11.85	-1.31	-11.41	-1.67	-10.85	-1.42
2400.0	-14.98	-22.06	-9.26	-5.3	-8.47	-5.52	-7.03	-5.43
2500.0	-13.78	-19.74	-9.99	-1.37	-9.43	-1.09	-8.33	-1.12
2600.0	-18.73	-26.38	-7.92	-4.67	-7.72	-4.03	-6.42	-4.09
2700.0	-17.15	-27.01	-6.54	-5.76	-6.45	-4.53	-4.62	-5.17
2800.0	-20.81	-27.02	-7.9	-6.44	-7.25	-5.6	-5.62	-5.83
2900.0	-18.89	-25.71	-7.21	-8.12	-7.17	-7.73	-6.2	-7.91
3000.0	-19.74	-27.44	-6.96	-7.67	-6.99	-7.93	-5	-8.76
3100.0	-19.74	-24.16	-7.26	-7.33	-7.13	-7.42	-5.36	-8.01
3200.0	-20.9	-23.98	-8.17	-8.81	-7.95	-9.43	-6.57	-11.06
3300.0	-20.69	-23.68	-5.48	-9.97	-5.09	-10.48	-3.54	-11.66
3400.0	-20.31	-23.89	-6.06	-10.59	-5.7	-10.48	-4.41	-9.92
3500.0	-24.79	-26.48	-6.17	-12.75	-4.9	-11.26	-4.21	-10.89
3600.0	-32.36	-34.51	-5.88	-10.49	-5.76	-8.8	-4.33	-7.91
3700.0	-21.54	-24.55	-6.17	-12.88	-5.99	-8.21	-4.57	-7.95
3800.0	-23.8	-25.22	-5.71	-11.89	-5.2	-8.34	-3.77	-8.34
3900.0	-25.66	-25.38	-7.14	-22.12	-5.54	-9.81	-4.45	-11.15
4000.0	-24.07	-23.72	-8.3	-10.82	-8.08	-6.78	-6.76	-8.14
4100.0	-21.27	-26.08	-7.75	-13.78	-7.3	-6.96	-6.12	-11.8
4200.0	-24.32	-27.26	-6.09	-9.43	-5.27	-6.23	-3.98	-8.09
4300.0	-24.72	-26.72	-7.77	-8.86	-6.63	-4.6	-5.8	-5.74
4400.0	-22.77	-26.54	-7.25	-7.24	-6.26	-6.36	-5.83	-5.32
4500.0	-21.69	-28.74	-7.18	-8.39	-6.02	-4.76	-5.73	-3.39
4600.0	-22.64	-29.87	-7.35	-9.47	-6.04	-5.9	-5.1	-3.93
4700.0	-26.14	-29.46	-7.37	-6.4	-6.08	-3.35	-5.44	-2.46
4800.0	-23	-29.57	-7.5	-7.23	-5.79	-2.8	-4.98	-2.56
4900.0	-24.41	-32.18	-7.58	-5.82	-5.25	-2.29	-5.49	-2.26
5000.0	-24.13	-31.22	-7.46	-4.38	-6.79	-1.3	-5.95	-1.35
5100.0	-23.05	-29.79	-7.66	-6.55	-6	-3.62	-4.75	-3.79
5200.0	-23.6	-32.76	-7.86	-2.07	-6.06	0.01	-4.7	-0.11
5300.0	-27.05	-33.38	-8.09	-4.43	-6.65	-2.98	-5.75	-3.36
5400.0	-24.2	-29.36	-8.47	-5.84	-6.38	-3.74	-4.77	-3.74
5500.0	-23.44	-34.37	-7.84	-2.25	-6	-1.23	-4.07	-0.17
5600.0	-22.81	-32.08	-7.61	-8.08	-5.92	-4.78	-4.55	-4.56
5700.0	-24.96	-32.28	-9.9	-6.98	-7.73	-4.85	-5.42	-4.61
5800.0	-24.4	-30.91	-7.64	-4.25	-5.75	-3.05	-3.95	-3.32
5900.0	-25.23	-33.35	-7.95	-5.4	-5.6	-3.67	-4.72	-4.33
6000.0	-26.54	-33.1	-9.6	-6.85	-7.97	-5.19	-6.3	-5.92

Table Appendix A. 2. Electromagnetic wave's absorption and reflection data of the batches made with WT and reinforced with steel fiber from the N series.

Frequency	Reference		WSN0-0		WSN0		WSN1	
MHz	**Absorption**	**Reflection**	**Absorption**	**Reflection**	**Absorption**	**Reflection**	**Absorption**	**Reflection**
900.0	-15	-17.1	-4.72	-8.24	-7.84	-7	-9.44	-4.24
1000.0	-26	-33.6	-0.56	2.72	-2.78	3.48	-6.67	6.41
1100.0	-24	-21.5	3.62	-2.97	1.08	-3.15	-1.87	0.42
1200.0	-22	-18.1	-2.25	0.53	-4.42	0.4	-5.54	-7.55
1300.0	-17	-19.2	-2.58	-8.06	-5.93	-8.92	-7.76	-4.6
1400.0	-15	-26.2	-3.85	2.29	-6.79	2.85	-10.96	3.1
1500.0	-16	-24.7	-5.26	0.85	-7.53	0.58	-8.69	4.91
1600.0	-16	-20.2	-6.28	-0.69	-9.14	-0.43	-11.75	2.44
1700.0	-15	-23.4	-3.29	0.98	-5.87	0.6	-9.6	3.17
1800.0	-15	-24.9	-5.03	0.69	-7.45	0.94	-8.49	3.64
1900.0	-15	-21.5	-3.88	-0.03	-6.51	0.44	-8.88	2.96
2000.0	-14	-20.4	-6.99	0.5	-9.46	1.08	-10.95	0.71
2100.0	-15	-22.9	-9.53	-0.1	-11.89	0.1	-11.87	-1.36
2200.0	-15	-22.8	-8.49	-2.76	-10.33	-1.9	-11.1	-3.01
2300.0	-15	-21.5	-10.11	-0.84	-12.5	-0.39	-10.9	-2.83
2400.0	-15	-22.1	-6.49	-5.41	-9.37	-4.34	-7.7	-6.08
2500.0	-14	-19.7	-7.89	-1.02	-9.51	-0.49	-10.1	-1.24
2600.0	-19	-26.4	-5.65	-4.66	-7.82	-3.54	-10.33	-1.38
2700.0	-17	-27	-4.7	-5.59	-7.05	-4.12	-8.99	-2.21
2800.0	-21	-27	-5.22	-6.4	-7.45	-4.93	-6.25	-3.13
2900.0	-19	-25.7	-4.71	-8.48	-7.23	-6.34	-9.51	-4.63
3000.0	-20	-27.4	-4.65	-7.64	-6.72	-6.53	-8.36	-10.1
3100.0	-20	-24.2	-4.26	-7.03	-9.17	-4.85	-8.8	-7.41
3200.0	-21	-24	-5.53	-8.96	-8.3	-7.93	-9.42	-8.92
3300.0	-21	-23.7	-2.66	-10.98	-5.51	-7.8	-8.11	-8.58
3400.0	-20	-23.9	-3.45	-10.61	-6.45	-9.62	-8.46	-12.5
3500.0	-25	-26.5	-2.4	-14.15	-5.45	-14.01	-7.66	-8.57
3600.0	-32	-34.5	-2.39	-9.59	-5.25	-12.24	-11.01	-10.2
3700.0	-22	-24.6	-3.05	-12.4	-5.44	-17.42	-10.51	-6.33
3800.0	-24	-25.2	-2.39	-11.61	-4.73	-19.2	-11.84	-7.05
3900.0	-26	-25.4	-2.62	-19.26	-5.94	-23.56	-10.89	-7.74
4000.0	-24	-23.7	-4.32	-10.18	-7.64	-15.69	-14.6	-8.32
4100.0	-21	-26.1	-4.53	-14.8	-7.15	-30.69	-12.12	-7.15
4200.0	-24	-27.3	-3.05	-10.55	-6.03	-16.91	-11.07	-7.37
4300.0	-25	-26.7	-3.42	-8.81	-6.6	-16.78	-11.98	-3.76
4400.0	-23	-26.5	-4.44	-7.35	-7.28	-14.11	-13.89	-5.54
4500.0	-22	-28.7	-4.15	-8.23	-6.44	-13.19	-12.92	-3.71
4600.0	-23	-29.9	-3.67	-8.65	-6.42	-16.24	-13.93	-2.26
4700.0	-26	-29.5	-4.09	-6.08	-6.57	-12.79	-14.47	-1.16
4800.0	-23	-29.6	-3.26	-8.65	-6.15	-16.19	-14.28	0.4
4900.0	-24	-32.2	-3.24	-6.84	-6.25	-11.89	-14.42	1.04
5000.0	-24	-31.2	-4.07	-8.02	-7.12	-12.15	-15.68	0.02
5100.0	-23	-29.8	-3.37	-12.44	-6.21	-15.83	-15.13	-0.52
5200.0	-24	-32.8	-3.03	-8.48	-6.42	-11.8	-15.4	3.18
5300.0	-27	-33.4	-4.13	-8.57	-7.68	-10.44	-14.95	-0.3
5400.0	-24	-29.4	-4.37	-9.6	-7.69	-13.94	-16.24	1.2
5500.0	-23	-34.4	-4.27	-5.45	-7.57	-11.15	-16.12	3.44
5600.0	-23	-32.1	-3.82	-13.78	-8.29	-19.91	-16.72	-0.49
5700.0	-25	-32.3	-5.16	-12.54	-10.11	-18.69	-18.96	0.9
5800.0	-24	-30.9	-3.55	-13.59	-8.44	-19.06	-17.77	0.84
5900.0	-25	-33.4	-2.86	-11.05	-7.93	-13.86	-20.66	1.49
6000.0	-27	-33.1	-5.45	-12.6	-10.57	-16.4	-21.15	1.92
Frequency	Reference		WSN2		WSN3		WSN3-0	
MHz	**Absorption**	**Reflection**	**Absorption**	**Reflection**	**Absorption**	**Reflection**	**Absorption**	**Reflection**
900.0	-15	-17.1	-12.55	-3.54	-11.14	-2.09	-11.14	-2.09
1000.0	-26	-33.6	-7.21	7.03	-11.18	6.1	-11.18	6.1
1100.0	-24	-21.5	-4.24	1.43	-3.69	-2.26	-3.69	-2.26
1200.0	-22	-18.1	-6.32	-6.5	-12.37	-11.47	-12.37	-11.5
1300.0	-17	-19.2	-10.63	-4.75	-11.57	-7.25	-11.57	-7.25
1400.0	-15	-26.2	-13.41	4.38	-16.33	0.23	-16.33	0.23
1500.0	-16	-24.7	-10.22	5.73	-14.84	6.29	-14.84	6.29
1600.0	-16	-20.2	-13.31	3.07	-19.39	-0.28	-19.39	-0.28
1700.0	-15	-23.4	-11.77	3.24	-14.44	2.64	-14.44	2.64

Frequency	Reference		WSN2		WSN3		WSN3-0	
MHz	**Absorption**	**Reflection**	**Absorption**	**Reflection**	**MHz**	**Absorption**	**Reflection**	**Absorption**
1800.0	-15	-24.9	-10.29	4.33	-13.15	0.92	-13.15	0.92
1900.0	-15	-21.5	-10.6	3.17	-13.01	-1.11	-13.01	-1.11
2000.0	-14	-20.4	-11.93	1.27	-15.04	-0.64	-15.04	-0.64
2100.0	-15	-22.9	-15.07	-0.78	-17.71	-6.36	-17.71	-6.36
2200.0	-15	-22.8	-13.18	-3.12	-18.43	-5.84	-18.43	-5.84
2300.0	-15	-21.5	-13.09	-2.3	-18.32	-4.37	-18.32	-4.37
2400.0	-15	-22.1	-9.98	-4.42	-12.85	-4.2	-12.85	-4.2
2500.0	-14	-19.7	-12.26	-0.09	-13.45	0.81	-13.45	0.81
2600.0	-19	-26.4	-12.85	0.32	-15.6	-0.85	-15.6	-0.85
2700.0	-17	-27	-10.51	0.2	-15.01	4.08	-15.01	4.08
2800.0	-21	-27	-9.09	-1.46	-11.56	3.08	-11.56	3.08
2900.0	-19	-25.7	-11.58	-1.99	-14.65	3.31	-14.65	3.31
3000.0	-20	-27.4	-11.21	-5.86	-14.64	3.92	-14.64	3.92
3100.0	-20	-24.2	-10.84	-6.2	-12.81	2.47	-12.81	2.47
3200.0	-21	-24	-12.28	-8.06	-14.77	1.78	-14.77	1.78
3300.0	-21	-23.7	-11.26	-7.58	-13.85	2.71	-13.85	2.71
3400.0	-20	-23.9	-11.06	-12.24	-15.67	2.99	-15.67	2.99
3500.0	-25	-26.5	-10.57	-7.98	-16.45	3.34	-16.45	3.34
3600.0	-32	-34.5	-14.29	-9.82	-18.2	3.52	-18.2	3.52
3700.0	-22	-24.6	-13.46	-5.92	-18.66	0.47	-18.66	0.47
3800.0	-24	-25.2	-15.72	-6.99	-19.22	0.97	-19.22	0.97
3900.0	-26	-25.4	-13.98	-7.52	-16.92	-0.92	-16.92	-0.92
4000.0	-24	-23.7	-18.29	-7.97	-20.7	-0.66	-20.7	-0.66
4100.0	-21	-26.1	-15.83	-7.16	-19.86	-0.29	-19.86	-0.29
4200.0	-24	-27.3	-13.31	-6.38	-17.38	-1.2	-17.38	-1.2
4300.0	-25	-26.7	-15.2	-3.9	-20.34	-0.52	-20.34	-0.52
4400.0	-23	-26.5	-17.17	-5.44	-20.92	-0.12	-20.92	-0.12
4500.0	-22	-28.7	-15.53	-4.41	-20.01	0.29	-20.01	0.29
4600.0	-23	-29.9	-16.54	-2.25	-20.33	0.31	-20.33	0.31
4700.0	-26	-29.5	-18.41	-1.98	-22.71	-0.38	-22.71	-0.38
4800.0	-23	-29.6	-17.51	0.14	-23.38	-0.07	-23.38	-0.07
4900.0	-24	-32.2	-17.9	0.61	-21.9	-0.99	-21.9	-0.99
5000.0	-24	-31.2	-19.53	-0.25	-24.23	-0.49	-24.23	-0.49
5100.0	-23	-29.8	-18.88	-0.72	-24.6	-1.36	-24.6	-1.36
5200.0	-24	-32.8	-19.48	3.41	-24.32	-1.93	-24.32	-1.93
5300.0	-27	-33.4	-19.99	-0.15	-26.76	-3.96	-26.76	-3.96
5400.0	-24	-29.4	-21.63	1.71	-28.57	-0.79	-28.57	-0.79
5500.0	-23	-34.4	-22.24	4.32	-28.66	3.53	-28.66	3.53
5600.0	-23	-32.1	-20.86	0.32	-27.65	-1.32	-27.65	-1.32
5700.0	-25	-32.3	-24.54	2.14	-31.29	0.27	-31.29	0.27
5800.0	-24	-30.9	-23.32	1.85	-28.18	-2.84	-28.18	-2.84
5900.0	-25	-33.4	-25.04	1.61	-29.03	-1.13	-29.03	-1.13
6000.0	-27	-33.1	-26.85	2.12	-29.75	-0.88	-29.75	-0.88

Table Appendix A. 3. Electromagnetic wave's absorption and reflection data of the batches made with GT and reinforced with PP fiber from the N series.

Frequency	Reference		GPN0-0		GPN0		GPN1	
MHz	**Absorption**	**Reflection**	**Absorption**	**Reflection**	**Absorption**	**Reflection**	**Absorption**	**Reflection**
900	-18.07	-17.07	-14.76	-5.18	-11.51	-8.22	-14.98	-5.89
1000	-31.95	-33.63	-15.39	4.04	-9.29	6.84	-12.44	6.45
1100	-22.45	-21.5	-4.8	-1.17	-2.14	2.65	-4.25	2.55
1200	-14.65	-18.14	-3.5	-10.6	2.11	-7.86	-0.07	-7.73
1300	-19.33	-19.17	-15.2	-9.6	-10.7	-4.87	-13.74	-5.16
1400	-17.56	-26.15	-17.39	1.71	-13.64	5.66	-15.95	4.9
1500	-18.83	-24.66	-14.94	4.66	-11.42	5.3	-13.31	5.17
1600	-17.19	-20.19	-17.19	-1.47	-12.1	2.07	-14.85	1.69
1700	-18.22	-23.39	-15.01	1.55	-11.82	3.09	-14.03	2.82
1800	-20.34	-24.91	-16.77	-1.07	-13.25	2.36	-15.21	2.43
1900	-18.01	-21.48	-15.88	-3.44	-12.81	0.44	-14.81	0.37
2000	-14.23	-20.39	-18.34	-4.6	-14.69	-0.89	-16.83	-1.17
2100	-19.36	-22.94	-19.76	-10.58	-17.19	-3.25	-19.35	-3.83
2200	-20.66	-22.78	-20.63	-11.27	-16.05	-5.37	-18.94	-6.24
2300	-18.88	-21.53	-18.98	-5.4	-13.36	-5.95	-15.92	-6.71
2400	-20.38	-22.06	-15.69	-3.25	-11.56	-6.27	-14.14	-7.04
2500	-16.15	-19.74	-12.7	-1.99	-8.6	-4.31	-11.16	-4.92
2600	-23.1	-26.38	-17.02	-0.48	-12.01	-3.6	-14.5	-4.16
2700	-22.59	-27.01	-16.01	3.85	-11.39	0.16	-14.29	-0.69
2800	-25.16	-27.02	-14.03	1.53	-8.9	-2.01	-12.21	-3.12
2900	-23.03	-25.71	-16.26	2.35	-10.89	-0.15	-14.67	-0.7
3000	-24.61	-27.44	-16.03	3.27	-10.34	-0.68	-13.85	-1.34
3100	-21.42	-24.16	-11.81	1.23	-7.22	-2.18	-10.81	-3.05
3200	-22.25	-23.98	-12.36	-0.37	-7.06	-4.78	-10.98	-5.42
3300	-21.34	-23.68	-10.12	0.58	-4.96	-5.14	-8.87	-5.58
3400	-21.47	-23.89	-12.95	0.49	-6.85	-3.5	-10.79	-4.98
3500	-24.31	-26.48	-9.12	1.38	-3.24	-3.28	-7.23	-3.61
3600	-29.86	-34.51	-11.49	-0.21	-5.62	-3.44	-10.29	-4.1
3700	-20.31	-24.55	-12.54	-0.4	-6.35	-3.63	-10.94	-3.33
3800	-21.36	-25.22	-12.4	-0.01	-5.93	-2.7	-10.79	-2.37
3900	-22.71	-25.38	-8.77	-2.19	-3.04	-8.83	-7.84	-6.42
4000	-19.82	-23.72	-10.8	-3.89	-4.41	-9.58	-10.15	-7.76
4100	-20.69	-26.08	-13.73	-1.18	-6.75	-10.08	-11.93	-8.22
4200	-23.18	-27.26	-11.19	-2.71	-5.58	-10.88	-10.26	-7.3
4300	-21.42	-26.72	-10.34	-2.4	-3.82	-10.62	-8.67	-6.84
4400	-20.43	-26.54	-12.01	-3.29	-5.99	-10.15	-11.08	-6.7
4500	-22.5	-28.74	-14.76	-0.85	-8.6	-7.63	-13.53	-3.45
4600	-22.94	-29.87	-12.93	-2.76	-7.06	-4.83	-11.69	-2.87
4700	-22.7	-29.46	-10.62	-5.19	-4.5	-6.54	-9.83	-4.45
4800	-22.66	-29.57	-13.5	-3.44	-7.16	-3.43	-12.34	-1.86
4900	-25.85	-32.18	-13.01	0.1	-7.04	0.13	-11.88	1.26
5000	-23.32	-31.22	-13.1	-5.28	-7.62	-3.89	-13.17	-3.07
5100	-22.05	-29.79	-11.01	-6.71	-6.18	-3.97	-11.32	-3.77
5200	-24.77	-32.76	-13.19	-3.36	-8.5	3.81	-13.3	3.35
5300	-26.91	-33.38	-12.89	-5.23	-8.43	-2.08	-13.77	-2.06
5400	-22.74	-29.36	-11.75	-8.2	-5.55	-3.1	-10.78	-3.44
5500	-25.79	-34.37	-16.05	0.2	-10.49	2.81	-15.24	2.11
5600	-24.52	-32.08	-15.92	-3.41	-10.86	-1.19	-16.06	-1.38
5700	-25.07	-32.28	-15.75	-4.46	-9.25	-0.55	-14.5	-0.89
5800	-23.23	-30.91	-13.53	-4.49	-8.4	-2.86	-13.03	-3.07
5900	-27.81	-33.35	-15.34	-2.8	-10	0.55	-15.45	0.3
6000	-27.55	-33.1	-16.3	-4.52	-10.11	-0.71	-15.47	-0.62
Frequency	Reference		GPN2		GPN3		GPN3-0	
MHz	**Absorption**	**Reflection**	**Absorption**	**Reflection**	**Absorption**	**Reflection**	**Absorption**	**Reflection**
900	-18.07	-17.07	-10.84	-9.23	-10.38	-10.15	-14.89	-5.89
1000	-31.95	-33.63	-8.07	6.44	-6.86	6.94	-17.74	3.06
1100	-22.45	-21.5	-1.62	2.64	-1.1	2.53	-6.55	-3.76
1200	-14.65	-18.14	2.61	-8.3	3.01	-8.12	-5.66	-13.83
1300	-19.33	-19.17	-10.02	-4.34	-9.3	-4.55	-15.88	-13.46
1400	-17.56	-26.15	-12.28	5.4	-11.78	5.86	-17.56	0.87
1500	-18.83	-24.66	-11.08	5.48	-11.27	5.88	-16.27	4.97
1600	-17.19	-20.19	-11.39	2.14	-10.66	2.37	-17.16	-4.07
1700	-18.22	-23.39	-11.18	3.31	-10.94	3.37	-15.67	-0.13

Frequency	Reference		GPN2		GPN3		GPN3-0	
MHz	**Absorption**	**Reflection**	**Absorption**	**Reflection**	**MHz**	**Absorption**	**Reflection**	**Absorption**
1800	-20.34	-24.91	-12.16	3.23	-11.65	3.42	-17.24	-3.12
1900	-18.01	-21.48	-11.94	1.34	-11.56	1.45	-16.82	-6.9
2000	-14.23	-20.39	-13.91	-0.14	-13.4	-0.22	-18.74	-5.9
2100	-19.36	-22.94	-16.09	-1.44	-15.19	-1.29	-20.85	-16.32
2200	-20.66	-22.78	-15.45	-4.03	-14.54	-4	-21.52	-14.67
2300	-18.88	-21.53	-12.69	-5.64	-12.23	-5.77	-19.46	-5.07
2400	-20.38	-22.06	-11.18	-6.78	-11.07	-7.42	-16.39	-2.27
2500	-16.15	-19.74	-9.01	-4.12	-8.41	-4.08	-13	-1.45
2600	-23.1	-26.38	-11.9	-3.39	-11.18	-3.93	-17.49	-0.04
2700	-22.59	-27.01	-11.14	-0.61	-10.36	-1.31	-16.85	4.31
2800	-25.16	-27.02	-9.09	-2.44	-8.29	-2.87	-14.88	1.82
2900	-23.03	-25.71	-11.36	-0.58	-10.14	-0.82	-17.29	2.29
3000	-24.61	-27.44	-10.68	-3.46	-9.78	-2.87	-17	3.75
3100	-21.42	-24.16	-7.85	-3.77	-6.46	-3.78	-12.38	1.71
3200	-22.25	-23.98	-7.27	-6.54	-6.32	-7.15	-13.7	0.16
3300	-21.34	-23.68	-5.28	-6.51	-4.05	-7.82	-11.02	1.12
3400	-21.47	-23.89	-6.76	-4.06	-5.78	-5.1	-14.67	0.65
3500	-24.31	-26.48	-3	-2.35	-1.91	-3.43	-10.31	1.1
3600	-29.86	-34.51	-6.62	-2.19	-4.61	-2.61	-12.05	-0.49
3700	-20.31	-24.55	-6.96	-2	-4.81	-2.74	-13.56	-1.22
3800	-21.36	-25.22	-6.51	-1.19	-4.58	-1.42	-13.45	-0.71
3900	-22.71	-25.38	-3.04	-6.33	-1.34	-7	-10.23	-2.77
4000	-19.82	-23.72	-4.99	-7.69	-2.84	-8.33	-12.17	-4.3
4100	-20.69	-26.08	-6.58	-7.47	-4.77	-8.36	-16.03	-1.45
4200	-23.18	-27.26	-5.42	-7.09	-3.68	-8.23	-13.09	-3.25
4300	-21.42	-26.72	-2.95	-6.24	-0.95	-7.21	-12.48	-3.21
4400	-20.43	-26.54	-5.26	-5.8	-3.38	-7.29	-13.38	-4.06
4500	-22.5	-28.74	-8.11	-3.83	-6.37	-4.59	-16.49	-2.03
4600	-22.94	-29.87	-5.38	-4.87	-4.52	-6.49	-14.24	-4.32
4700	-22.7	-29.46	-2.98	-4.41	-1.74	-4.84	-11.86	-8.47
4800	-22.66	-29.57	-5.45	-2.45	-4.56	-3.53	-14.89	-7.63
4900	-25.85	-32.18	-5.31	-0.61	-4.2	-2.77	-14.85	-4.37
5000	-23.32	-31.22	-5.66	-3.91	-4.35	-5.55	-14.09	-8.15
5100	-22.05	-29.79	-4.35	-5.25	-3.58	-6.25	-13.5	-9.01
5200	-24.77	-32.76	-6.56	1.28	-5.61	0.67	-14.59	-7.1
5300	-26.91	-33.38	-6.09	-3.08	-4.95	-4.21	-15.35	-7.5
5400	-22.74	-29.36	-3.37	-6.33	-2.25	-6.69	-13.53	-10.22
5500	-25.79	-34.37	-8.55	-1.05	-7.13	-1.17	-17.86	-0.22
5600	-24.52	-32.08	-8.78	-4.27	-7.93	-4.77	-17.73	-3.34
5700	-25.07	-32.28	-6.22	-3.92	-5.57	-3.5	-16.7	-3.63
5800	-23.23	-30.91	-5.54	-6.46	-4.88	-6.33	-15.39	-4.26
5900	-27.81	-33.35	-8.52	-1.73	-7.64	-1.14	-16.88	0.2
6000	-27.55	-33.1	-7.55	-3.1	-6.86	-2.57	-18	-2.18

Table Appendix A. 4. Electromagnetic wave's absorption and reflection data of the batches made with GT and reinforced with steel fiber from the N series.

Frequency	Reference		GN0-0		GN0		GSN1	
MHz	**Absorption**	**Reflection**	**Absorption**	**Reflection**	**Absorption**	**Reflection**	**Absorption**	**Reflection**
900	-18.07	-17.07	-14.76	-5.18	-11.51	-8.22	-8.4	-3.52
1000	-31.95	-33.63	-15.39	4.04	-9.29	6.84	-4.61	7.42
1100	-22.45	-21.5	-4.8	-1.17	-2.14	2.65	-1.31	3
1200	-14.65	-18.14	-3.5	-10.6	2.11	-7.86	-4.76	-5.71
1300	-19.33	-19.17	-15.2	-9.6	-10.7	-4.87	-8.18	-8.69
1400	-17.56	-26.15	-17.39	1.71	-13.64	5.66	-12	6.07
1500	-18.83	-24.66	-14.94	4.66	-11.42	5.3	-9.27	6.19
1600	-17.19	-20.19	-17.19	-1.47	-12.1	2.07	-12.08	1.77
1700	-18.22	-23.39	-15.01	1.55	-11.82	3.09	-8.66	4.16
1800	-20.34	-24.91	-16.77	-1.07	-13.25	2.36	-7.57	2.11
1900	-18.01	-21.48	-15.88	-3.44	-12.81	0.44	-10.64	1.08
2000	-14.23	-20.39	-18.34	-4.6	-14.69	-0.89	-14.38	1.01
2100	-19.36	-22.94	-19.76	-10.58	-17.19	-3.25	-12.22	-4.18
2200	-20.66	-22.78	-20.63	-11.27	-16.05	-5.37	-10.25	-2.12
2300	-18.88	-21.53	-18.98	-5.4	-13.36	-5.95	-8.97	-3.29
2400	-20.38	-22.06	-15.69	-3.25	-11.56	-6.27	-6.93	-4.63
2500	-16.15	-19.74	-12.7	-1.99	-8.6	-4.31	-7.18	-2.08
2600	-23.1	-26.38	-17.02	-0.48	-12.01	-3.6	-8.14	1.07
2700	-22.59	-27.01	-16.01	3.85	-11.39	0.16	-7.55	2.42
2800	-25.16	-27.02	-14.03	1.53	-8.9	-2.01	-6.9	-1.63
2900	-23.03	-25.71	-16.26	2.35	-10.89	-0.15	-8.68	1.21
3000	-24.61	-27.44	-16.03	3.27	-10.34	-0.68	-7.29	0.48
3100	-21.42	-24.16	-11.81	1.23	-7.22	-2.18	-7.21	-2.13
3200	-22.25	-23.98	-12.36	-0.37	-7.06	-4.78	-7.52	-3.35
3300	-21.34	-23.68	-10.12	0.58	-4.96	-5.14	-8.21	-3.45
3400	-21.47	-23.89	-12.95	0.49	-6.85	-3.5	-8.72	-3.54
3500	-24.31	-26.48	-9.12	1.38	-3.24	-3.28	-8.35	-3.8
3600	-29.86	-34.51	-11.49	-0.21	-5.62	-3.44	-11.38	-5.7
3700	-20.31	-24.55	-12.54	-0.4	-6.35	-3.63	-10.55	-4.54
3800	-21.36	-25.22	-12.4	-0.01	-5.93	-2.7	-9.88	-5.54
3900	-22.71	-25.38	-8.77	-2.19	-3.04	-8.83	-9.07	-9.93
4000	-19.82	-23.72	-10.8	-3.89	-4.41	-9.58	-10.8	-11.01
4100	-20.69	-26.08	-13.73	-1.18	-6.75	-10.08	-11.43	-7.25
4200	-23.18	-27.26	-11.19	-2.71	-5.58	-10.88	-8.86	-7.16
4300	-21.42	-26.72	-10.34	-2.4	-3.82	-10.62	-11.53	-5.35
4400	-20.43	-26.54	-12.01	-3.29	-5.99	-10.15	-10.38	-9.68
4500	-22.5	-28.74	-14.76	-0.85	-8.6	-7.63	-10.72	-4.1
4600	-22.94	-29.87	-12.93	-2.76	-7.06	-4.83	-9.77	-2.82
4700	-22.7	-29.46	-10.62	-5.19	-4.5	-6.54	-11.13	-4.13
4800	-22.66	-29.57	-13.5	-3.44	-7.16	-3.43	-11.61	-1.23
4900	-25.85	-32.18	-13.01	0.1	-7.04	0.13	-9.16	0.5
5000	-23.32	-31.22	-13.1	-5.28	-7.62	-3.89	-12.54	-1.71
5100	-22.05	-29.79	-11.01	-6.71	-6.18	-3.97	-12.3	-2.2
5200	-24.77	-32.76	-13.19	-3.36	-8.5	3.81	-11.48	4.03
5300	-26.91	-33.38	-12.89	-5.23	-8.43	-2.08	-13.17	-0.42
5400	-22.74	-29.36	-11.75	-8.2	-5.55	-3.1	-13.02	-2.44
5500	-25.79	-34.37	-16.05	0.2	-10.49	2.81	-13.61	3.78
5600	-24.52	-32.08	-15.92	-3.41	-10.86	-1.19	-15.48	-0.28
5700	-25.07	-32.28	-15.75	-4.46	-9.25	-0.55	-16.03	-3.03
5800	-23.23	-30.91	-13.53	-4.49	-8.4	-2.86	-16.7	-3.69
5900	-27.81	-33.35	-15.34	-2.8	-10	0.55	-13.76	-1.28
6000	-27.55	-33.1	-16.3	-4.52	-10.11	-0.71	-16.73	-1.76
Frequency	Reference		GSN2		GSN3		GSN3-0	
MHz	**Absorption**	**Reflection**	**Absorption**	**Reflection**	**Absorption**	**Reflection**	**Absorption**	**Reflection**
900	-18.07	-17.07	-12.53	-2.83	-14.93	-2.58	-16.99	-1.96
1000	-31.95	-33.63	-6.88	7.83	-10.06	8.2	-16.86	6.39
1100	-22.45	-21.5	-4.06	4.39	-5.45	4.24	-8.08	-1.83
1200	-14.65	-18.14	-6.21	-4.96	-8.41	-4.94	-15.45	-9.66
1300	-19.33	-19.17	-10.56	-8.54	-13.21	-7.43	-18.06	-15.23
1400	-17.56	-26.15	-12.81	7.78	-14.77	6.84	-22.47	0.97
1500	-18.83	-24.66	-10.69	6.75	-11.2	6.41	-21.3	5.47
1600	-17.19	-20.19	-12.56	2.21	-15.13	3.32	-23.97	-1.79
1700	-18.22	-23.39	-10.2	4.5	-11.67	4.87	-21.92	2.5

Frequency	Reference		GSN2		GSN3		GSN3-0	
MHz	**Absorption**	**Reflection**	**Absorption**	**Reflection**	**MHz**	**Absorption**	**Reflection**	**Absorption**
1800	-20.34	-24.91	-9.8	3.52	-11.63	4.4	-19.67	-1.18
1900	-18.01	-21.48	-12.71	2.66	-13.21	3.81	-20.36	-2.15
2000	-14.23	-20.39	-16.03	1.87	-18.11	2.77	-24.55	-0.49
2100	-19.36	-22.94	-14.06	-2.41	-13.97	-0.93	-23.25	-5.78
2200	-20.66	-22.78	-12.48	-1.86	-13.09	-0.69	-27.77	-5.06
2300	-18.88	-21.53	-13.4	-3.77	-13.52	-2.61	-25.73	-1.57
2400	-20.38	-22.06	-13.07	-7.84	-12.62	-6.76	-23.97	-2.13
2500	-16.15	-19.74	-14.11	-3.97	-13.85	-3.25	-28.75	-0.99
2600	-23.1	-26.38	-13.68	-1.16	-13.31	-0.46	-26.62	2.13
2700	-22.59	-27.01	-13.88	-0.85	-13.22	0.12	-21.02	5.04
2800	-25.16	-27.02	-14.13	-2.8	-14.24	-2.16	-25.09	2.03
2900	-23.03	-25.71	-16.1	0.2	-15.15	0.46	-26.98	3.9
3000	-24.61	-27.44	-16.23	-3.94	-15.42	-3.32	-28.73	5.13
3100	-21.42	-24.16	-15.1	-5.21	-15.2	-3.99	-21.96	1.83
3200	-22.25	-23.98	-15.12	-7.02	-14.46	-5.86	-23.76	1.74
3300	-21.34	-23.68	-15.65	-9.65	-15.9	-7.67	-22.86	1.56
3400	-21.47	-23.89	-15.96	-6.62	-15.8	-5.51	-27.05	1.41
3500	-24.31	-26.48	-16.24	-6.46	-16.71	-5.33	-24.99	1.17
3600	-29.86	-34.51	-18.95	-4.56	-18.92	-3.12	-30.75	0.06
3700	-20.31	-24.55	-19.48	-2.78	-19.83	-1.54	-31.68	0.52
3800	-21.36	-25.22	-19.77	-4.47	-19.74	-3.25	-37.42	0.83
3900	-22.71	-25.38	-18.72	-8.68	-19.94	-7.52	-32.27	-2.35
4000	-19.82	-23.72	-20.43	-8.51	-19.92	-7.84	-34.73	-2.78
4100	-20.69	-26.08	-21.25	-4.49	-20.87	-4.22	-33.29	-0.07
4200	-23.18	-27.26	-18.83	-3.9	-17.96	6.53	-31.56	-0.08
4300	-21.42	-26.72	-21.21	-2.27	-20.56	-1.95	-33.88	-0.12
4400	-20.43	-26.54	-23.09	-5.11	-21.81	-4.3	-36.97	-1.07
4500	-22.5	-28.74	-22.12	-0.05	-20.42	0.17	-34.98	1.2
4600	-22.94	-29.87	-21.63	0.16	-20.98	0.66	-33.5	-0.24
4700	-22.7	-29.46	-23.81	-2.21	-21.64	-2.06	-37.26	-2.17
4800	-22.66	-29.57	-25.21	0.88	-22.77	1.09	-36.57	0.48
4900	-25.85	-32.18	-22.65	0.22	-20.68	0.46	-31.45	2.52
5000	-23.32	-31.22	-25.71	1.1	-23.38	1.33	-35.45	-1.4
5100	-22.05	-29.79	-25.36	-0.74	-22.83	-0.82	-36.09	-2.39
5200	-24.77	-32.76	-25.04	4.47	-22.21	4.42	-34.23	2.03
5300	-26.91	-33.38	-27.12	1.8	-23.27	1.75	-37.86	0.01
5400	-22.74	-29.36	-27.62	-2.01	-23.18	-2.18	-39.79	-3.14
5500	-25.79	-34.37	-27.31	5.29	-24.67	5.76	-39.98	3.85
5600	-24.52	-32.08	-28.73	3.25	-23.74	3.24	-38.48	0.88
5700	-25.07	-32.28	-31.4	1.95	-27.49	1.92	-43.14	-1.21
5800	-23.23	-30.91	-30.88	-0.67	-27.8	-0.23	-44.49	-1.77
5900	-27.81	-33.35	-30.25	4.48	-25.06	5.02	-39.59	-0.01
6000	-27.55	-33.1	-30.29	1.79	-27.5	2.25	-40.97	-0.34

RESUME

Iyad AHMED completed his primary, secondary, and high school education in Jeddah. After that, he started undergraduate program in Applied Sciences Private University Department of Civil Engineering in 2014 and graduated in 2018. After graduation, Iyad worked for a year in Saudi Arabia as a technical engineer at an infrastructure project. Then in 2019, he started his Civil Engineering master's degree program at Karabuk University. And during his master's degree program, Iyad participate in two international symposiums with three papers. In 2020, he started to work as a scholar in a fully funded project from the Scientific and Technological Research Council of Turkey (TÜBİTAK) concerning about Alkali-Activated Materials and this project belongs to his supervisor Assoc. Prof. Dr. İlker TEKİN.